THE ROLE OF MATRICELLULAR SIGNALING IN POLYCYSTIC

KIDNEY DISEASE

By

Archana Raman

Submitted to the graduate degree program in Molecular and Integrative Physiology and the Graduate Faculty of the University of Kansas in partial fulfillment of the requirements for the degree of Doctor of Philosophy.

_____

Darren P. Wallace, Ph.D., Co-Chair

_____

Gustavo Blanco, M.D., Ph.D., Co-Chair

_____

Udayan Apte, Ph.D.

_____

James P. Calvet, Ph.D.

_____

Reena Rao, Ph.D.

_____

Alan S.L. Yu, M.B., B.Chir.

Date Defended: June 12th 2017

The dissertation committee for Archana Raman certifies that this is the
approved version of the following dissertation:

THE ROLE OF MATRICELLULAR SIGNALING IN POLYCYSTIC

KIDNEY DISEASE

_____

Darren P. Wallace, Ph.D., Co-Chair

_____

Gustavo Blanco, M.D., Ph.D., Co-Chair

Date Approved: July 25th 2017

ABSTRACT

Polycystic kidney disease (PKD) is characterized by excessive enlargement of the kidney, due to the hyperplastic growth of renal epithelial cells, giving rise to fluid-filled cysts. Autosomal dominant PKD (ADPKD), the most common renal disorder, affects 12.5 million people and accounts for 10% of the patients receiving renal replacement therapy. In PKD, the cyst-lining epithelia display several molecular patterns characteristic of tissue development and repair. The expanding cysts are associated with aberrant proliferation and extensive extracellular matrix (ECM) remodeling and deposition, causing interstitial fibrosis, which results in the progressive decline of renal function in PKD patients. Our lab discovered that periostin, a matricellular protein involved in tissue repair, is highly overexpressed in kidneys of human ADPKD, Autosomal Recessive PKD (ARPKD) and several animal models of PKD. Periostin accumulates in the ECM adjacent to cysts and binds to the cell surface integrins to stimulate the proliferation of cystic cells. Genetic knockout of periostin in *pcy/pcy* mice, a slowly progressive model of PKD, significantly reduced cystic growth and fibrosis, demonstrating that periostin significantly contributes to the progression of renal cystic disease. The molecular mechanisms behind periostin-induced ADPKD progression remain unclear. Here, we show that periostin stimulates integrin-linked kinase (ILK), a scaffold protein essential for ECM-cell communication, leading to activation of the Akt/mTOR pathway and proliferation of human ADPKD cells. In addition, periostin induced the activation of focal adhesion kinase (FAK) and Rho-dependent actin stress fiber formation and migration of ADPKD cells. Periostin also regulates the expression of genes involved in integrin signaling, ECM deposition and cytoskeletal reorganization in ADPKD cells, consistent with periostin activation of cellular pathways involved in tissue repair. To determine if overexpression of periostin in the cyst-lining

cells accelerates PKD progression, we generated *pcy/pcy* mice with selective overexpression of periostin in the collecting duct (CD) cells, the predominant site of cyst formation. CD-specific periostin overexpression accelerated the progression of cystic disease by significantly increasing renal mTOR activity, cell proliferation, cyst growth and interstitial fibrosis. In parallel studies, we found that pharmacologic inhibition and shRNA knockdown of ILK prevented periostin-induced Akt/mTOR signaling and ADPKD cell proliferation. Furthermore, selective knockdown of ILK in the CD cells of *Pkd1$^{fl/fl}$;Pkhd1-Cre* mice, a rapidly progressive model of ADPKD, and in *pcy/pcy* mice, decreased renal Akt/mTOR activity, cell proliferation, cyst growth, and interstitial fibrosis, and significantly improved renal function and survival. Our results indicate that aberrant expression of periostin stimulates ILK-Akt-mTOR mediated cell proliferation, FAK-Rho mediated cytoskeletal rearrangement and migration, and ECM production. We propose that blockade of ECM-integrin signaling holds potential to slow cyst growth and fibrosis in PKD.

DEDICATION

I dedicate this dissertation to my parents, Raman Ananthakrishna and Sarada Raman, my brother Adithya Raman, and my uncle, Easwar Narayanan.

You are my pillars of strength. You wholeheartedly supported my decision to live on the other side of the world to pursue my dreams. I cannot adequately express my thankfulness for your undying love and constant encouragement.

ACKNOWLEDGEMENTS

Graduate school has been a tremendous learning experience fueled by many ups, and downs. I would like to thank all the people who have taught, helped and supported me during these six years as a graduate student.

I owe everything I have to my parents, my brother and my uncle, who have always believed in me, and loved and supported me. My father and mother have taught me always to persevere, and they constantly inspire me to grow into a bigger and better human being. There are not enough words to express my love for you, Dad and Mom.

I am indebted to my thesis advisor, Dr. Darren Wallace. He is an unfaltering and dedicated mentor and has taught me a great deal in terms of both science and life values. I am constantly inspired by his knowledge, humbleness, helpfulness, and integrity, and I consider myself extremely fortunate to have chosen his laboratory to pursue my Ph.D. Thank you for everything, and I hope that my growth as a scientist will make you proud.

I sincerely thank my committee members, Dr. Udayan Apte, Dr. Gustavo Blanco, Dr. James Calvet, Dr. Reena Rao, and Dr. Alan Yu, for their advice, patience, and support through the course of my thesis project. I am fortunate to have the most constructive and helpful dissertation committee. Despite being well-established and constantly busy, they are extremely humble and have always taken the time to answer even minor queries. Their insightful questions and comments on my thesis project helped me broaden my horizons, think more critically and develop my scientific acumen.

I want to thank each past and current member of the Wallace laboratory for their help and support. Special thanks to Dr. Stephen Parnell and Gail Reif, who trained me, and helped me

also like to thank the KUMC Biomedical Research Training Program (BRTP) program for providing financial support for my research project from 2014-2016.

I cannot adequately express my depth of gratitude to Cynthia Duffer for providing me with a home away from home (with two adorable cats) and treating me like family. Special thanks to my ever-encouraging family of friends in Kansas City.

Lastly, I must thank two very important people, my best friends and my partners in crime, Ashwin Kumar, and Aarthi Gopal. Thank you for always being there with me through all the ups and downs. I have bored you with so many stories about my project, knowing full well that you are not biologists. Thanks to technology, I have never felt closer to two people, who were physically so far away. Thanks for your inundating support and for always cheering me up.

TABLE OF CONTENTS

LIST OF FIGURES

LIST OF TABLES

LIST OF ABBREVIATIONS

cAMP: 3', 5' cyclic adenosine monophosphate

AC: adenylyl cyclase

ANOVA: analysis of variance

AQP-2: aquaporin-2

ATP: adenosine triphosphate

AVP: arginine vasopressin

ADPKD: autosomal dominant polycystic kidney disease

ARPKD: autosomal Recessive polycystic kidney disease

BUN: blood urea nitrogen

BW: body weight

CTR: carboxyl-terminal domain

Cl: chloride

CKD: chronic kidney disease

CD: collecting duct

CFTR: cystic fibrosis transmembrane conductance regulator

DMEM/F12: Equal mixture of Dulbecco's modified Eagle's medium and Ham's F-12 medium

ER: endoplasmic reticulum

ESRD: end-stage renal disease

EGF: epidermal growth factor

EGFR/ Erb-1: Epidermal growth factor receptor

ECM: extracellular matrix

ERK: extracellular signal-regulated kinase

FAK: focal adhesion kinase

FBS: fetal bovine serum

GSK3β: Glycogen synthase kinase 3 beta=

HGF: hepatocyte growth factor

ILK: integrin-linked kinase

IPP: ILK-PINCH-Parvin

KW: kidney weight KW

KW/ (%BW): kidney weight as a percent of body weight

mTOR: mammalian target of rapamycin

MMP: matrix metalloproteinase

NPHP3: nephronophthisis type 3

NHK: normal human kidney

S6K: p70 - S6 kinase

Pcy: *pcy/pcy* mice

PTEN: phosphatase and tensin homolog on chromosome 10

PIP3: phosphatidylinositol (3)-triphosphate

PDE: phosphodiesterase

PI3K: phosphoinositide 3-kinase

P-S6: phosphorylated S6

PKD: polycystic kidney disease

PC1: polycystin-1

PC2: polycystin-2

PN: postnatal day

RTK: receptor tyrosine kinase

SE: standard error

TGFβ: transforming growth factor beta

βig-H3: TGFβ -induced gene clone 3

TSC: tuberous sclerosis complex

V2R: vasopressin V2 receptors

CHAPTER 1. PATHOPHYSIOLOGY OF AUTOSOMAL DOMINANT POLYCYSTIC KIDNEY DISEASE

1.1. Polycystic Kidney Disease

"Though of simple design, epithelial cysts are, arguably, the most important multicellular biological structures in medicine. Every one of us was once a cyst – a blastocyst" - Jared. J. Grantham [13].

Polycystic kidney disease (PKD) is a genetic disorder characterized by a persistent growth of fluid-filled cysts in the kidney leading to massive enlargement, often culminating in end-stage renal disease (ESRD) [13]. A normal adult kidney weighs less than one-third of a pound; by contrast, PKD kidneys can weigh over 25 lbs. (**Figure 1**). There is a wide variability in the onset, progression, and severity among individuals affected by PKD. There are two PKD subtypes based on genetic inheritance: autosomal dominant PKD (ADPKD) and autosomal recessive PKD (ARPKD).

ADPKD is the more prevalent, slowly progressive form of PKD and is caused by mutations in *PKD1* and *PKD2* encoding for polycystin-1 (PC1) and polycystin-2 (PC2) [14, 15]. ARPKD is the more severe, early-onset form of PKD and is associated with mutations in *PKHD1*, which encodes the protein fibrocystin/polyductin [16-19], causing dysregulation in cellular proliferation and differentiation.

A

B
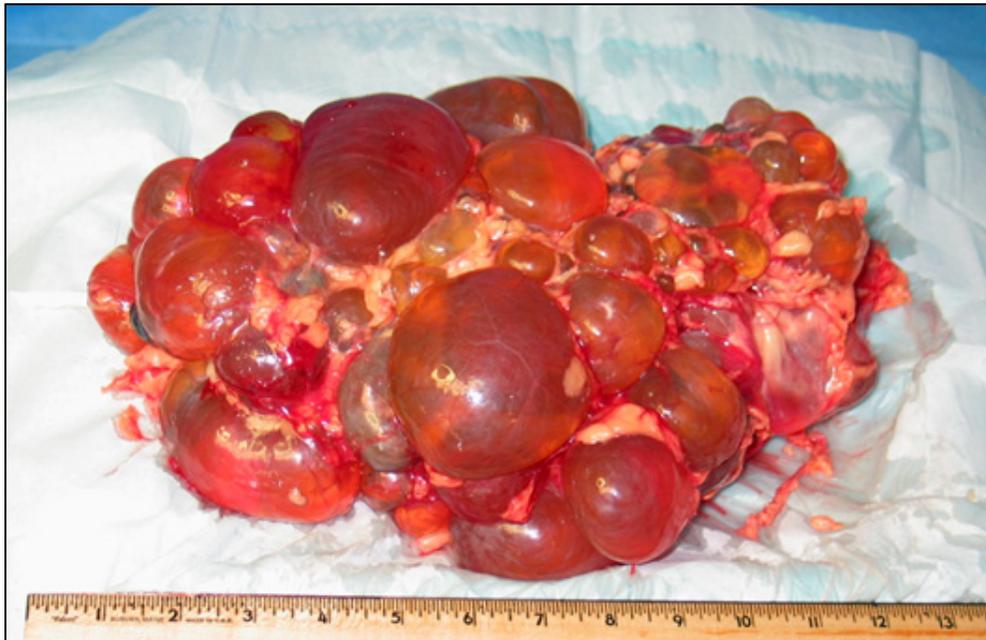
Figure 1-1. Images of normal and ADPKD kidneys. (A) A normal human kidney is typically the size of a human fist. (B) By contrast, an ADPKD kidney is the size of a football. Picture courtesy of PKD Biomarkers and Biomaterials Core in the Jared Grantham Kidney Institute at the University of Kansas Medical Center.

1.2. Autosomal Dominant Polycystic Kidney Disease (ADPKD)

ADPKD is the most prevalent monogenic disorder that affects around 12.5 million people worldwide [20]. It occurs more commonly than sickle cell anemia, cystic fibrosis, Huntington's disease and muscular dystrophy combined. Cysts arise from all segments of the nephron but are predominantly derived from the collecting ducts (CDs) [21]. The cysts appear to be benign neoplasms that arise due to epithelial cell proliferation and fluid secretion, leading to massive enlargement of the kidneys to about 4-8 times the normal size [1, 22]. Growth of the cysts causes damage to the neighboring tubules, impeding renal function [7]. Expanding cysts are associated with a thickened tubular basement membrane due to excessive deposition of extracellular matrix (ECM), replacing normal parenchyma with fibrosis, leading to renal insufficiency [23]. While cyst formation begins in utero, ADPKD is typically slowly progressive with many patients remaining asymptomatic for the first 25 years. Approximately 50% of the patients progress to ESRD by 60 years of age [24]. ADPKD is a systemic disorder - vascular abnormalities and cysts in the liver, pancreas, seminal vesicles and arachnoid membrane, are associated complications of ADPKD. Hypertension is a key symptom and complication of ADPKD and may precede the clinical disease manifestations. Patients suffer from reduced quality of life due to flank pain, nephrolithiasis and cyst-related complications of the kidney including infections, hemorrhage, and hematuria.

PKD1 mutations account for 85% of the reported cases and patients progress towards ESRD by 58 years of age. Within the *PKD1* mutations cohort, individuals with truncating mutations are affected more severely, progressing towards ESRD by ~55 years, compared to patients with non-truncating mutations with a median age at ESRD onset of 67 years. *PKD2* mutations account for most of the remaining 15% of the ADPKD patients. Although individuals

with *PKD2* mutations show similar systemic manifestations as seen with *PKD1* mutations, the onset and disease progression is slower, and patients have longer renal survival rates (typical age of ESRD onset is ~79 years) and have fewer complications [25, 26]. ADPKD accounts for 6-10% of the ESRD patients receiving renal replacement therapies. Based on a study performed between 2007 -2009, total health care costs for ADPKD patients were estimated to be more than USD $2 Billion per year in the US, averaging about USD $51,048 per patient/year [27].

Currently, there is no FDA approved treatment for ADPKD. The slowly progressive nature of the disease necessitates the use of long-term therapeutic interventions and hence potential treatment options need to be safe with minimal side effects.

1.3. Genetics of ADPKD

*PKD*1 has 46 exons with a long coding sequence of 12,912 bp (NM_001009944.2) and is located on chromosome 16p13.3. The region spanning exons 1 to 33 is duplicated, generating six pseudogenes that are located on the same chromosome [15, 28, 29]. Additionally, *PKD1* has a high GC content. These complexities necessitate long-range PCRs followed by nested PCRs to analyze specific mutations, making the process time-consuming and technically demanding. Despite this, a staggering 868 pathogenic *PKD1* mutations, mostly from unique pedigrees, and registered in the ADPKD mutation database (http://pkdb.mayo.edu; as of March 2017). *PKD2* is located on chromosome 4q21 [14] and is composed of 15 exons with a coding sequence of 2,907 bp (NM_000297.3). 162 *PKD2* pathogenic mutations have been identified. All the cells in an ADPKD patient harbor the heterozygous PKD mutation; however, cysts arise only from a few nephrons, suggesting that a second hit is necessary to initiate cyst formation in the kidney [21]. Qian *et al.* [30] isolated human cystic epithelial cells and showed that they harbored a somatic

mutation in the other PKD allele, consistent with the concept of a second hit. Supporting this observation, mice carrying a hypermutable *Pkd2* allele develop cystic disease due to loss of function [31]. More recently, mice with hypomorphic *Pkd1* alleles and reduced expression of normal PC1 (15–20%) also developed cystic disease [32, 33], demonstrating that a somatic mutation is not required for cyst initiation. The presence of incompletely penetrant, hypomorphic *PKD1* alleles (*PKD1p.R3277C*) causes a folding/trafficking defect lowering PC1 expression, and initiates cyst formation in humans and mice, demonstrating that a reduction in the expression of the polycystins below a certain threshold is sufficient to induce the cystogenic pathway (**Figure 1-2**). The presence of homozygous hypomorphic *PKD1* alleles resulted in a moderate to severe ADPKD phenotype in humans and mice [34, 35]. Patients that harbored a hypomorphic mutation in trans with an inactivating *PKD1* allele displayed ARPKD like phenotype with aggressive and early cystic disease [36]. Thus, the 'dosage' of polycystin appears to be critical for the onset and severity of the cystic phenotype. Further, the initiation and progression of the cystic disease is vastly affected by the timing at which polycystin expression/function is reduced/lost. In an elegant study, Piontek *et al.* [37] showed that inactivation of the *Pkd1* gene within the postnatal day (PN) 13, induced rapid and aggressive cystic disease. By contrast, *Pkd1* knockout after this time point resulted in delayed cyst formation and slowly progressive disease. It appears that developmental and proliferative genes dramatically change before and after this window of time, and the expression of polycystins may be critical at this stage. Further, the timing of polycystin loss could be influenced by genetic modifiers, and environmental factors, thus governing the course of cyst development. Thus, the threshold expression of the polycystins and the timing at which their reduction/loss occurs influences cyst formation and disease progression in ADPKD patients.
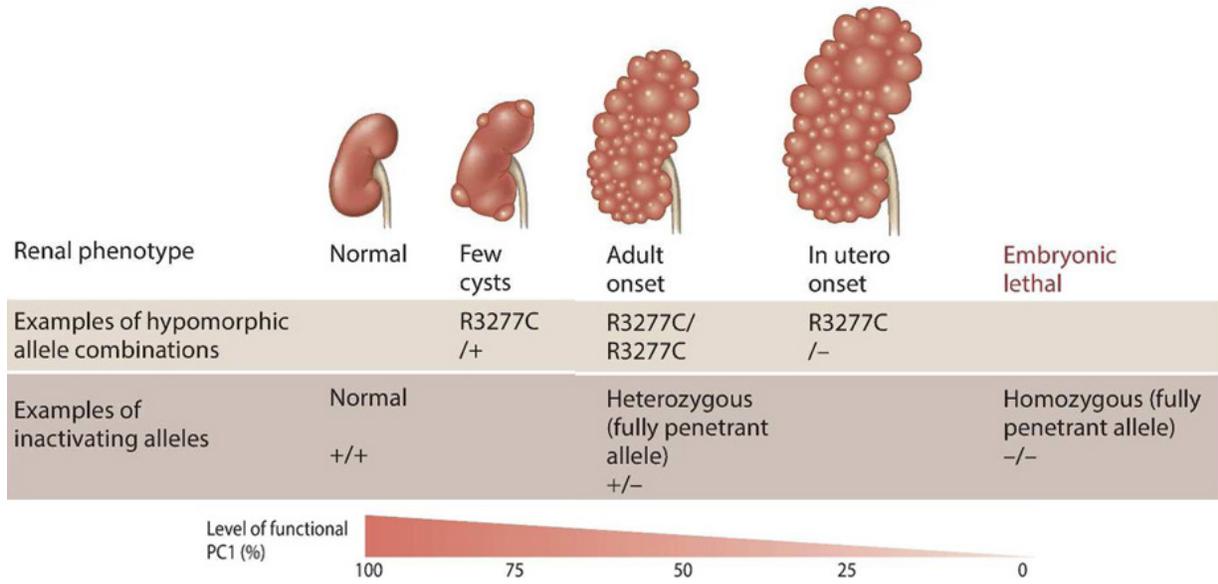
Figure 1-2. Polycystin gene dosage influences the cystic phenotype. PC1 levels (bottom) appears to directly influence cystogenesis. A ~50% reduction in PC1 expression, with 2 incompletely penetrant alleles (*R3277C*), is associated with adult onset disease. Inheriting an incompletely penetrant *PKD1* allele, in trans with an inactivating *PKD1* mutation, leads to more aggressive cystic disease. Adapted from reference [3].

1.4. The Polycystins

PC1 is an integral membrane protein that is thought to interact with PC2, a Ca^{2+} permeable cation channel, and regulate its activity (**Figure 1-3**). It has a large extracellular N-terminal region of about 3000 amino acids, containing unique domains and motifs, eleven transmembrane domains, and a small C-terminal cytosolic tail [3, 15, 29, 38]. The extracellular region contains 1) a signal peptide, 2) two leucine-rich repeats (LRR), thought to be involved in cell adhesion, 3) a WSC domain responsible for interaction with carbohydrates, 4) a type-C lectin motif, likely to participate in cellular signaling and exocytosis, 5) an LDL-A domain, 6) a PKD domain with 16 immunoglobulin-like repeats which is thought to make the extracellular tail highly extensible, suggesting that PC1 may be involved in mechanical coupling of cells, 7) a region homologous to the sea urchin receptor for egg jelly (REJ) that extends over 1000 amino acids, potentially involved in ion transport, and 8) the GAIN (G protein-coupled receptor-autoproteolysis inducing) regulatory domain that contains a G protein–coupled receptor proteolysis site (GPS) motif [39-41]. GPS-cleavage of PC1 generates an N-terminus and C-terminus product (composed of the TM domains and the C-terminal tail), which may remain non-covalently bound to each other [42]. Missense mutations in the GPS domain that prevent the cleavage event have been reported in human ADPKD. GPS cleavage of PC1 is not seen in all cell types, and both the cleaved and uncleaved forms coexist in the cells; however, *PKD1*-GPS cleavage mutant mice develop an aggressive postnatal cystic disease suggesting that the loss of cleaved PC1 promotes cyst formation [43]. Between the transmembrane domains, there is a highly-conserved lipoxygenase α-toxin (PLAT) domain which appears to be involved in lipid/protein binding potentially integrating PC1 signaling and trafficking [44, 45]. PC1 shares many conserved motifs with the egg jelly receptors, including the PKD repeats, GPS, REJ, C-type lectin, PLAT

and the transmembrane domains, suggesting that PC1 could be a cell surface receptor [46]. The C-terminal tail of PC1 contains a coiled-coil (CC) domain that aids in interaction with PC2, and a domain for binding heterotrimeric G-proteins [38], that activates transcription factors such as nuclear factor of activated T-cells (NFAT) and AP-1, regulating signaling pathways including, mammalian target of rapamycin (mTOR), JNK, WNT, JAK/STAT, and intracellular calcium signaling [47-50]. In vitro, the C-terminal tail can be phosphorylated by PKA [51, 52], and could also interact with protein phosphatases, possibly altering the phosphorylation state of PC1, PC2 and other proteins [53]. Furthermore, it appears that proteolytic cleavage of the C-terminal tail can lead to its translocation to the nucleus, directly regulating gene expression [54].

PC2 shows high sequence homology to transient receptor potential (TRP) channel proteins and is also referred to as TRP2. Several groups have shown that it functions as a non-selective Ca^{2+} permeable channel [55-58]. PC2 also forms tetrameric structures with other TRP channels [59]. PC2 contains 1) 6 transmembrane helices that display high permeability to Ca^{2+} ions, a cytoplasmic C-terminal tail including 2) a G-protein activating peptide (GPAP), 3) an endoplasmic reticulum retention (ERR) signal, 4) a coil-coiled (CC2) domain that is thought to mediate its C-terminal oligomerization and bind to PC1 C-terminus [56], 5) a Ca^{2+} binding EF-hand domain that regulates Ca^{2+}-dependent interactions [60], and 6) the N-terminus, which is relatively small and faces the cytosol, in contrast to the N-terminus of PC1. Very recently, three groups have deciphered the cryo-EM structures of PC2 in different conformational states, and have shown that it can exist in single or multi-ionic states and can reciprocally regulate, as well as be regulated by Ca^{2+} binding [58, 61, 62]. The lipid composition at various PC2 localization sites may also potentially regulate its functional conformation states.

PC1 is expressed in most organs including the kidney, brain, liver, pancreas, heart, and lungs. It is localized in the focal adhesions, membrane junctions such as desmosomes, tight junctions, and adherens junctions, apical vesicles, primary cilia, endoplasmic reticulum (ER), and the urinary exosomes [3, 63-66]. Polycystin-2 predominantly localizes to the ER. Other sites of PC2 expression are the basolateral membranes, primary cilia, mitotic spindles, lamellipodia and the urinary exosomes. The differential localization of PC1 and PC2 suggest that they may also act independently. Although mutations in *PKD1* or *PKD2* causes low intracellular Ca^{2+}, the primary sites of the TRP2 channel activity and its regulation by PC1 remain unclear [1]. Considering the literature on the coupling and interaction of TRP channels in the plasma membrane and receptors like inositol-1,4,5 triphosphate (IP3) in the ER, it is possible that PC1 in the plasma membrane and PC2 in the ER may interact and capacitate calcium signaling [55, 67, 68]. Both PC1 and PC2 may localize to the primary cilium to maintain mechanosensation. However, it was recently shown that the cilia are not calcium-responsive mechanosensors [69]. It is possible that the polycystins can control flow-dependent cell volume regulation via the mTOR signaling pathway [70].
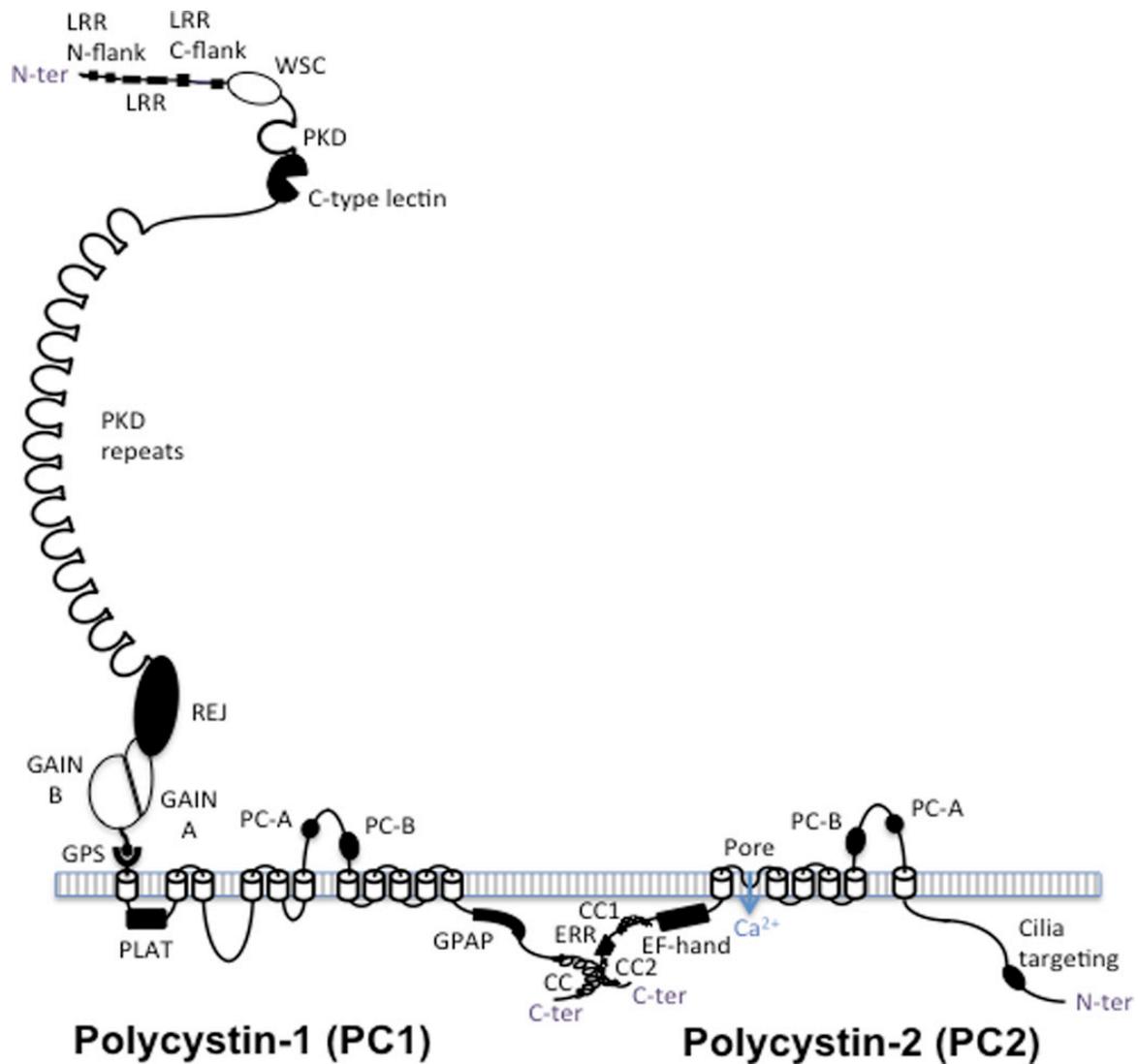
Figure 1-3. Proposed structures of PC1 and PC2. Reproduced with permission from reference [6]. PC1 has 11 transmembrane domains with a large N- terminal extracellular domain, and a short cytoplasmic C-terminal tail. The coiled coil (CC) domain in the C-terminal end of PC1 interacts with the C-terminal tail of PC2. PC2 has cytoplasmic N and C-terminus and 6 transmembrane domains.

1.5. Mechanisms of cyst formation

1.5.1. Role of cAMP

In ADPKD, cyst formation is characterized by abnormal cell proliferation and fluid secretion. The tubule epithelial cells relentlessly proliferate, stretching the tubule walls and accumulate the non-reabsorbed luminal fluid. These microcysts expand and eventually bud away from the parent tubule to become isolated cysts. The exact molecular mechanisms responsible for cyst formation remain unclear [71]. It appears that the dysregulation of the polycystin complex disrupts Ca^{2+} homeostasis, reducing intracellular Ca^{2+} levels. Primary ADPKD cells derived from human cyst epithelium have lower baseline Ca^{2+} compared to normal human kidney (NHK) cells [72]. Interestingly, there is elevated levels of the second messenger, 3', 5' cyclic adenosine monophosphate (cAMP) in cystic epithelial cells of PKD kidneys [73-75]. cAMP is anti-mitogenic to NHK cells; by contrast, cAMP increases ADPKD cell proliferation by phosphorylation of extracellular signal-regulated kinase (ERK), a mitogen-activated protein kinase (MAPK). The addition of a Ca^{2+} channel activator or a Ca^{2+} chelator prevented the cAMP-mediated proliferative response in ADPKD cells [72, 76, 77]. Further studies showed that in NHK cells, BRAF, a kinase that regulates MEK/ERK signaling, is repressed by a Ca^{2+}-dependent mechanism, preventing cAMP activation of the MEK/ERK pathway and cell proliferation. By contrast, in ADPKD, low intracellular Ca^{2+} relieves BRAF inhibition, allowing cAMP stimulation of the BRAF/MEK/ERK pathway and cell proliferation [78, 79](**Figure 1-4**).

cAMP also induces PKA phosphorylation of the cystic fibrosis transmembrane conductance regulator (CFTR), causing secretion of chloride (Cl) into the lumen leading to fluid accumulation in the cysts [1, 80, 81]. *Pkd* null embryonic kidneys showed cAMP-mediated formation of cyst-like tubule dilatations in organ culture; by contrast, *Cftr* and *Pkd* double knockout

embryonic kidneys did not form these cystic structures in the presence of cAMP [82]. Taken together, these results suggest that cAMP promotes ERK-mediated cell proliferation and Cl-dependent fluid secretion.

Arginine vasopressin (AVP) is a key cAMP agonist for the kidney. Binding of AVP to the vasopressin V2 receptors (V2R) on the renal CD cells causes increased cAMP and PKA-mediated phosphorylation of aquaporin-2 (AQP-2). This activated AQP-2 is inserted into the apical membrane, leading to increased water reabsorption and a concentrated urine. Upon hydration, plasma AVP levels drop resulting in a diluted urine. ADPKD patients have elevated V2R and circulating AVP, yet many patients have a compromised concentrating capacity, likely due to the disruption of the renal architecture [74, 75, 83]. Gattone and colleagues [75, 83, 84] reasoned that V2 receptor inhibition would decrease cAMP-mediated cyst growth in PKD. They administered OPC-31260, a V2R inhibitor, to 1) *cpk/cpk* mice, an aggressive model of recessive PKD, 2) *pcy/pcy* mice, a slowly progressive model of PKD, 3) PCK rats, an orthologous model of ARPKD and 4) *Pkd2^{WS25/-}* mice, a slowly progressive orthologous model of ADPKD. Inhibition of V2R dramatically slowed cyst growth and preserved renal function in all these models, suggesting that AVP is a key modulator of cAMP-mediated cyst growth. Further, in an elegant study, Nagao *et al.* [74] found that increased water intake in PCK rats also mirrored the effects of V2R inhibition and showed a marked reduction in cystic disease. Using a genetic approach, Torres and associates crossed the Battleboro rats, which lack AVP, to the PCK rats [85] to show that AVP depletion reduces cystic disease similar to increased water intake. Further, administration of vasopressin analog (DDAVP) to the AVP depleted PCK rats, restored the cystic phenotype, highlighting that AVP and cAMP are key modulators of cystogenesis. OPC-41061 or tolvaptan, a highly selective potent V2R inhibitor, also shown to reduce PKD in animal

studies [86], was tested in a three-year double blinded, placebo-controlled clinical trial (TEMPO) for ADPKD. Although some patients were discontinued due to complications from aquaresis or elevated liver enzyme levels, the drug was found to reduce total renal volume and improve renal function [87].

The balance involved in cAMP production by adenylyl cyclases (ACs) and its degradation by phosphodiesterases (PDEs) can be perturbed by the low intracellular Ca^{2+} in ADPKD. Ca^{2+}-regulated ACs and PDEs can locally or globally alter cAMP. Earlier work from our lab showed that ADPKD cells have increased calcium-inhibited ACs 5/6; however, cAMP mediated cell proliferation appeared to be more dependent on the Ca^{2+}/calmodulin-stimulated AC3, suggesting that there was a change in the regulation of the AC isoforms [88]. Consistent with these findings, others have shown that conditional deletion of AC6 significantly reduces cystic disease [89]. Further, expression and activity of the PDE isoforms influence global and compartmentalized cAMP pools. We found altered regulation of the PDE isoforms in ADPKD [90]. The expression of PDE3 and PDE4 were reduced in ADPKD cells, compared to NHK cells. PDE4 was involved in alterations in global intracellular cAMP and chloride secretion, whereas, the Ca^{2+}/calmodulin-regulated PDE1 was specifically affected AVP-induced activation of the BRAF/MEK/ERK pathway and ADPKD cell proliferation. Consistent with these findings, knockout of *Pde1a*, *Pde1c*, or *Pde3a* accelerated PKD progression in *Pkd2* mutant mice. Furthermore, Glycogen synthase kinase 3 beta (GSK3β), a serine-threonine kinase, can promote cAMP production by modulating AC activity, and there is an abnormal expression of GSK3β in ADPKD, which promotes cAMP-mediated cyst expansion. Recently, it has been shown that cAMP can also regulate GSK3β expression, thereby resulting in a feed-forward mechanism in ADPKD [91-93].
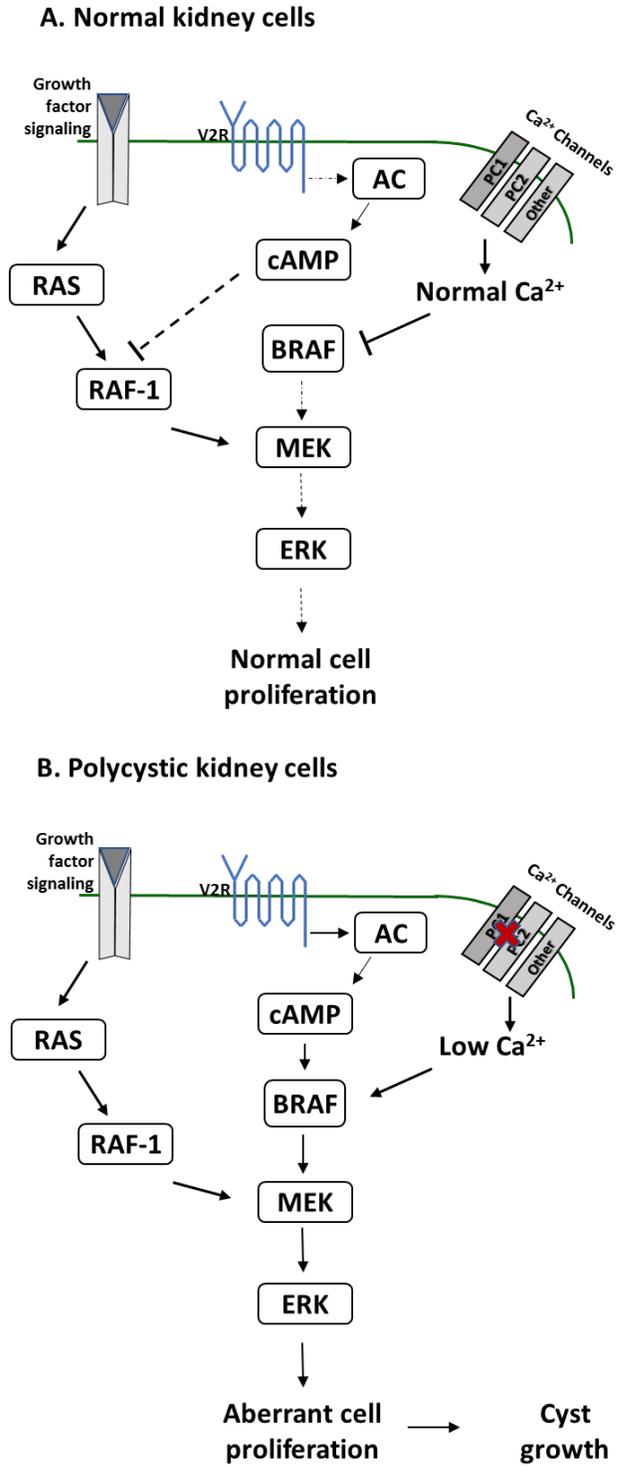
Figure 1-4. Proposed mechanism for cAMP-mediated cell proliferation. Redrawn from reference [1]. (A) cAMP inhibits ERK and proliferation of normal human kidney cells. In normal cells, BRAF is repressed by a Ca^{2+}-dependent mechanism, preventing cAMP activation of ERK B) By contrast, cAMP agonists, stimulate the MEK/ERK pathway and proliferation of ADPKD cells. Mutations in the PKD genes reduce intracellular Ca^{2+} de-repressing BRAF, resulting in cAMP-dependent cell proliferation and cyst growth.

1.5.2. Role of growth factor signaling

Epidermal growth factor receptor (EGFR; Erb-1) and Erb-B2, belong to the receptor tyrosine kinase (RTK) family and are aberrantly expressed in PKD. They bind to the epidermal growth factor (EGF) and stimulate cell proliferation via the MEK/ERK pathway. Although renal EGF expression is downregulated in some animal models of PKD, mitogenic concentrations of EGF-like peptides have been identified in cyst fluids from human ADPKD, ARPKD and rodent PKD [94, 95]. Inhibition of EGFR and Erb- B2 activity appears to reduce cystic disease in several rodent models of PKD [96-99]. ERK inhibition also slowed cystic disease progression in *pcy/pcy* mice; however, MEK inhibition did not affect cyst growth in an aggressive model of cystic disease [100, 101]. Interestingly, inhibition of Src, a tyrosine protein kinase downstream of RTKs, reduces cystic disease in *bpk* mice and PCK rats. Effects of long-term inhibition of RTK signaling remains to be determined.

1.5.3. Role of mTOR in ADPKD

The mammalian target of rapamycin (mTOR) complex regulates cell proliferation, cell growth, and protein translation by phosphorylating 4E-BP1 and the p70 - S6 kinase (S6K), regulators of translation initiation and ribosomal function.

The tuberous sclerosis complex (TSC) proteins hamartin and tuberin (encoded by *TSC1* and *TSC2*, respectively), regulate mTOR activity. The *TSC* genes themselves appear to be important cystogenic modifiers of ADPKD. *TSC2* and *PKD1* lie in a tail-to-tail orientation [102] in the human genome. Tuberous sclerosis is associated with renal lesions, and epithelial cysts and some TSC patients who have ADPKD are thought to have a contiguous gene syndrome due to

loss of expression of *TSC2* and *PKD1* [103]. In rodents, inactivation of *TSC1* or *TSC2* leads to renal cysts potentially through downregulation of PC1 expression [104, 105]. At the protein level, tuberin functions as a GTPase activating protein (GAP), and hamartin binding regulates its GAP activity. Tuberin maintains Rheb, a GTP-binding protein in its inactive state. Inactivation of the tuberin/hamartin complex by mechanisms including AKT or ERK-mediated phosphorylation of tuberin releases Rheb which in turn activates mTOR [106].

PC1 appears to bring tuberin and mTOR proximal to each other by forming a complex, hence inhibiting mTOR, and functional loss of the polycystins leads to aberrant activation of the Akt/mTOR signaling pathway [48, 107-109]. Inhibition of mTOR using rapamycin or its derivatives reduces cystic disease and fibrosis in several murine models of PKD, suggesting that mTOR activation is a common phenomenon in renal cystic diseases [4, 109-113]. While clinical trials for mTOR inhibitors in PKD did not yield promising results, limiting factors including the use of suboptimal doses, recruitment of patients who had already progressed to stage III chronic kidney disease (CKD), and discounting the effects of reduction in total kidney volume, may have affected the outcomes [114].

1.6. Futile repair in PKD

Many developmental genes and signaling pathways are aberrantly regulated in PKD, and cystic epithelial cells are thought to be incompletely differentiated [115, 116]. In a detailed review, Tran *et al.* [117] proposed that dysregulation of developmental pathways including the Hedgehog, Wnt and Notch pathways may play a key role in renal cystogenesis. Song *et al.* performed a genome-wide expression analysis to study the genes and pathways differentially regulated in human ADPKD [118]. They found that several genes involved in epithelial differentiation, integrin-

ECM signaling, growth factor-induced proliferation, fibrosis, and inflammation, were altered in ADPKD. Weimbs and colleagues [106, 119, 120] postulated that mutations in the polycystins might initiate uncontrolled activation of renal repair pathways, including mTOR, that promote cell de-differentiation, cytoskeletal reorganization and proliferation, hallmarks of cystic disease. Interestingly, several independent groups showed that an external renal injury accelerates cystic disease progression in slowly progressive murine models of PKD [121-125]. Thus, the loss of polycystin function perhaps predisposes the cells to form cysts when presented with an insult or a mitogenic modifier. Additionally, the process of cyst expansion along with inflammation and fibrosis may compress the neighboring nephrons, activating repair programs that could initiate additional cyst formation. Identifying and targeting such maladaptive repair pathways can lead to potential therapeutic avenues.

CHAPTER 2. ECM-INTEGRIN SIGNALING

2.1. The extracellular matrix dynamics during repair and disease

The extracellular matrix (ECM) was originally conceptualized as a structural scaffold for the cells that provides tissue integrity. Recently, the ECM has been recognized as a dynamic structure that undergoes constant remodeling to maintain tissue homeostasis [126]. The ECM is an elaborate and complex assembly of 1) fibrous structural proteins, including collagens, laminins and fibronectins, 2) specialized proteins such as growth factors, matricellular proteins, and 3) proteoglycans, which interact with the cell surface receptors and integrins. The composition of the ECM is also highly dynamic and depends on the localization and state of the tissue or cell type. It undergoes rapid remodeling during tissue development and repair in response to external stimuli that are transmitted to the cell through integrins, syndecans, and laminin receptors, and other receptors located on the plasma membrane [127]. The ECM is an important part of wound healing [128]; however, excessive matrix deposition leads to fibrosis, a common feature of chronic kidney disease [129]. ECM components also undergo proteolytic cleavage during remodeling by proteinases including matrix metalloproteinases (MMPs), and other serine and cysteine proteases. They cleave structural molecules, release small peptides and growth factors, and can directly affect degradation of matrix proteins. Unchecked MMP activity is also noted during injury and fibrosis.

Matricellular proteins represent a family of soluble ECM molecules that regulate collagen fibrillogenesis and bind to heterodimeric integrin receptors, facilitating communication between the cell and the ECM [130, 131]. Integrin engagement leads to the formation of cellular focal adhesion junctions, characterized by the aggregation of cytoskeletal proteins including focal adhesion kinase (FAK), integrin-linked kinase (ILK), and paxillin, activating pathways involved

in cell adhesion, migration, and proliferation. Thus, ECM proteins regulate intracellular dynamics, a process called "outside-in signaling" [132-134]. Persistent expression of these proteins is associated with chronic inflammation and tissue fibrosis [8, 23, 135-138].

2.2. Dysregulation of ECM signaling in PKD

The concept of altered ECM signaling in PKD arose from earlier observations that the basement membranes of the cysts appeared thickened and abnormal[139-141]. Since then, aberrant expression of ECM molecules and integrin receptors have been reported in several human and rodent models of PKD[2, 142, 143]. While the *PKD* genes could themselves cause dysregulated ECM production [144], increasing literature suggests that abnormalities in the matrix are not seen before cyst initiation, rather, they may arise due to factors produced by the cysts (**Figure 2-1**) [2, 7, 23, 116]. Thickening of the tubular basement membrane due to deposition of ECM, and increased accumulation of fibroblasts and inflammatory cells in the interstitium are the forerunners of fibrosis in ADPKD. Indeed, fibrosis causes loss of functional renal parenchyma and leads to end stage renal disease (ESRD). Currently, the molecular mechanisms leading to aberrant ECM signaling and its role in PKD progression remain unclear.

Among factors that govern ECM composition and turnover, MMPs appear to be dysregulated in PKD. The expression of *MMP2* was decreased in the Han:SPRD Cy/+ rat, a nonorthologous model of ADPKD [145]. By contrast, *MMP14* was found to be upregulated in the cyst-lining epithelia. Batimastat, an MMP inhibitor, reduced cystic disease progression in this rat model[146]. Murine PKD kidneys showed increased expression of MMPs[147, 148]. Consistent with these observations, serum samples from human PKD patients also showed elevated MMPs [149, 150]. It is speculated that breakdown of matrix molecules can induce an immune response. For

instance, breakdown of collagen I into a proline-glycine-proline (PGP) fragment, is thought to drive the progression of chronic obstructive pulmonary disease [151]. In sum, these data suggest that matrix-degrading proteases may contribute to PKD progression, although their functional relevance remains to be determined.

Several integrins, including α_V, α_8, β_1, and β_4, are aberrantly expressed by cyst-lining cells in PKD [2, 143, 152-154] and deletion of β_1- integrin prevented cystogenesis in a *Pkd1* mutant mouse model [154]. We and others have shown that abnormal and extensive expression of ECM molecules, including laminins, collagens, and matricellular proteins, accelerate cyst growth through activation of integrin signaling [2, 23, 118, 143, 155]. Laminin-332 (α_3, β_3, γ_2), also called laminin-5, has been shown to be abnormally expressed in PKD and contributes to cell adhesion and cyst epithelial cell proliferation [143, 155].
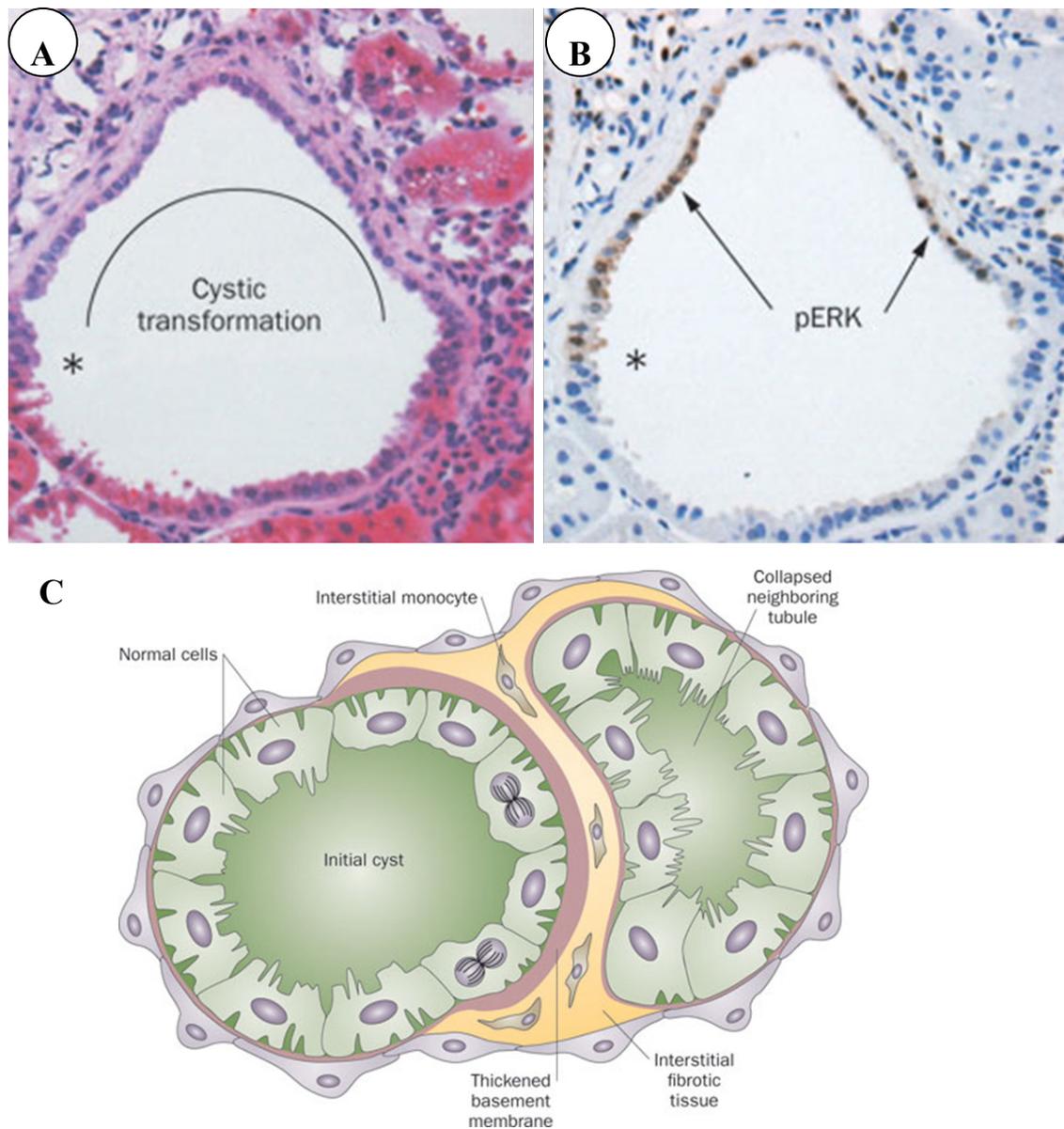
Figure 2-1. Factors affecting ADPKD progression. Reproduced with permission from reference [7]. (A) Hematoxylin and eosin stained section from Han:SPRD Cy/+ rat, showing the transition between a cyst and the neighboring tubules (asterisk). Thickened tubule basement membrane and ECM beneath the tubule, labeled as 'cystic transformation'. (B) Immunohistochemical staining shows that phosphorylated ERK (pERK; arrows) exclusively stains the cystic portion of the hemi-cyst. (C) An expanding cyst associated with thickened basement membrane material. Macrophages and fibroblasts, and ECM molecules appear in the interstitium subjacent to the evolving cystic portion.

2.3. Periostin - the multifaceted matricellular molecule

2.3.1. Structure of periostin and its functions in normal physiology and pathophysiology

Periostin, known originally as osteoblast-specific factor-2[156], was discovered and identified in a mouse osteoblast cell line. The protein was later renamed periostin because of its predominant expression in the periosteum and the periodontal ligament [157]. Human periostin is located on chromosome 13q, while murine periostin is located on chromosome 3[158]. It is a 90 kDa secreted glycoprotein (**Figure 2-2**) composed of 1) an amino-terminal secretory sequence, 2) an EMI domain, 3) four fasciclin1 (Fas1) domains with structural homology to the insect axon guidance protein fasciclin1 and the Drosophila adhesion protein Fas1, and 4) a carboxyl-terminal domain (CTR) [8]. Periostin also shares structural homology to a 68 kDa protein - transforming growth factor (TGF)-β-induced gene clone 3 (βig-H3) [159]. The EMI domain is cysteine-rich and is responsible for protein-protein interactions, enabling periostin to interact directly with proteins including βig-H3 [160], collagen type I [161] and fibronectin [162]. Fas1 domains 2 and 4, contain a central Asp-Ile amino acid dimer that appears to bind $\alpha_V\beta_3$, and $\alpha_V\beta_5$ integrin receptors. This binding motif is conformationally similar to the traditional integrin-binding RGD motif [163, 164]. Additionally, the Fas1 domains also bind to an array of cell adhesion proteins including tenascin-C and bone morphogenic protein-1 (BMP-1) [165]. These potential protein interactions involving periostin underline its importance as a cell adhesion and migration molecule. The CTR domain of periostin, containing exons 15-23, is the least conserved region across species and is the least studied. It contains a heparin binding site, several proteolytic cleavage sites that can give rise to different splice variants, and a puzzling nuclear localization signal, which is at odds with periostin being a secreted protein [166].

A

Periostin

EMI domain

CTR

Fas1 domains

Cleavage

B

Periostin | EMI | Fas1 | Fas1 | Fas1 | Fas1 | CTR
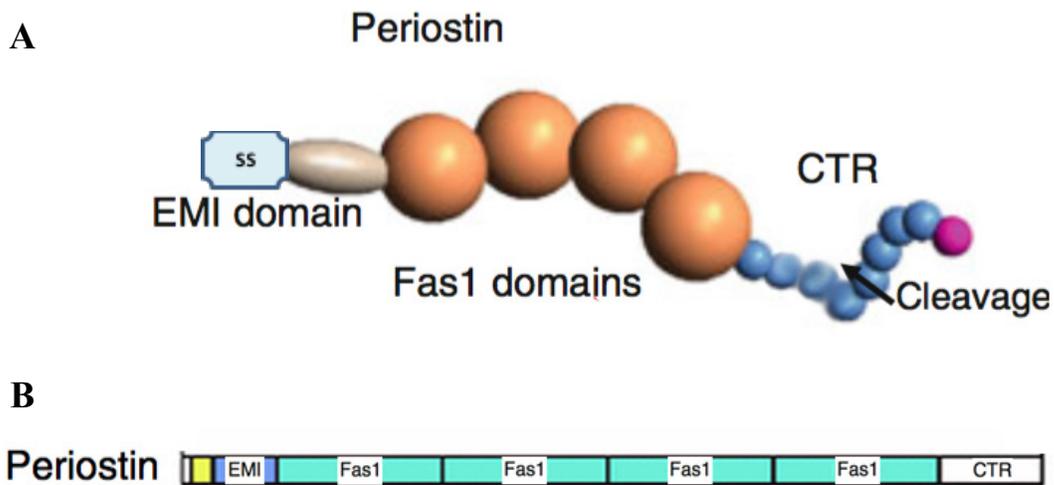
Figure 2-2. Key structural domains of periostin. Periostin is a 90 kDa secreted glycoprotein composed an amino-terminal secretory sequence (SS in A; yellow box in B), an EMI domain, four fasciclin1 (Fas1) domains, and a carboxyl-terminal domain (CTR) with several proteolytic cleavage sites that can give rise to different splice variants. Adapted from [8].

Periostin is expressed in tissues involved in mechanical stress, such as periodontal ligaments, periosteum, and cardiac valves; and is secreted into the ECM following acute injury to heart, skin and other tissues [157]. It directly interacts with components of the ECM, including collagen and fibronectin, and promotes collagen cross-linking through activation of lysyl oxidase[167, 168]. Periostin-induced fibrillogenesis is important to maintain tissue integrity [161]. In addition to modulating biomechanical properties of tissues, periostin binds αv-integrins on the cell surface and activates cellular pathways involved in 1) cell proliferation, 2) survival, 3) profibrotic TGF-β signaling, and 4) angiogenesis [2, 8, 137, 164, 169-171]. Application of periostin to cardiac tissue, following an infarction, stimulates proliferation of differentiated cardiomyocytes leading to myocardial repair [172, 173].

Global periostin knockout mouse (*Postn*$^{-/-}$) [174] was generated by inserting a *lacZ* reporter gene at the first exon site in the mouse periostin gene, and subsequent studies elucidated the role of periostin in development and disease [131, 135]. *Postn*$^{-/-}$ mice are viable and appear normal at birth. However, ~ 15% of the mice die before weaning age (2-3 weeks), potentially due to valvular insufficiency. Upon examination, valve leaflets of the *Postn*$^{-/-}$ mice displayed large acellular ECM deposits and ectopic smooth muscle cell clusters [174]. Norris *et al*. observed that adult *Postn*$^{-/-}$ mice had a reduction in skin thickness and tensile strength, potentially due to a reduction in crosslinking of type I collagen fibers in the skin [161]. These mice also exhibited mild growth retardation and early onset periodontal disease, coupled with incisor enamel defects [174]. A soft diet regime partially rescued the growth retardation in the *Postn*$^{-/-}$ mice by reducing the mechanical strain on the periodontal ligament. These observations suggest that periostin plays important roles in ECM maturation and organization.

Periostin is overexpressed in several cancers, including lung, ovarian, breast and colon, where it binds to α_V-integrins ($\alpha_V\beta3$, $\alpha_V\beta5$), stimulating Akt/mTOR, leading to increased cell proliferation, survival, and angiogenesis of the tumor [158, 164, 171, 175-178]. Serum periostin is also being considered as a potential biomarker for some cancers [179, 180]. Aberrant expression of periostin, perhaps due to inappropriate tissue adaption to injury, has pathological consequences in heart and other tissues, including tissue fibrosis [136, 181-183]. Matricellular proteins, such as periostin, and their cell signaling pathways are being considered as potential therapeutic targets to reduce fibrosis.

2.3.2. Role of Periostin in ADPKD

Periostin is normally expressed briefly within the nephrogenic zone during renal development; however, it does not appear to have a role in the adult kidney [2, 5, 184]. Previously, we showed that periostin was one of the most highly overexpressed genes (overexpressed 13.6-fold) in the ECM of ADPKD cells compared to normal human kidney (NHK) cells. Periostin is secreted by the ADPKD cyst-lining epithelial cells and accumulates within the extracellular space adjacent to the cysts and within cyst fluid (**Figure 2-3**). Periostin stimulates ADPKD cell proliferation, and cell-cycle analysis revealed that the percentage of cells in S and G_2/M phases were increased with periostin-treatment. However, this mitogenic effect of periostin was not observed in NHK cells, suggesting that periostin-induced proliferation was unique to cystic cells and that periostin does not induce cyst initiation, but rather promotes cyst progression. ADPKD cells have a 9-fold overexpression of α_V-integrins, receptors for periostin, compared to NHK cells [2]. This implies that the specific response to periostin by ADPKD cells can be attributed to the altered phenotype of the ADPKD cells, because of the abnormal expression of the integrins.

Recently, we showed that periostin was also overexpressed in autosomal recessive PKD (ARPKD) and several animal models of PKD, including *pcy/pcy* mice, *cpk/cpk* mice, *jck/jck* mice [5] and PCK rats (unpublished observation), suggesting that periostin expression is a general feature of PKD regardless of the underlying genetic mutation. Global knockout of periostin in *pcy/pcy* mice, a slowly progressive model of PKD, decreased kidney weight (KW) as a percent of body weight (%BW) (**Figure 2-4**) and interstitial fibrosis (**Figure 2-5**). There was also a decrease in renal mTOR activity, consistent with a reduction in the number of actively proliferating cells (not shown) [5]. Ablation of periostin also resulted in a significant improvement in the survival of *pcy/pcy* mice. These results highlight that periostin is an important mediator of cyst growth and fibrosis in PKD.
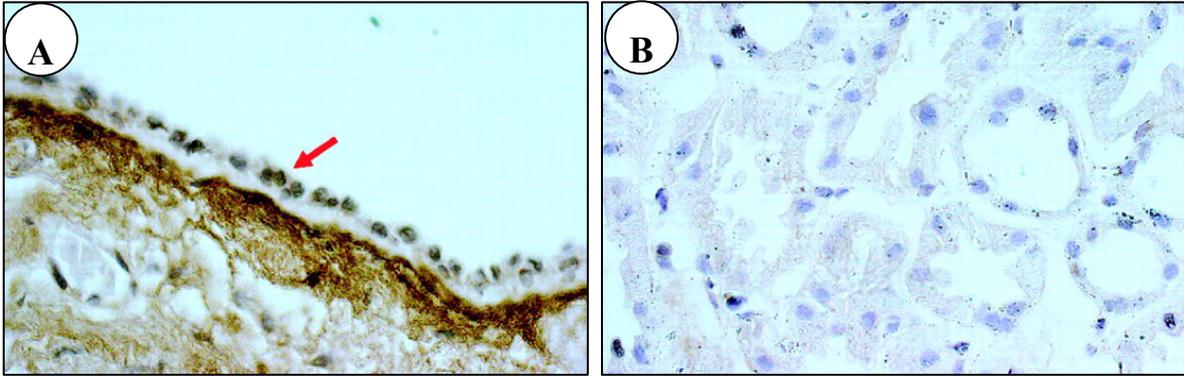
Figure 2-3. Periostin expression in ADPKD and NHK kidneys. (A) Representative section of a human ADPKD cyst displaying punctuate staining for periostin in mural epithelial cells (arrow) and robust staining in the extracellular matrix lining the basal surface of the cyst. By contrast, periostin was not detected in normal human kidney (NHK; B). Adapted from reference[2].
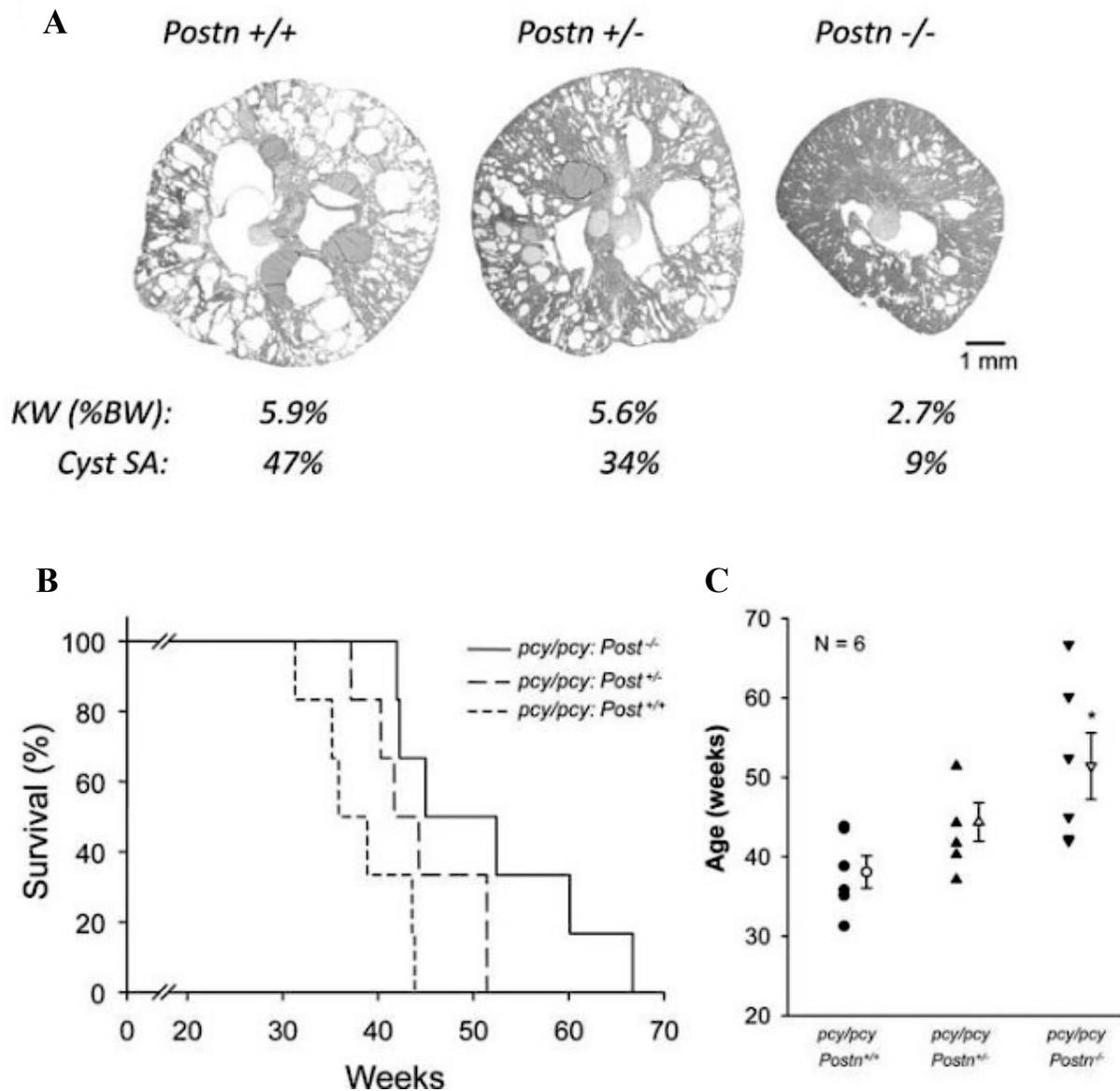
Figure 2-4. Periostin accelerates the progression of cystic disease in *pcy/pcy* mice. (A) Representative images of kidney sections, kidney weight (KW) as %BW, and % cystic area from *pcy/pcy;Postn*^{+/+}, *pcy/pcy;Postn*^{+/−} and *pcy/pcy;Postn*^{−/−} mice at 20 weeks of age. (b) Kaplan-Meier curve of *pcy/pcy;Postn*^{+/+}, *pcy/pcy;Postn*^{+/−} and *pcy/pcy;Postn*^{−/−} mice. (c) Summary of the age of death. pcy/pcy: Postn+/+ mice died at 38.1 ± 2.0 weeks. By contrast, *pcy/pcy* mice with the loss of one Postn allele (*pcy/pcy;Postn*^{+/−}) survived to 44.4 ± 2.4 weeks and *pcy/pcy* mice with a complete loss of periostin expression survived to 51.4 ± 4.2 weeks (*P < 0.05, compared to *pcy/pcy;Postn*^{+/+}). Reproduced with permission from reference [5].
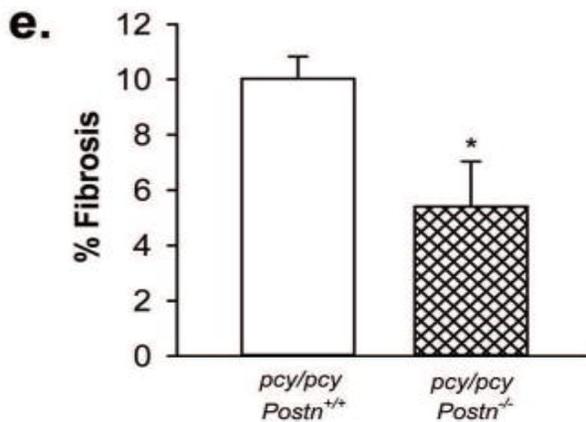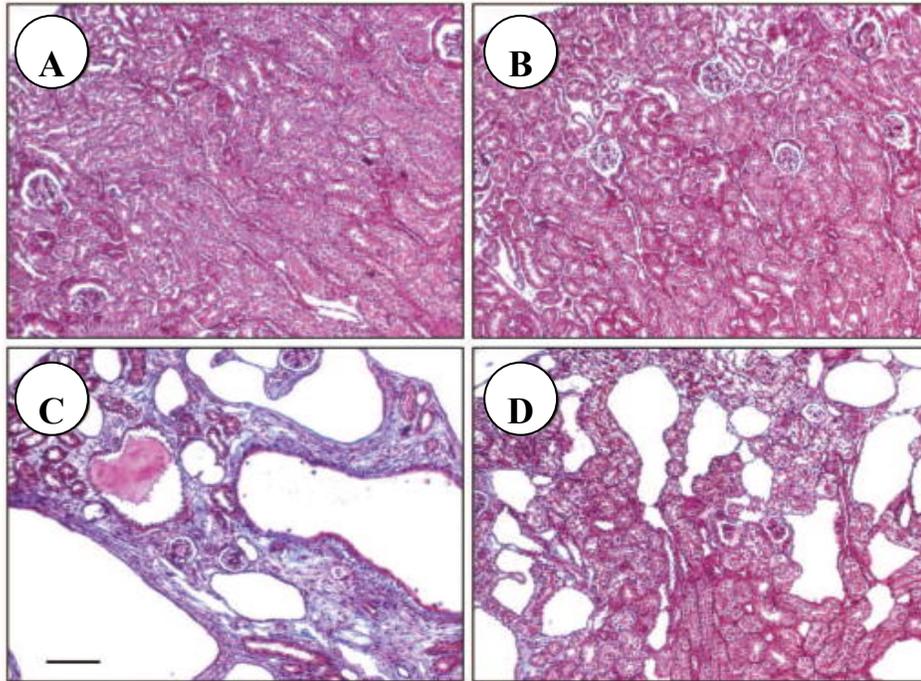
Figure 2-5. Periostin promotes renal interstitial fibrosis in *pcy/pcy* mice. Representative kidney sections from (A) *Postn*$^{+/+}$, (B) *Postn*$^{-/-}$, (C) *pcy/pcy: Postn*$^{+/+}$ and (D) *pcy/pcy: Postn*$^{-/-}$ mice were stained with Masson trichrome to visualize interstitial collagen (blue color). All images are the same magnification. Bar scale is 100 μm. (e) Fibrosis was determined by visual assessment of the trichrome-stained slides and represented as % fibrotic area to total area of the whole tissue section. (n = 6 per group) Data are means ± SE. Statistical analysis was determined by unpaired t-test. *P < 0.05, compared to *pcy/pcy: Postn*$^{+/+}$ kidney. Reproduced with permission from reference [5].

2.4. Integrin-linked kinase signaling

ILK was originally characterized as a serine/ threonine kinase that phosphorylates and interacts with β integrins and mediates integrin signaling. ILK is composed of an ankyrin domain, a pleckstrin homology-like motif (PH domain) and a catalytic C-terminal domain (**Figure 2-6**) [185, 186]. The PINCH scaffolding proteins bind to the ankyrin domain. The C-terminal domain of ILK harbors the integrin binding domain (for β1 and β3 integrin binding) [187] and an atypical kinase-like domain that also appears to bind α- parvin or β-parvin [188, 189]. The ILK-PINCH-Parvin (IPP) ternary complex is responsible for recruiting focal adhesions components that mediate cell migration via actin cytoskeleton remodeling [187]. Upon binding ILK, PINCH also associates with an adaptor molecule Nck2 to activate receptor tyrosine kinase (RTK) signaling [190-192]. The PH domain is activated by binding of phosphatidylinositol (3, 4, 5)-triphosphate (PIP3), the second messenger of phosphoinositide 3-kinase (PI3K) [193]. Further, the ankyrin domain also binds to the ILK-associated protein, ILKAP, a protein phosphatase which can inhibit ILK signaling [194].

In breast cancer, colon cancer, prostate cancer, malignant melanoma and non-small cell lung cancer, ILK activity is upregulated (in a PI3K dependent manner) and correlates with the stage and grade of cancer [195-198]. Phosphatase and tensin homolog on chromosome 10 (PTEN) is a tumor suppressor that is mutated at a high frequency in glioblastomas and is known to regulate the phosphatidylinositol-3'-kinase (PI3K), potentially repressing the ILK PH domain. Edwards *et al*. showed that ILK and Akt are aberrantly activated in human glioblastoma cells that harbor a loss-of-function PTEN mutation. Treatment of antisense oligonucleotides targeted against ILK reduces the growth of the tumors in mice with glioblastoma xenografts [199].

2.4.1. Arguments for and against ILK as a bona fide kinase

Several studies have indicated that ILK can directly phosphorylate proteins and substrates *in* vitro. In-gel kinase assays showed that purified ILK could phosphorylate Akt (serine 473) and other substrates such as myosin light chain 20 (MLC-20) and a GSK-3αβ/ crosstide peptide [200-202]. ILK lacks certain conserved residues typically found in catalytic kinase domains [203]. These finding led to a huge controversy in the field questioning if ILK is a bona fide kinase. Fukuda *et al*. resolved a high-resolution 3D structure of the catalytic domain of ILK fused to the C-terminal of α-parvin. This study revealed that the ILK catalytic domain shows characteristics of pseudokinase activity, including a non-hydrolyzed ATP in the crystal with an unusual ATP orientation, and an abnormal catalytic loop that lacked key catalytic residues [189]. However, the effect of α-parvin binding on the conformation of kinase domain was not considered. The same group also demonstrated using biochemical studies, that minute traces of heterogeneous components present in partially purified ILK could lead to false-positive results, compromising the validity of *in vitro* kinase assays [204]. In an elegant study, Lange *et al.* made knock-in mice harboring various mutations in the ILK domains and showed that both kinase-dead (S344A) and constitutively active (S344D) ILK knock-in mice develop normally, suggesting that the kinase activity may not be critical for normal physiological development and function [205]. Interestingly, they saw that mice that harbored a mutation in the α-parvin binding site (also required for ATP-binding), displayed renal agenesis. Taken together, it appears that the kinase and the scaffold functions of ILK may be interdependent. Resolution of the complete crystal structure of ILK will be required to answer this question.

2.4.2. ILK signaling in normal physiology and pathophysiology

Despite the debate on the kinase properties of ILK, it is widely accepted that ILK serves as a master regulator of cellular behavior and ECM signaling. The scaffold property of ILK is critical for the formation of a multi-protein complex with adaptor proteins PINCH and α/β-parvin: ILK-PINCH-Parvin (IPP) complex [190, 206]. The IPP ternary complex and plays a central role in ECM-integrin signaling [192, 207] and is responsible for binding β-integrins to the actin cytoskeleton and recruiting focal adhesion components that mediate cell proliferation, survival, and migration during tissue repair [187, 189]. IPP is critical for the phosphorylation of downstream molecules such as Akt and the mitogen-activated protein kinases [208-211]. Persistent ILK signaling to Akt and mTOR mediates carcinogenic cell proliferation. By contrast, in a mouse model of Duchenne muscular dystrophy, overexpression of α_7-integrin reduced the muscle pathology by upregulating ILK signaling to the Akt-mTOR pathway [212, 213]. In summary, ILK is an important physiological regulator of cellular homeostasis.

A

IPP complex

B
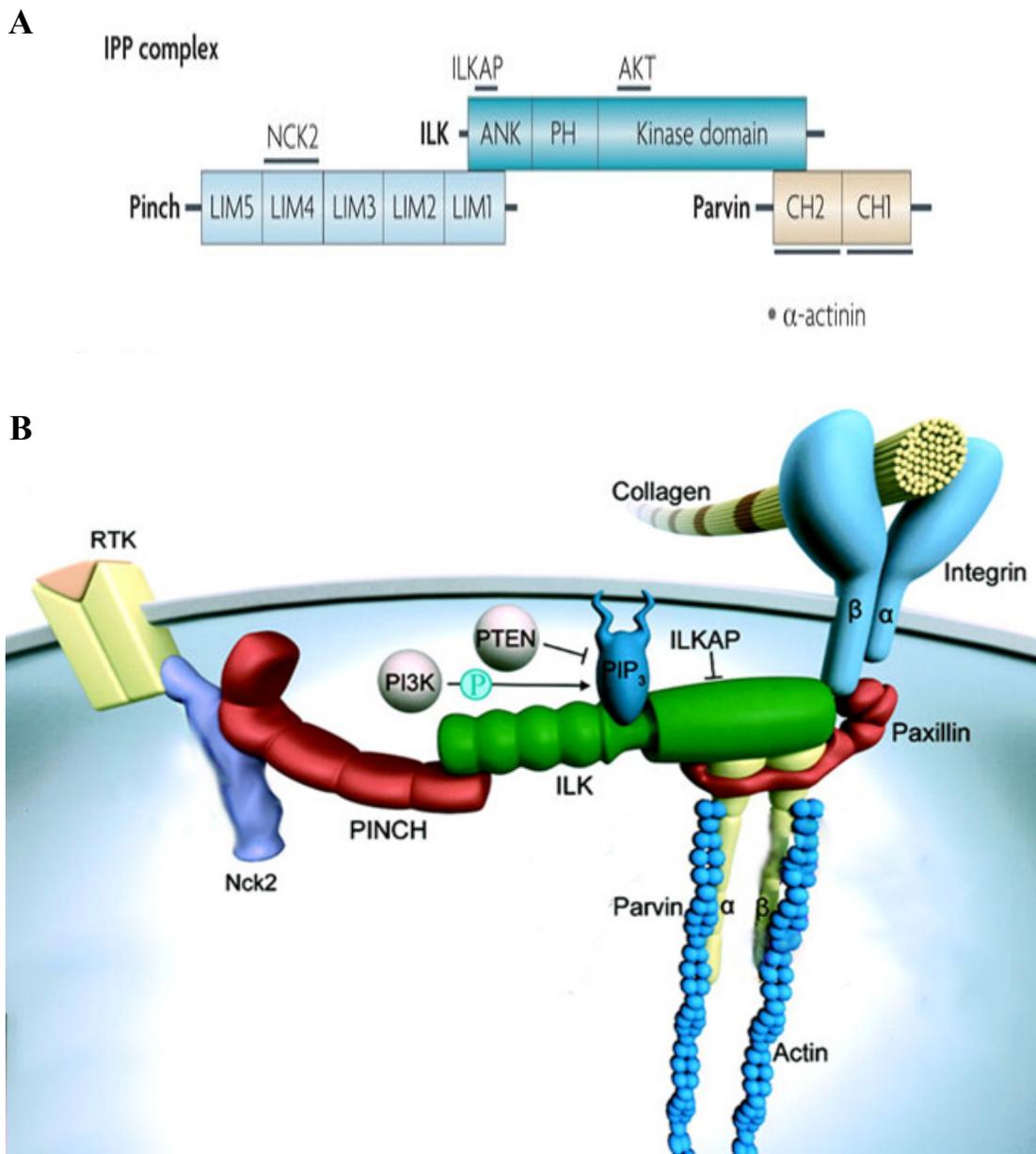
Figure 2-6. ILK structural domains and interactors. (A) ILK is composed of an ankyrin (ANK) domain, a pleckstrin homology-like motif (PH) and a catalytic C-terminal (kinase) domain. The ILK-PINCH-Parvin (IPP) ternary complex is responsible for recruiting focal adhesions components that mediate cell migration via actin cytoskeleton remodeling. Adapted from reference [9]. (B) IPP associates with Nck2 to activate receptor tyrosine kinase (RTK). Phosphoinositol (3, 4, 5)-triphosphate (PIP3) activates the kinase domain. PI3K activates PIP3 while PTEN inactivates it. Adapted from reference [12].

2.5. Specific Aims

ADPKD is the most commonly inherited renal disorder characterized by hyperplastic growth of renal epithelial cells that form fluid-filled cysts, leading to excessive kidney enlargement, interstitial fibrosis and progressive decline in renal function [13, 22, 214]. Despite recent advances in ADPKD, there remains a need for better understanding of the molecular mechanisms involved in cyst growth and fibrosis in order to develop targeted therapies. Periostin, a matricellular protein, is aberrantly expressed in human ADPKD, ARPKD and several animal models of renal cystic disease. Periostin binds components of the extracellular matrix (ECM) and promotes collagen fibrillogenesis, leading to fibrosis. It also binds cell surface integrins, leading to changes in cell adhesion, migration, proliferation, and survival. We found that periostin promotes the proliferation of human ADPKD cystic epithelial cells, but does not affect the proliferation of normal human kidney cells [2]. Global knockout of periostin in *pcy/pcy* mice, a slowly progressive model of PKD, caused a marked reduction in kidney volume, renal mTOR activity, number of proliferating cells, cystic area and renal interstitial fibrosis, and preserved renal function [5]. Loss of periostin also significantly extended the lifespan of the *pcy/pcy* mice demonstrating that periostin contributes importantly to the progression of renal cystic disease.

Currently, the cellular mechanism for periostin-induced cyst growth and fibrosis in ADPKD remains unclear. We propose that cyst-lining cells are involved in a futile repair mechanism causing persistent expression of periostin and activation of ILK signaling, leading to aberrant cell proliferation, cyst growth, interstitial fibrosis, and decline in renal function. Our long-term goals are to delineate the cellular and molecular mechanisms underlying the mitogenic and fibrotic effects of matricellular molecules including periostin, in renal cystic diseases.

Aim 1: To determine if knockdown of ILK in human ADPKD cells inhibits periostin-induced Akt/mTOR signaling and cell proliferation, and slows cyst growth and fibrosis in PKD mice (Chapter 3). We employed pharmacologic inhibition and shRNA knockdown of ILK in ADPKD cells to determine if the loss of ILK prevents periostin-induced activation of mTOR and cell proliferation. Next, we determined if knockdown/knockout of ILK in the collecting ducts (CDs), a predominant site for cyst formation, reduced cyst growth and fibrosis in two relevant murine models of PKD.

Aim 2: To determine if periostin promotes cytoskeletal remodeling, cell migration and ECM production by human ADPKD cells, and accelerates cyst growth and fibrosis in *PKD* mice (Chapter 4). We hypothesize that aberrant expression of periostin by cystic epithelial cells stimulates a futile repair mechanism that promotes cyst growth and fibrosis in PKD kidneys. We determined if periostin induced pathways involved in tissue repair, including cell proliferation, actin remodeling, ECM-integrin signaling, integrin clustering and the migration of human ADPKD cells. To examine the role of periostin in vivo, we generated periostin transgenic mice and determined if CD-specific overexpression of periostin accelerates cyst growth and fibrosis in *PKD* mice.

CHAPTER 3. INTEGRIN-LINKED KINASE SIGNALING PROMOTES CYST GROWTH AND FIBROSIS IN POLYCYSTIC KIDNEY DISEASE

3.1. Abstract

Autosomal dominant polycystic kidney disease (ADPKD) is characterized by innumerous fluid-filled cysts and progressive deterioration of renal function. Previously, we showed that periostin, a matricellular protein involved in tissue repair, is markedly overexpressed by cyst epithelial cells. Periostin promotes cell proliferation, cyst growth, interstitial fibrosis and the decline in renal function in PKD mice. Here, we show that the binding of periostin to α_V-integrins stimulates integrin-linked kinase (ILK), a scaffold protein that is essential for linking the extracellular matrix to the actin cytoskeleton, leading to activation of the Akt/mTOR pathway and proliferation of human ADPKD cells. Pharmacologic inhibition and shRNA knockdown of ILK prevented periostin-induced Akt/mTOR signaling and ADPKD cell proliferation. Homozygous deletion of ILK in renal collecting ducts (CD) of *Ilk$^{fl/fl}$;Pkhd1-Cre* mice caused tubule dilations, apoptosis, fibrosis, and organ failure by 10 weeks of age, confirming that ILK is critical for maintaining the CD epithelium and renal function. By contrast, *Ilk$^{fl/+}$;Pkhd1-Cre* mice had normal renal morphology and function and survived beyond one year. Reduced expression of ILK in *Pkd1$^{fl/fl}$;Pkhd1-Cre* mice, a rapidly progressive model of ADPKD, decreased renal Akt/mTOR activity, cell proliferation, cyst growth, and interstitial fibrosis, and significantly improved renal function and survival. In addition, CD-specific knockdown of ILK strikingly reduced renal cystic disease and fibrosis and extended the life of *pcy/pcy* mice, a slowly progressive PKD model. We conclude that ILK is a key intermediate for periostin activation of signaling pathways involved in cyst growth and fibrosis in PKD.

3.2. Introduction

Autosomal dominant polycystic kidney disease (ADPKD) is caused by mutations in *PKD1* or *PKD2*, which encode for polycystin-1 and 2, respectively [3]. The disorder is characterized by the formation of fluid-filled cysts, leading to loss of functional parenchyma, interstitial fibrosis, and enlarged kidneys. Several signaling pathways have been implicated in PKD [20]; however, the mechanisms involved in disease progression remain unclear. Cyst-lining cells are characterized as being incompletely differentiated and express factors involved in tissue repair [106, 115, 116, 119]. Tissue injury caused by compression of neighboring nephrons as cysts expand may activate repair mechanisms, including the stimulation of the Akt/mTOR pathway [106, 215, 216], contributing importantly to cyst growth [119, 120] and formation of new cysts.

We found that periostin, a matricellular protein involved in tissue repair, was highly overexpressed in ADPKD, autosomal recessive PKD (ARPKD) and rodent models of PKD, suggesting that periostin expression is a common feature of renal cystic disease [2]. Knockout of periostin reduced mTOR activity, cyst growth, and interstitial fibrosis, and significantly improved the survival of *pcy/pcy* mice [5].

$\alpha v \beta_3$-integrins, the receptors for periostin, promote proliferation of cancer cells [176] by activating integrin-linked kinase (ILK) [217] and stimulating downstream Akt/mTOR and GSK-3β/β-catenin signaling pathways [132, 218]. ILK interacts with β_1- integrin and was originally characterized as a kinase [132, 185, 188, 201, 219-221]. However, it remains unclear if ILK is a bona fide kinase since the kinase domain lacks conserved motifs found in conventional kinases and mutations that should render the kinase inactive failed to alter mouse development [187, 188, 204, 205]. Nevertheless, it is generally agreed that ILK serves as a scaffolding protein critical for the formation of a multi-protein complex with adaptor proteins PINCH and α-parvin [190, 206]. ILK-

PINCH-Parvin (IPP) signaling affects phosphorylation of downstream molecules such as Akt and the mitogen-activated protein kinases [208-211] and plays a central role in ECM-integrin signaling [192, 207]. The IPP ternary complex is responsible for binding β-integrins to the actin cytoskeleton and recruiting focal adhesion components that mediate cell proliferation, survival, and migration during tissue repair [187, 189]. ILK activation of Akt and mTOR mediates proliferation of cancer cells [212, 213]. In addition, PINCH interacts with adaptor protein NCK2, leading to crosstalk between the ILK and receptor tyrosine kinase (RTK) pathways [190-192].

We determined if ILK mediates periostin-induced ADPKD cell proliferation and if knocking down ILK in renal collecting ducts (CD) reduces cystic disease in two models of PKD. The results indicate that ILK is a key intermediate in the activation of cellular pathways involved in cyst growth. We propose that targeting the periostin-integrin-ILK axis may be a potential therapeutic approach to slow cyst growth and fibrosis in PKD.

3.3. Materials and Methods

Human ADPKD and normal human kidney cells. Primary cultures of ADPKD and normal human kidneys (NHK) cells were generated by the PKD Biomaterials and Biomarkers Core in the Kansas PKD Center at the Kansas University Medical Center (KUMC). ADPKD kidneys were obtained from the surgery department at KU hospital and other hospitals participating in the Polycystic Kidney Research Retrieval Program through the assistance of the PKD Foundation. Normal human kidneys, unsuitable for transplantation, were obtained from the Midwest Transplant Network (MTN; Kansas City, KS), an organ retrieval agency. The protocol for the use of discarded human tissues for research complies with federal regulations and was approved by the Institutional Review Board at KUMC. Primary cell cultures were prepared as described

previously [90, 222]. Cells were propagated in DMEM/F12 supplemented with 5% FBS, 5 µg/ml insulin, 5 µg/ml transferrin, and 5 ng/ml sodium selenite (ITS) and penicillin G and streptomycin (P/S). After cells had reached 70-80% confluence in the flasks, they were lifted from the plastic with a trypsin-EDTA solution (Sigma Chemical, Saint Louis, MO) and counted using a hemocytometer.

Cell Proliferation measurements. ADPKD cells (7.5×10^4) were seeded into individual wells of 6-well plates containing DMEM/F12, ITS, 1% FBS and P/S. After cells reached approximately 50% confluence, the serum was reduced to 0.002%. After 24 h, cells were treated with 250 ng/ml human recombinant periostin (75 kDa; Biovendor, Asheville, NC) or 100 ng/ml epidermal growth factor (EGF; Sigma Chemical) alone or in the presence of 1 µM CPD 22 (EMD Millipore, Billerica, MA), an ILK inhibitor [223], for an additional 24 h. Each treatment was performed in triplicate. Cells were harvested by trypsinization, counted using an automated cell counter (Bio-Rad, Hercules, CA) and normalized to the control-treated group. In some experiments, cell proliferation was determined by an MTT assay [224]. Briefly, ADPKD cells (4×10^3) were seeded into the wells of a 96-well plate (six wells per experimental condition) and grown under similar conditions as described above. After the 24-h treatment, cell proliferation was measured using CellTiter 96 non-radioactive cell proliferation (MTT) assay (Promega, Madison, WI).

ILK knockdown in human ADPKD cells. ILK was knocked down in human ADPKD cells using shRNA lentiviral approach. Six unique ILK shRNA constructs (RHS4531-EG3611), each with a high specificity for the ILK mRNA, and a scrambled non-silencing shRNA construct (RHS4346)

were purchased from GE Healthcare (Waukesha, WI). HEK293T cells were transfected with 4.5 µg ILK or scrambled shRNA plasmid DNA and the packaging vectors (4.5 µg *psPAX2* and 1.8 µg *pMD2.G*) using Lipofectamine 200 (Invitrogen, Carlsbad, CA). The cells were incubated for 18 h for lentivirus production. Fresh media was added, and the conditioned media containing the lentivirus was harvested at 24 h and 48 h. Human ADPKD cells were seeded into 100 mm petri dishes for 24 h. Lentiviral harvest media from the two time points was added successively to the ADPKD cells. After viral infection, media bathing the ADPKD cells was switched to DME/F12 + 1% FBS for two days. Using immunoblot analysis, ILK knockdown efficiency was determined by band densitometry of ILK protein from ADPKD cells infected with ILK shRNA compared to the scrambled shRNA. We selected two shRNAs with the best knockdown efficiencies (mature antisense sequences for ILK shRNA1: ACACTACGGCTATTGAGTG, and ILK shRNA2: ATACGGTTGAGATTCTGGC). Alignment of the reverse complement of the antisense sequences targeted only ILK and no other mRNAs. To determine if ILK knockdown inhibits periostin-induced cell proliferation, ADPKD cells were infected with individual ILK shRNA or the scramble shRNA and then treated with 250 ng/ml periostin or EGF (positive control) for 24 h. Cell proliferation was determined by either cell count ($N = 1$) or MTT assay ($N = 3$).

Collecting duct-specific ILK knockdown and knockout in mice. Ilk$^{fl/fl}$ mice [225] were crossed to mice expressing *Pkhd1-Cre,* which maximally express Cre recombinase in the CD at postnatal (PN) day 7 [226] to generate *Ilk$^{fl/+}$;Pkhd1-Cre* mice. These mice were crossed to produce *Ilk$^{+/+}$;Pkhd1-Cre (*WT: *Ilk$^{+/+}$ CD), Ilk$^{fl/+}$;Pkhd1-Cre (Ilk$^{+/-}$ CD), Ilk$^{fl/fl}$;Pkhd1-Cre (Ilk$^{-/-}$ CD)* mice. We observed normal Mendelian inheritance. Mice were provided food and water *ad libitum* and monitored daily. At five and 10 wk of age, mice were water-restricted for three h and

urine was collected for measurement of osmolality using a vapor pressure osmometer. Afterward, the mice were euthanized in an isoflurane chamber, and blood was collected by cardiac puncture for measurement of blood urea nitrogen (BUN) followed by exsanguination and removal of the kidneys, as described previously [5]. The protocol for use of these mice was approved by the Institutional Animal Care and Use Committee at KUMC.

CD-specific knockout of ILK in Pkd1 mutant mice and pcy mice. To study the effect of ILK knockdown in PKD, we bred *Pkd1$^{fl/fl}$* mice [37] with *Ilk$^{fl/fl}$* mice. *Ilk$^{fl/+}$;Pkd1$^{fl/fl}$* mice were crossed with *Ilk$^{fl/+}$;Pkd1$^{fl/+}$;Pkhd1-Cre* mice to generate litters of *PKD* mice (*Pkd1$^{fl/fl}$;Pkhd1-Cre*) with *Ilk$^{+/+}$;Pkd1$^{fl/fl}$;Pkhd1-Cre* (*Ilk$^{+/+}$ PKD*), *Ilk$^{fl/+}$;Pkd1$^{fl/fl}$;Pkhd1-Cre* (*Ilk$^{+/-}$PKD*) and *Ilk$^{fl/fl}$;Pkd1$^{fl/fl}$;Pkhd1-Cre* (*Ilk$^{-/-}$ PKD*) ILK alleles in CD cells. Non-cystic littermate controls (*Ilk$^{+/+}$ CD, Ilk$^{+/-}$ CD, Ilk$^{-/-}$ CD*) were also generated using this breeding strategy. One group of mice was set aside for survival study where food and water were provided *ad libitum* and mice were monitored every day until death or euthanized when there were signs of imminent death, including labored breathing and inability to move [227]. A second group of mice was assessed at PN day 25. These mice were anesthetized, and serum and tissues were harvested as described above, and killed by exsanguination. All mice were F3-F5 generations on the C57BL/6 background. To confirm the results in a slowly progressive model of PKD, we knocked down ILK expression in CDs of *pcy/pcy (pcy)* mice, a model orthologous to human nephronophthisis type 3 (NPHP3). Disease progression in *pcy* mice is similar to ADPKD with kidney enlargement to several times normal size and progressive interstitial fibrosis [228]. Previously, we showed that kidney volume increased exponentially up to 20 weeks of age, after which there was a plateau as renal parenchyma was replaced with fibrosis [228]. In general, these mice survive to ~40 weeks of

age [5]. *Ilk*$^{fl/+}$ mice and *Pkhd1-Cre* mice were bred to *pcy* mice and backcrossed for eight generations. These mice were then bred to obtain *Ilk*$^{+/+}$*;pcy/pcy* (*Ilk*$^{+/+}$ *pcy*) and *Ilk*$^{fl/+}$*;Pkhd1-Cre;pcy/pcy* (*Ilk*$^{+/-}$ *pcy*) mice. Since mice with complete loss of ILK died by 10 weeks, *Ilk*$^{-/-}$ *pcy* mice were not used. In one group, the mice were euthanized for tissue analysis at 10 weeks of age, as described above. Mice in the survival study had free access to food and water *ad libitum*. At 25 weeks, 50-100 μl of blood was collected from the tail vein for BUN analysis. These mice were monitored for survival as described above.

Genotyping. We used a PCR method for genotyping ILK floxed mice. The forward primer sequence was 5′-GTTTCGCGGTGCTTCTGTG-3′, and the reverse sequence was (5′-AAAAGCCTTTGATCCTTGAATGG-3′). For genotyping wildtype and floxed Pkd1 alleles, the forward primer was 5′-CCTGCCTTGCTCTACTTTCC -3′, and the reverse primer was 5′-AGGGCTTTTCTTGCTGGTCT -3′. For genotyping for Cre alleles, the forward sequence was 5′- GCGGTCTGGCAGTAAAAACTATC -3′, and the reverse primer was 5′-GTGAAACAGCATTGCTGTCACTT -3′.

Western blot analysis. ADPKD and NHK cells were seeded onto plastic petri dishes (100 mm diameter) containing DMEM/F12 medium with 1% FBS. Serum was reduced to 0.002% at 75% confluency. Cells were then treated as indicated and lysates were prepared in triton lysis buffer at specific time points. Lysates were also prepared from renal tissues as described previously [229]. Total protein content was determined using BCA protein assay (Pierce, Rockford, IL) and 50 μg of protein was used for immunoblot analysis [224]. The following antibodies were used P-Akt [9271 Cell Signaling Technology, Beverly, MA (CS)], Akt (CS 9272), GAPDH (CS 2118), ILK

(EP-1593Y, Origene, Rockville, MD) and sc13075 (Santa Cruz, CA), P-S6K (CS 9234), S6K (CS 9292). Following incubation with an HRP-linked secondary antibody against rabbit or mouse (NA934, NA931; GE Healthcare), the blots were detected with ECL (RPN2232, GE Healthcare), imaged in AI 600 imager and quantified with Biorad Quantity One program.

Histology, immunohistochemistry, and immunofluorescence. Kidney cross sections were fixed in 4% paraformaldehyde overnight, embedded into paraffin blocks and 5 μm sections were placed on glass slides. Immunohistochemical staining for cleaved caspase-3 (CS 4858) was performed by the Department of Pathology and Laboratory Medicine core facility at KUMC. For quantification of cleaved caspase-3 staining, sections were blinded for the experimental condition, and the total number of cleaved caspase-3 stained cells were manually counted and normalized to the total non-cystic surface area of the kidney (% cleaved caspase-3). For immunofluorescence, tissue slices were deparaffinized, rehydrated and incubated with the following primary antibodies: Ki-67 (Abcam [ab] Inc., Cambridge, MA; ab15880) and Ki-67 blocking peptide (ab15881), ILK (EP-1593Y, Origene), P-S6 (CS 4858) followed by incubation with fluorescent conjugated secondary antibody (ab 150084). Sections were co-stained with FITC-conjugated DBA (FL-1031; Vector Laboratories, Burlingame, CA) to label CD cells and mounted with DAPI (ThermoFisher Scientific P36931). Slides were coded to conceal the group assignment and three non-overlapping fields per section were imaged using a Nikon Eclipse Ti microscope (Nikon Instruments, Melville, NY). Quantification of nuclear Ki-67 and cytoplasmic P-S6 staining was performed with a multi-wavelength cell scoring application in Metamorph Image Analysis software (Molecular Devices, Sunnyvale, CA).

Measurement of renal cystic area. Tissue sections were stained with hematoxylin and eosin and imaged using a dissecting microscope connected to a digital camera (Leica Microsystems, Buffalo Grove, IL). Slides were coded, and total number of cysts, cystic area and total area of the kidney were measured using Image Pro Premiere (Media Cybernetics Inc, Silverspring, MD) [5].

Measurement of tissue fibrosis. Tissue sections were stained with Masson's trichrome, causing collagen fibers to appear blue [5]. *Pkd1^{fl/fl};Pkhd1-Cre* mice have aggressive disease and die of massively enlarged kidneys, before excessive collagen/ECM deposition. Accordingly, we observed only mild collagen deposition within the cortex, whereas there were dramatic pre-fibrotic edematous areas in the cortex and detectable fibrosis within the medulla. Tissues were scored by the naïve observer assigning a percent of cortical area with pre-fibrotic edema and collagen deposition per total area of the cortex within the section. We also measured renal fibrosis in *pcy* mice which develop significant renal fibrosis by 10 wk. Percent fibrosis was scored based on both pre-fibrotic and fibrotic areas.

Measurement of blood urea nitrogen (BUN). Serum was isolated from blood collected at the time of euthanasia by centrifugation at 10,000 RPM for 10 min. Urea concentration was estimated using a colorimetric QuantiChrom Urea assay kit (DIUR 500; Bioassay Systems, Hayward, CA) and BUN was calculated using the formula BUN = (Urea/2.14).

Statistics. Data are expressed as mean ± standard error (SE). Unless noted otherwise, statistical significance was determined by one-way analysis of variance (ANOVA) and Student-Newman-

Keuls (SNK) post-test for multiple comparisons or unpaired t-test for comparison between control and treated groups. For survival studies, the Gehan-Breslow analysis was performed to determine statistical significance of the survival curves, and pairwise analysis was performed using the Bonferroni Method.

3.4. Results

3.4.1. Effect of periostin on ILK-mTOR signaling and proliferation of ADPKD cells

ILK was immunoprecipitated from primary ADPKD and normal human kidney (NHK) cells and incubated with GSKα/β protein or myelin basic protein in a kinase assay [185, 200]. Consistent with previous reports, ILK appeared to be capable of phosphorylating these substrates (**Figure 3-1**); however, it is unclear if other components of the complex were immunoprecipitated with ILK [204, 208, 221]. Basal ILK activity was higher in ADPKD than NHK cells, and periostin caused a further increase in ILK activity in ADPKD cells.
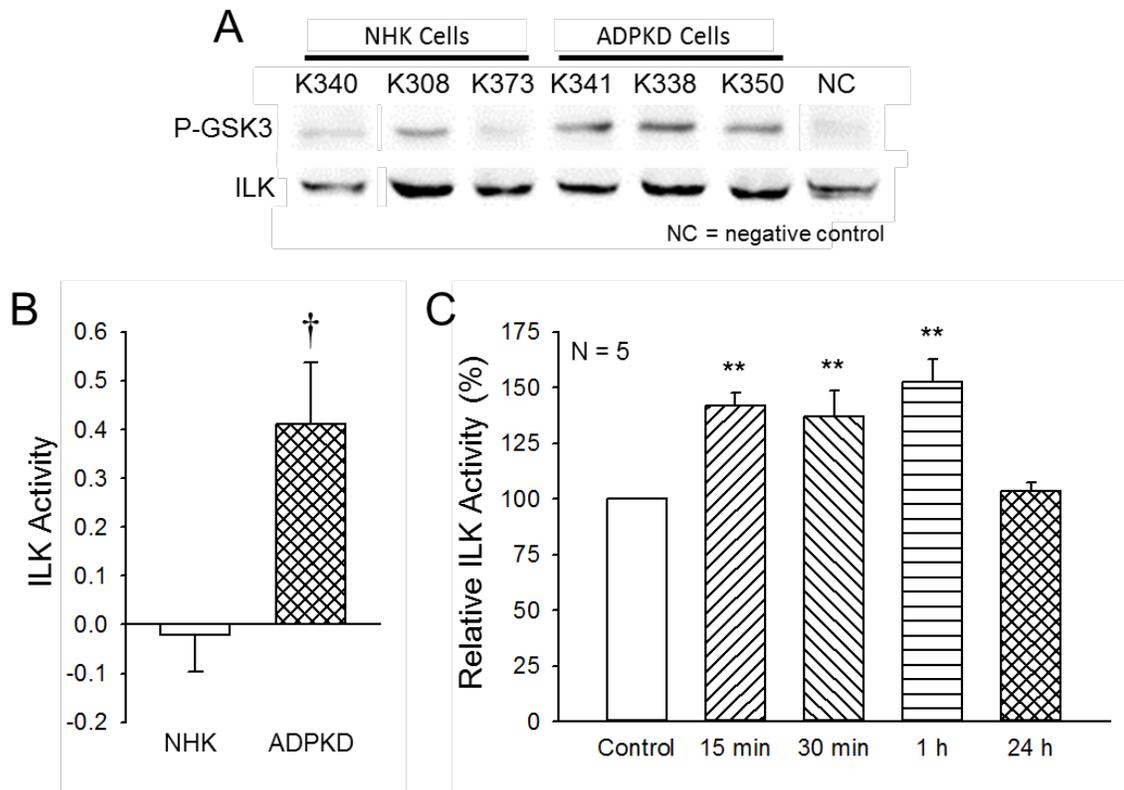
Figure 3-1. Effect of periostin on ILK activity in cultured ADPKD cells. (A) Primary ADPKD and normal human kidney (NHK) cells were grown to confluency, and then ILK was immunoprecipitated from cell lysates using an ILK antibody attached to magnetic beads. ILK activity was determined from the phosphorylation of GSK3α/β fusion protein (P-GSK3). Numbers above the bands indicate the kidney number in the PKD biospecimen repository. The negative control (NC) represents the level P-GSK3 in a kinase assay containing ILK that was immunoprecipitated from ADPKD cells, and all other reagents, except ATP. (B) ILK activity was defined as the P-GSK3 band intensity minus the band intensity of the NC, divided by the intensity of the total ILK band. N = 8 for NHK cells and N = 6 for ADPKD cells. †P< 0.05 (C) ADPKD cells were treated with 250 ng/ml periostin from 15 min to 24 h, and ILK activity was determined. Baseline activity (control treatment) was set to 100%. ILK activity increased as early as 15 min and remained elevated for at least 1 h. **P < 0.01, compared to control treated ADPKD cells.

Previously, we found that periostin stimulated the proliferation of ADPKD cells, but not NHK cells, a difference that may be related to increased expression of α_V-integrin in the cystic cells [2]. Periostin increased phosphorylated Akt (P-Akt/Akt) and S6K (P-S6K/S6K), a target of mTOR, in as early as 15 min and levels remained elevated for 24 h (**Figure 3-2**). Incubation with CPD 22, an ILK inhibitor [223], blocked periostin-induced phosphorylation of Akt and S6K (**Figure 3-3 A, B**). Periostin and epidermal growth factor (EGF) increased ADPKD cell proliferation to similar levels. Incubation with CPD 22 blocked periostin-induced cell proliferation (**Figure 3-3 C**) but did not affect the EGF response.

To confirm the results, we used a lentiviral shRNA approach to knock down ILK expression in ADPKD cells. In three separate experiments, two ILK shRNA constructs were used, achieving 46-54% reduction in ILK expression (**Figure 3-4 A**). Periostin increased P-Akt/Akt and P-S6K/S6K to the same level in the absence and presence of scrambled shRNA (data not shown). By contrast, ILK knockdown prevented periostin stimulation of the Akt/mTOR pathway (**Figure 3-4 B, C**) and blocked periostin-induced cell proliferation (**Figure 3-4 D**). In contrast to ILK inhibition with CPD 22, disruption of the IPP complex by ILK knockdown decreased EGF-induced ADPKD cell proliferation, supporting a role for the IPP complex in RTK signaling [192, 230, 231].
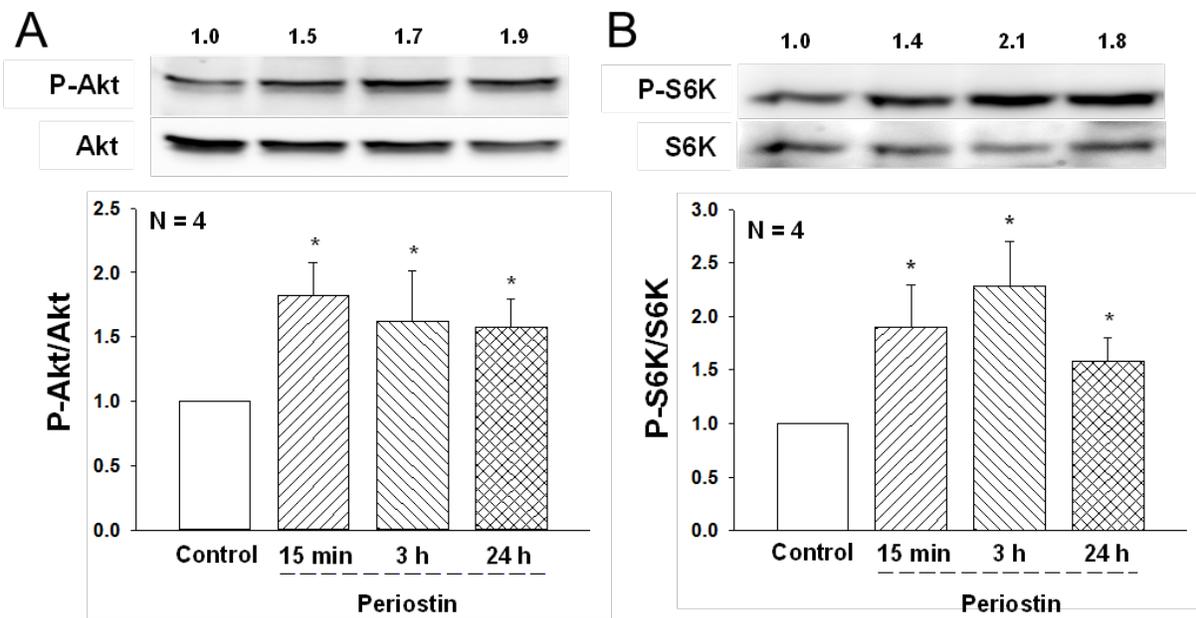
Figure 3-2. Effect of periostin on the Akt/mTOR pathway in human ADPKD cells. ADPKD cells (N = 4) were incubated in media containing 250 ng/ml periostin for 15 min, 3 h or 24 h. Levels of (A) phosphorylated (P-Akt) and (B) phosphorylated (P-S6K), a downstream target of mTOR, were determined by immunoblot analysis. Numbers above representative immunoblots are (A) P-Akt/Akt and (B) P-S6K/S6K, normalized to control (set to 1.0). Bar graphs represent the mean and standard error (S.E.) for (A) P-Akt/Akt and (B) P-S6K/S6K from cell preparations from four different ADPKD kidneys. *$P < 0.05$, versus control treatment.
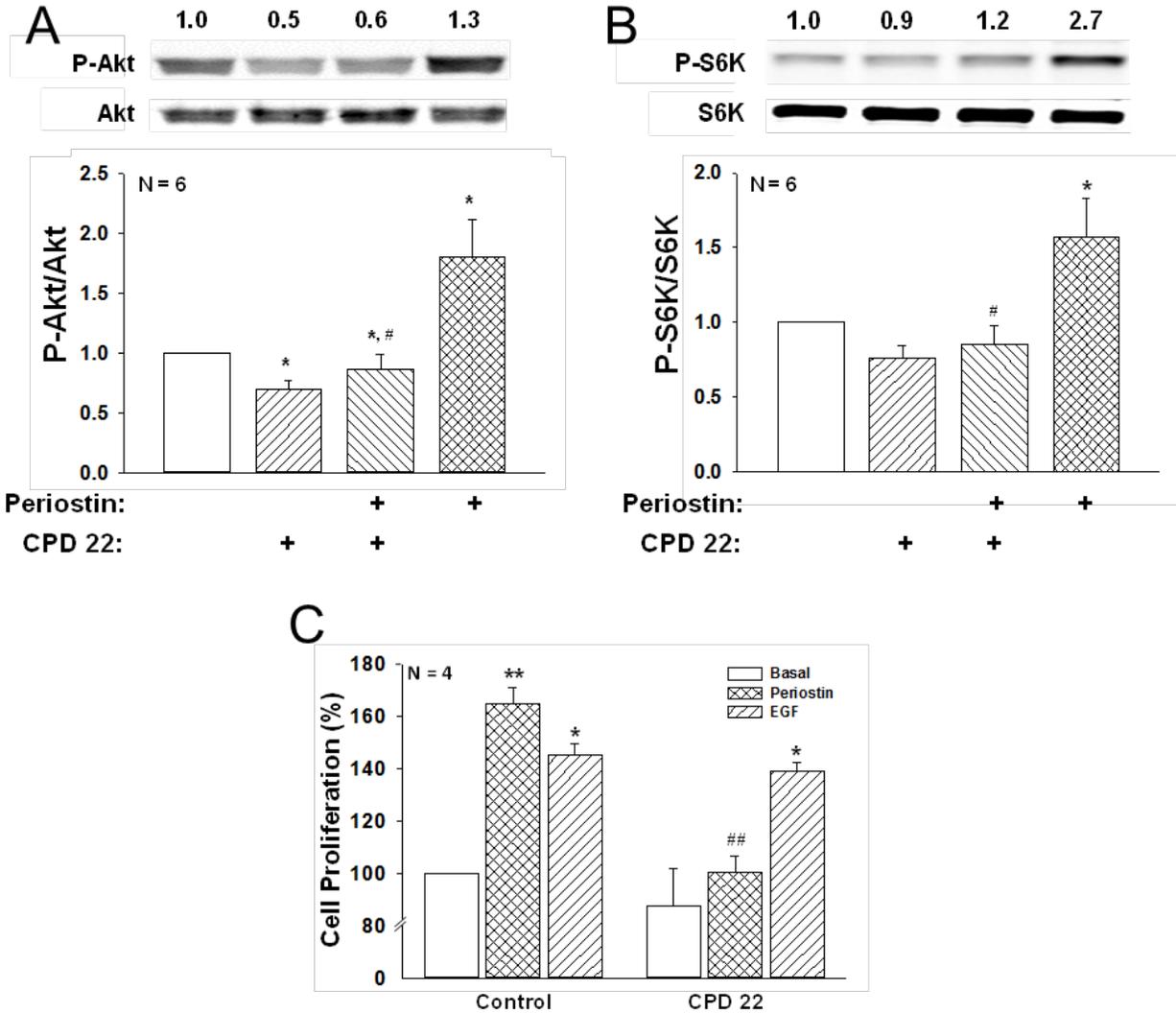
Figure 3-3. Effect of ILK inhibition on periostin-induced Akt/ mTOR activation and proliferation of ADPKD cells. ADPKD cells were treated with or without 2.5 μM CPD22 for 1 h and then stimulated with periostin for 15 min. Numbers above representative immunoblots are (A) P-Akt/Akt and (B) P-S6K/S6K. (C) The effect of ILK inhibition on ADPKD proliferation was determined by treating cells with either 250 ng/ml periostin or 25 ng/ml epidermal growth factor (EGF) for 48 h in the presence or absence of 1 μM CPD 22. Cell numbers were counted using BioRad TC20 cell counter. *P < 0.05 and **P< 0.01, compared to control and [#]P < 0.05, [##]P <0.01, compared to periostin alone.
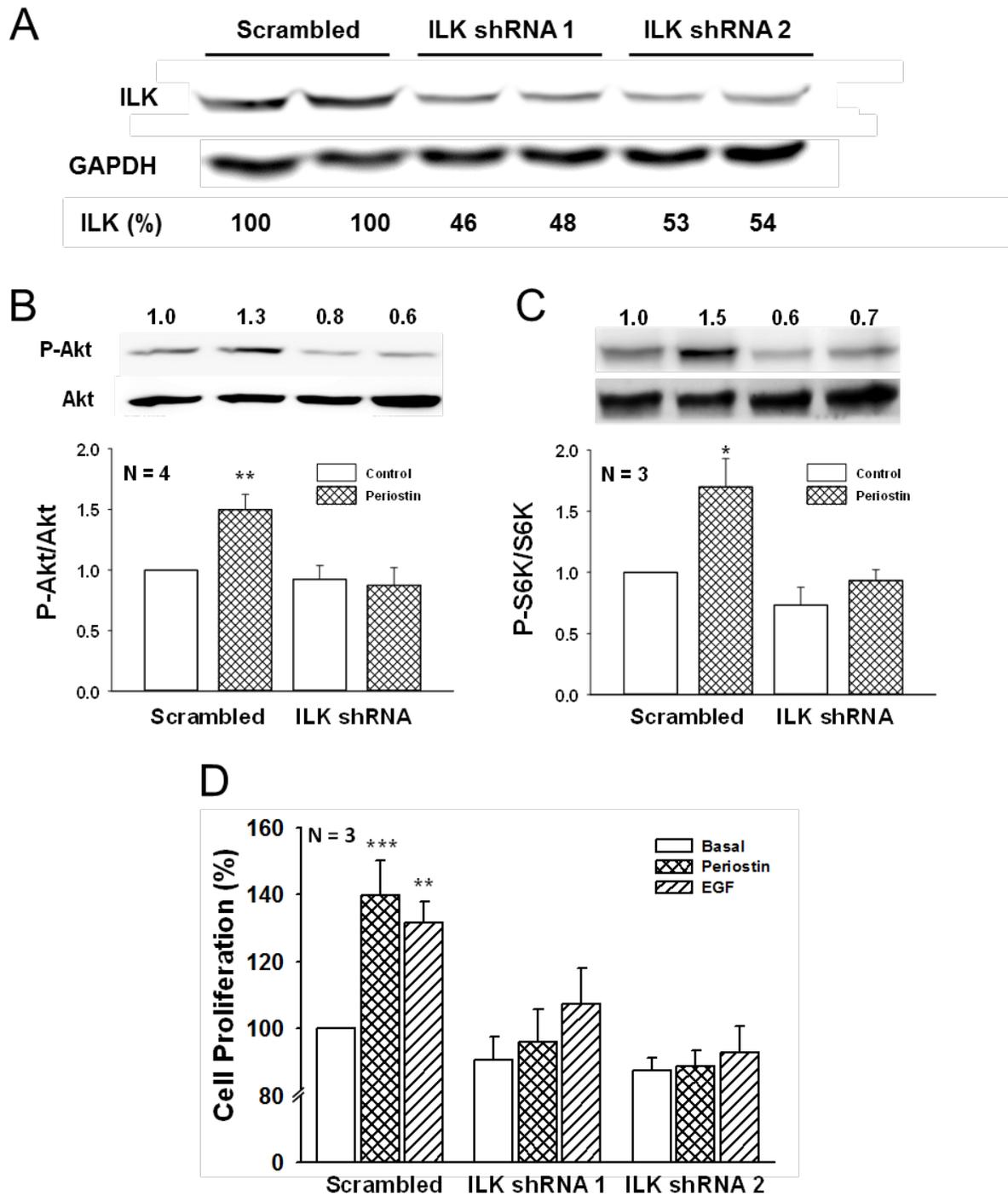
Figure 3-4. Effect of ILK knockdown on periostin-induced Akt/mTOR signaling and ADPKD cell proliferation. To confirm the role of ILK, ADPKD cells were infected with lentivirus containing shRNA against ILK or a non-specific (scrambled) sequence. (A) Representative immunoblot of ILK in ADPKD cells after infection by lentiviral ILK shRNA (ILK shRNA 1 or ILK shRNA 2) or a non-specific (Scrambled) sequence. Numbers below the bands indicate the percentage of ILK, relative to scrambled shRNA cells. Cells were treated with 250 ng/ml periostin for 15 min and levels of (B) P-Akt/Akt and (C) P-S6K/S6 were measured by immunoblot analysis. Summary data for (D) P-Akt/Akt and (E) P-S6K/S6 were normalized to basal conditions of scrambled shRNA cells (set to 1.0). (D) ADPKD cells were infected with an ILK (shRNA 1 or shRNA 2) or a scrambled shRNA lentivirus, and then treated with periostin or 100 ng/ml EGF for 24 h. Cell proliferation was measured by Promega MTT assay and normalized to basal proliferation of cells infected with the scrambled shRNA (set to 100%). *$P < 0.05$, **$P < 0.01$ and ***$P < 0.001$, compared to control or basal conditions of scrambled shRNA infected cells.

3.4.2. Generation of mice with CD-specific deletion of ILK

Ilk $^{fl/fl}$ mice [225] were crossed with *Pkhd1-Cre* mice [226] to generate wild type (WT: *Ilk* $^{+/+}$ CD), *Ilk* $^{fl/+}$*;Pkhd1-Cre* (*Ilk* $^{+/-}$ *CD*) and *Ilk* $^{fl/fl}$*;Pkhd1-Cre* (*Ilk* $^{-/-}$ *CD)* mice. ILK deletion in CDs was confirmed by co-immunofluorescence using an ILK antibody and Dolichos *biflorus* agglutinin (DBA, green) (**Figure 3-5**).

Ilk $^{-/-}$ *CD* mice had lower body weight (BW) and developed a urine concentrating defect (**Table 3-1**), consistent with a previous report [232]. Kidneys of *Ilk* $^{-/-}$ *CD* mice had caspase-3-mediated anoikis [10] with apoptotic cells in the lumen and dilated cortical tubules (**Figure 3-6**). There was a significant increase in blood urea nitrogen (BUN) as early as 25 days. By 10 weeks of age, *Ilk* $^{-/-}$ *CD* mice had reduced kidney size (**Table 3-1**), massive levels of apoptosis and renal fibrosis, and the mice died by 10.4 ± 0.34 weeks (N = 14). By contrast, *Ilk* $^{+/-}$ *CD* mice had normal renal morphology and function, urine osmolality and BW and survived beyond one yr.
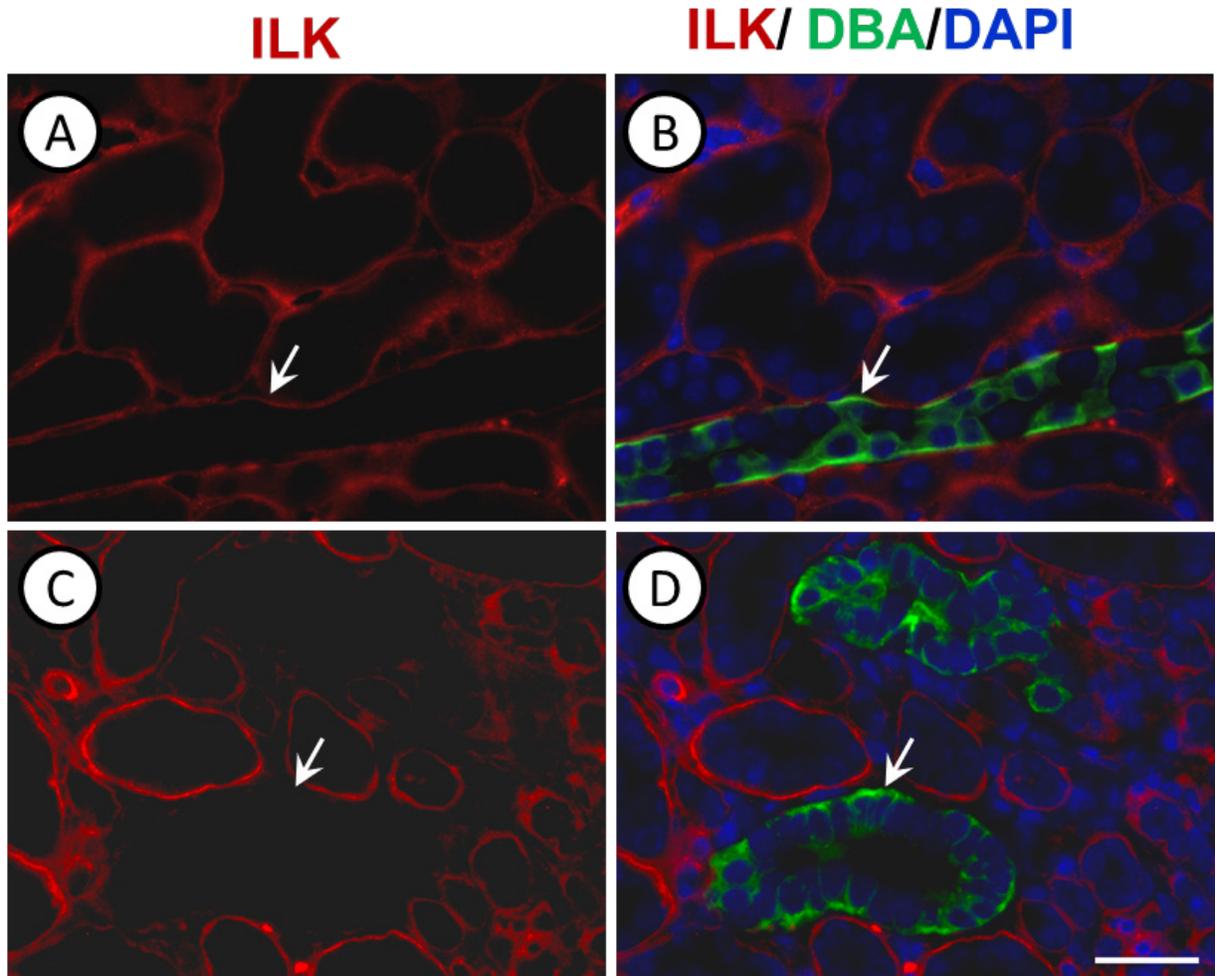
Figure 3-5. Collecting-duct specific ILK knockout in mice. At postnatal (PN) day 25, *Ilk^{+/+};Pkhd1-Cre* (Ilk^{+/+} CD) and *Ilk^{fl/fl};Pkhd1-Cre* (*Ilk^{-/-} CD*) mice were euthanized, and kidney sections were stained for ILK (red), Dolichos *biflorus* agglutinin (DBA, green) and DAPI nuclear stain (blue). Left panels (A, C) are images of kidney sections that were stained for ILK expression (red). Right panels (B, D) are merged images in which ILK, DBA, and DAPI staining was superimposed. Top panels (A, B) show an Ilk^{+/+} CD mouse kidney section with normal ILK expression in a collecting duct (arrow). Bottom panels (C, D) show that Ilk^{-/-} CD mouse kidney sections lack ILK expression in the collecting ducts. Scale bar = 5 μm.

52

Genotype	Age	N	BW (g)	KW (g)	KW/BW (%)	Urine OsM
Ilk$^{+/+}$ CD	25 d	6	11.5 ± 0.9	0.15 ± 0.01	1.31 ± 0.07	2621 ± 116
Ilk$^{+/-}$ CD	25 d	4	13.1 ± 1.1	0.17 ± 0.02	1.32 ± 0.04	2336 ± 143
Ilk$^{-/-}$ CD	25 d	5	8.7 ± 1.0	0.18 ± 0.02	2.02 ± 0.10*	655 ± 175*
Ilk$^{+/+}$ CD	10 wk	4	24.5 ± 1.8	0.33 ± 0.02	1.36 ± 0.11	3337 ± 193
Ilk$^{+/-}$ CD	10 wk	3	22.6 ± 2.0	0.30 ± 0.04	1.35 ± 0.06	3066 ± 86
Ilk$^{-/-}$ CD	10 wk	4	10.2 ± 1.6*	0.17 ± 0.02*	1.66 ± 0.13	535 ± 26*

Table 3-1. Effect of collecting duct (CD)-specific knockout of ILK on body weight, kidney weight, and urine concentrating ability. Body and kidney weights and urine concentrating ability were determined at 25 days and 10 weeks of age for wild type ILK (*Ilk*$^{+/+}$ CD), *Ilk*$^{fl/+}$*;Pkhd1-Cre* (*Ilk*$^{+/-}$ CD) and *Ilk*$^{fl/fl}$*;Pkhd1-Cre* (*Ilk* $^{-/-}$ CD) mice. To evaluate urine concentrating ability, drinking water was removed for 3 h, spot urine was collected, and urine osmolality (OsM, mosmoles/kg water) was measured using a vapor pressure osmometer. *Ilk*$^{-/-}$ CD mice had decreased body weight (BW) and lower urine osmolality (OsM, mosmoles/kg) compared to *Ilk*$^{+/+}$ CD and *Ilk*$^{+/-}$ CD mice, confirming that ILK ablation leads to a defect in concentrating ability of the kidneys [11]. *Ilk*$^{+/-}$ CD mice had normal BW, KW (%BW) and urine OsM.
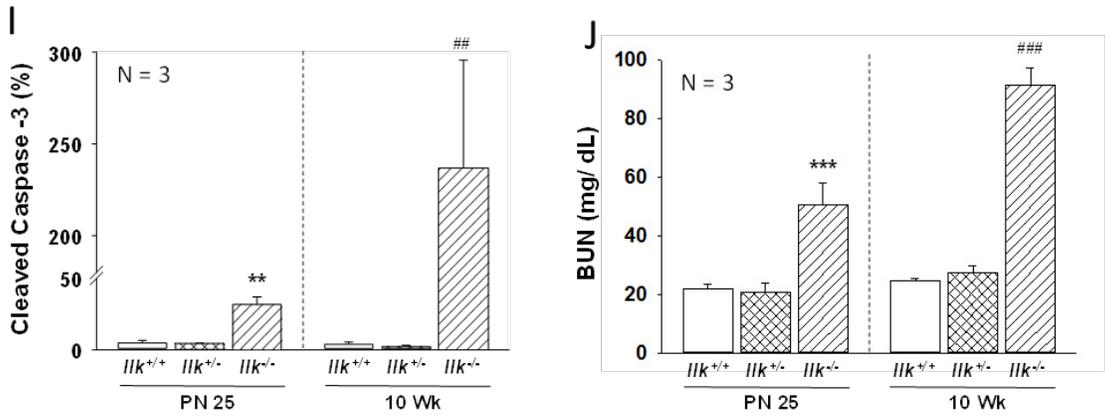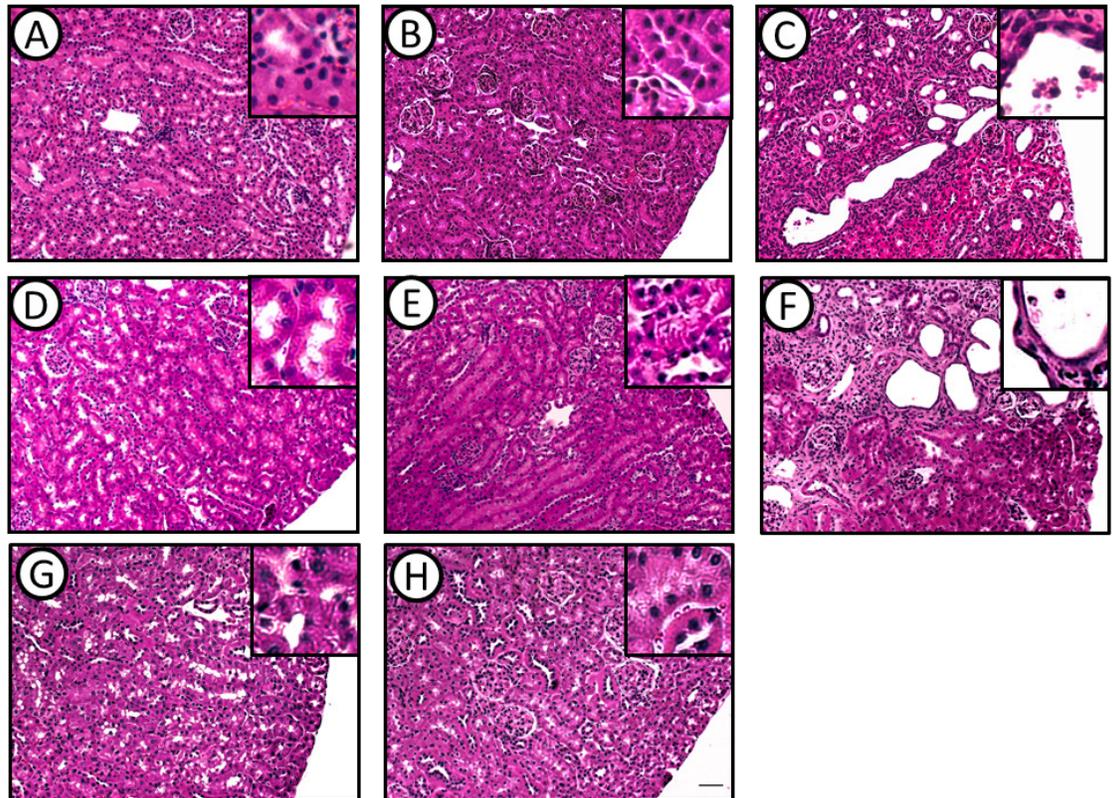
Figure 3-6. Effect of collecting duct-specific ILK deletion. Kidney sections from wild type ILK (*Ilk^{+/+}* *CD;* A, D, G), *Ilk^{fl/+};Pkhd1-Cre* (*Ilk^{+/-} CD;*B, E, H) and *Ilk^{fl/fl};Pkhd1-Cre* (*Ilk^{-/-} CD;*C, F) mice at 25 days (A, B, C), and 10 (D, E, F) and 51 weeks (G, H) were stained with hematoxylin and eosin. All images are the same magnification. Scale bar = 50 µm. (I) Tissue sections were stained for cleaved caspase-3 to determine if the cellular loss of ILK caused apoptosis/anoikis[10]. The number of cleaved caspase-3 positive cells in the kidney sections were counted and represented as a percentage of non-cystic surface area (% cleaved caspase-3). (J) Blood collected from mice at postnatal day 25 (PN 25) and 10 wk, were analyzed for blood urea nitrogen (BUN).

54

3.4.3. Effect of ILK on cystic disease progression in ADPKD mice

ILK expression was knocked down in CDs of *Pkd1$^{fl/fl}$;Pkhd1-Cre* (*PKD*) mice, an orthologous ADPKD model with aggressive disease [226]. These mice typically die by 33 days with massively enlarged kidneys. We generated *Ilk$^{+/+}$;Pkd1$^{fl/fl}$;Pkhd1-Cre* (*Ilk$^{+/+}$ PKD*), *Ilk$^{fl/+}$;Pkd1$^{fl/fl}$;Pkhd1-Cre* (*Ilk$^{+/-}$PKD*) and *Ilk$^{fl/fl}$;Pkd1$^{fl/fl}$;Pkhd1-Cre* (*Ilk$^{-/-}$ PKD*) mice (Figure 4). By 25 days, the PKD mice had massively enlarged kidneys (**Figure 3-7 A, B**) with percent kidney weight (KW) to BW equaling 18.0% (**Figure 3-7 D**), compared to 1.3% for WT mice (**Table 3-1**). Loss of one or both alleles of ILK reduced KW(%BW) to 12.7% or 5.1%, respectively. There was no difference in BW among the three genotypes. Cystic area of the kidneys was reduced from 55% in *Ilk$^{+/+}$ PKD* mice to 43% and 28% in *Ilk$^{+/-}$ PKD* and *Ilk$^{-/-}$ PKD* mice, respectively (**Figure 3-7 B, E**). There were also fewer cysts in *Ilk$^{+/-}$ PKD* and *Ilk$^{-/-}$ PKD* kidneys; however, this difference was not significant (data not shown).

To determine if CD-specific knockdown of ILK decreased cell proliferation, the number of Ki-67 positive cells in DBA-positive tubules was determined using immunofluorescence (**Figure 3-8**). We found that Ki-67 positive cells were dramatically decreased with the loss of one or both alleles of ILK in CD cells (**Figure 3-8 E**).
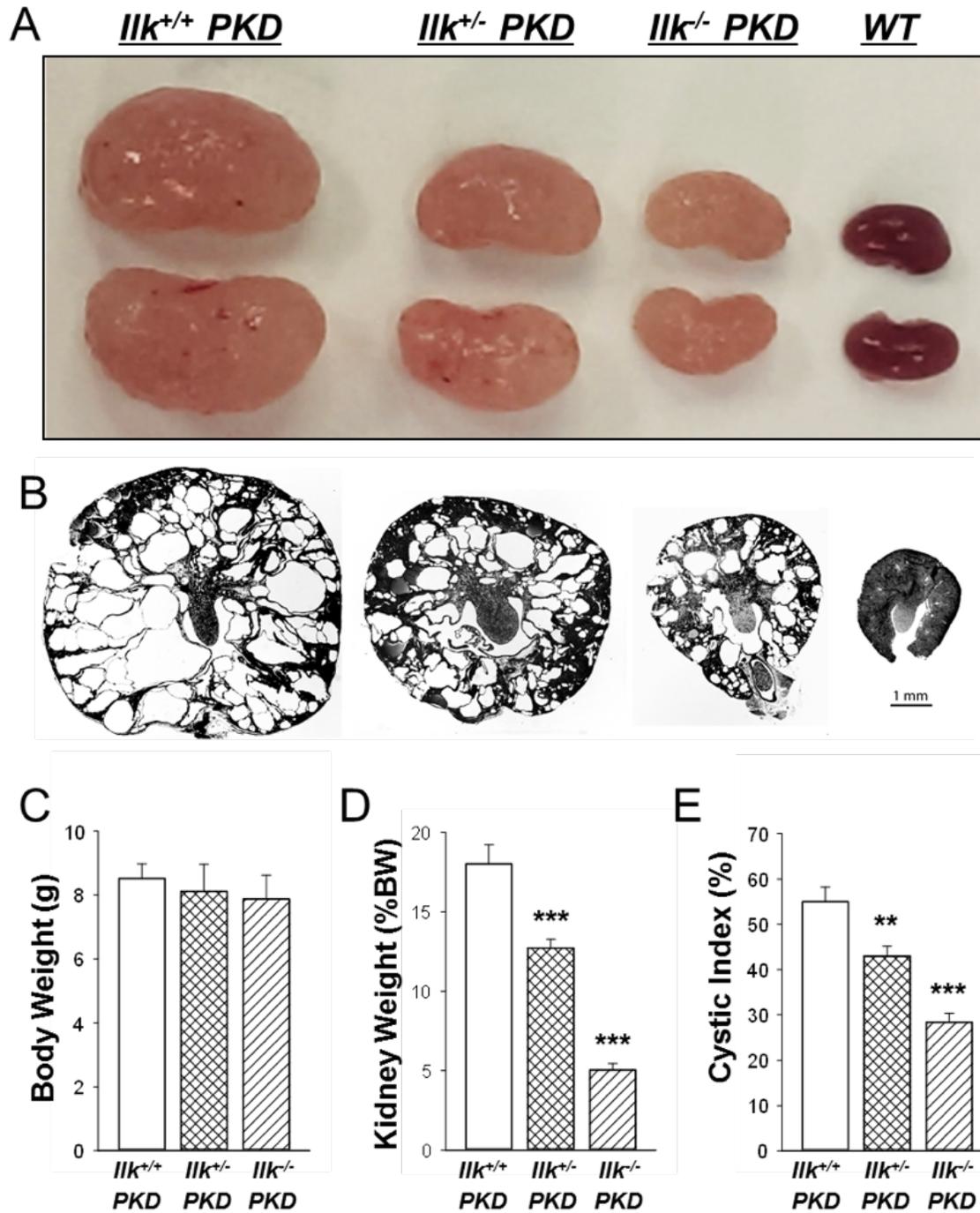
Figure 3-7. Effect of ILK expression on cyst growth in PKD mice. Representative images of (A) kidneys and (B) kidney sections from *Ilk$^{+/+}$;Pkd1$^{fl/fl}$;Pkhd1-Cre* (*Ilk$^{+/+}$ PKD*), *Ilk$^{+/-}$;Pkd1$^{fl/fl}$;Pkhd1-Cre* (*Ilk$^{+/-}$PKD*) and *Ilk$^{fl/fl}$;Pkd1$^{fl/fl}$;Pkhd1-Cre* (*Ilk$^{-/-}$ PKD*) and wild type (WT) mice demonstrate that the loss of ILK expression in CD cells reduced cyst growth in PKD mice. All images were taken at the same magnification. Scale Bar = 1 mm. Bar graphs are mean ± S.E. for (C) Body weight and (D) kidney weight as a percentage of body weight (%BW) for N = 10 mice per group. (E) Cystic index is represented as the percentage of cystic area per total kidney cross-sectional surface area for N = 7 mice per group. **P < 0.01 and ***P < 0.001, compared to *Ilk$^{+/+}$ PKD* mice.

Ki-67 / DBA/ DAPI
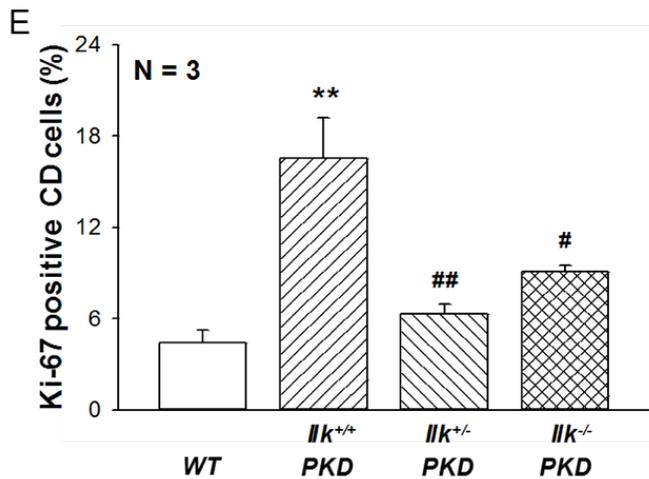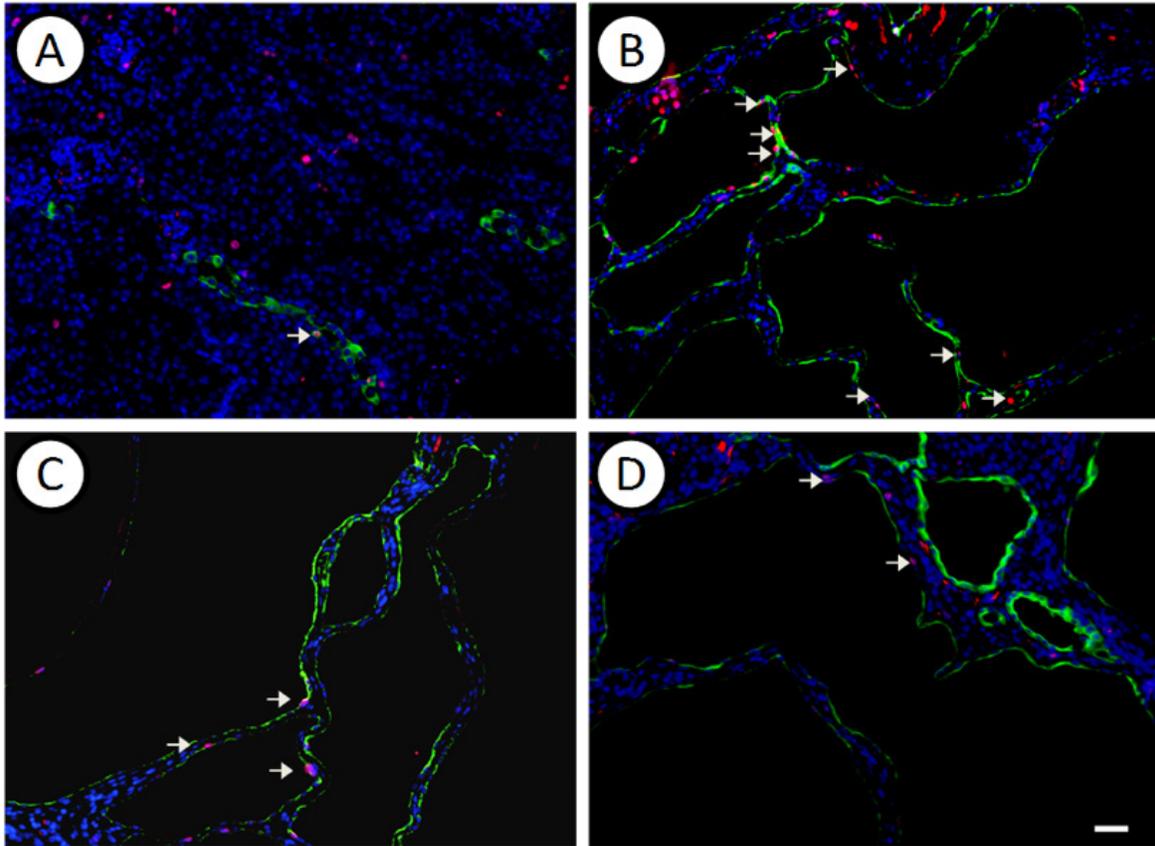
Figure 3-8. Effect of ILK expression on renal cell proliferation in PKD mice. Representative kidney sections from (A) wild type, WT, (B) $Ilk^{+/+};Pkd1^{fl/fl};Pkhd1-Cre$ ($Ilk^{+/+}$ PKD), (C) $Ilk^{fl/+};Pkd1^{fl/fl};Pkhd1-Cre$ ($Ilk^{+/-}$PKD) and (D) $Ilk^{fl/fl};Pkd1^{fl/fl};Pkhd1-Cre$ ($Ilk^{-/-}$ PKD) mice were stained with an antibody to Ki-67, a marker for cell proliferation (red). Tissues were also stained for DBA (green) to detect collecting ducts (CD) and the DAPI nuclear stain (blue). Arrows indicate Ki-67 positive CD cells. Scale bar = 5 µm. (E) Summary for the number of cells positive for nuclear Ki-67, normalized to the total nuclei in DBA-positive positive CD. Data are mean ± S.E. for kidneys from three mice per group. **$P<0.01$ compared to WT, #P <0.05 and ##P <0.01 compared to $Ilk^{+/+}$ PKD.

Pkd1^{fl/fl};Pkhd1-Cre kidneys had higher P-Akt/Akt levels than WT kidneys [154, 215] and partial loss or complete ablation of ILK reduced P-Akt/Akt (**Figure 3-9 A, F**). Percentage of CD cells with phosphorylated S6 (P-S6) was higher in *Ilk^{+/+} PKD* compared to WT mice, and partial or complete loss of ILK significantly diminished P-S6 in CD-derived cysts (**Figure 3-9 B-E, G**). These data support the hypothesis that ILK is a key regulator of Akt/mTOR signaling in PKD.

To determine the effect of ILK on RTK signaling, we examined levels of ERK activity (P-ERK/ERK) (**Figure 3-10**). *Ilk^{+/+} PKD* kidneys showed a significant increase in ERK activity compared to WT [93]. Loss of one allele of ILK decreased P-ERK; however, this was not significant. By contrast, ILK ablation in *Ilk^{-/-} PKD* kidneys significantly reduced P-ERK. We think that disruption of IPP complex due to loss of ILK also affects RTK signaling [192, 230, 231]

There was an increase in cleaved caspase-3-positive nuclei in PKD kidneys (**Figure 3-11**). Complete loss of ILK further increased the number of apoptotic cells and caused CD cells to be shed into the lumen. Previously, loss of cystic cells due to apoptosis was shown to reduce PKD progression [233, 234].
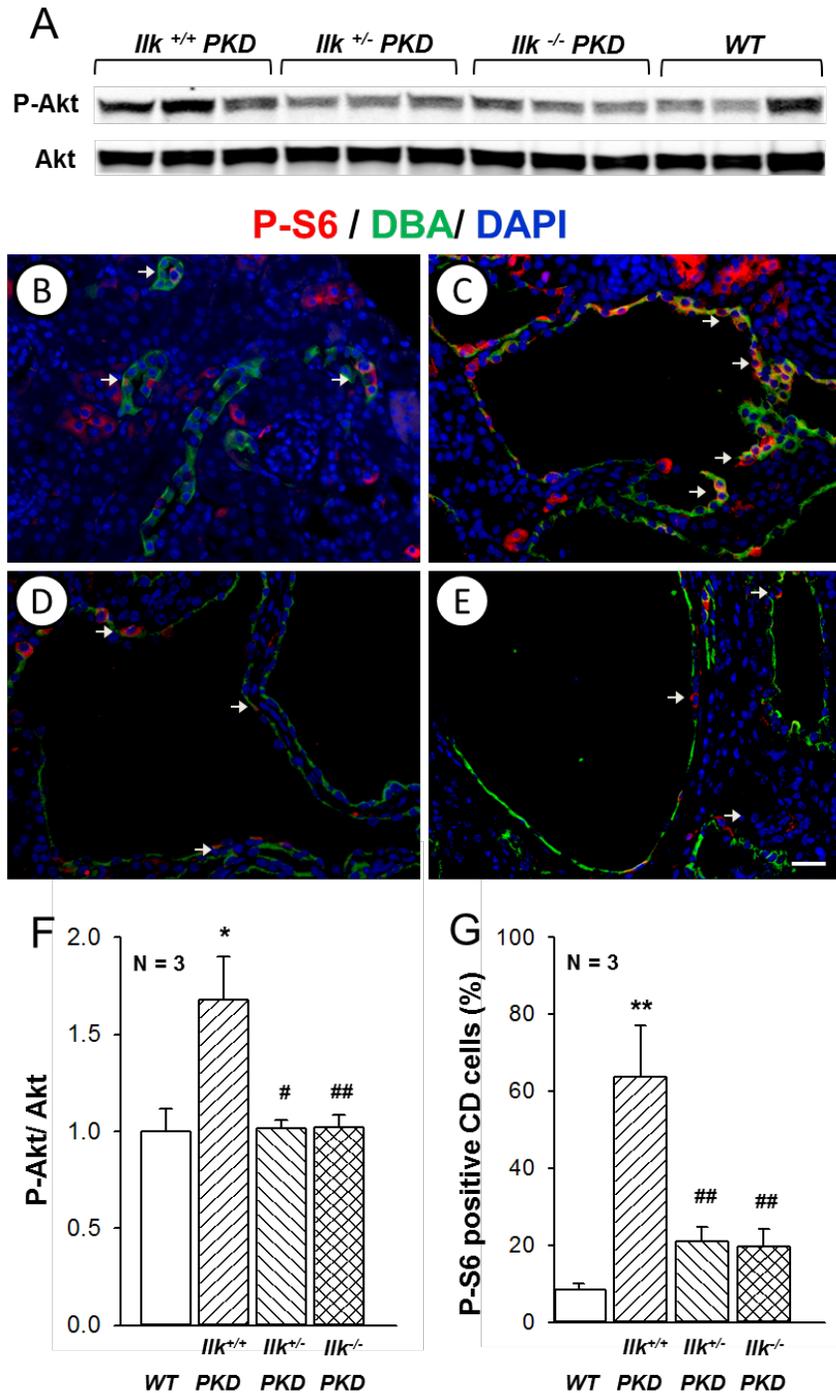
Figure 3-9. Effect of ILK expression on Akt/mTOR signaling in PKD kidneys. (A) Immunoblot analysis was used to compare phosphorylated levels of renal Akt (P-Akt) in $Ilk^{+/+};Pkd1^{fl/fl};Pkhd1\text{-}Cre$ ($Ilk^{+/+}$ PKD), $Ilk^{fl/+};Pkd1^{fl/fl};Pkhd1\text{-}Cre$ ($Ilk^{+/-}$ PKD), $Ilk^{fl/fl};Pkd1^{fl/fl};Pkhd1\text{-}Cre$ ($Ilk^{-/-}$ PKD) and wildtype (WT) mice. Representative sections from (B) WT, (C) $Ilk^{+/+}$ PKD, (D) $Ilk^{+/-}$PKD and (E) $Ilk^{-/-}$ PKD mice were stained with an antibody to P-S6 (red). Tissues were also stained for DBA (green) to detect collecting ducts (CD) and the DAPI nuclear stain (blue). Arrows indicate cytoplasmic P-S6 in CD cells. All images were taken at the same magnification. Scale bar = 5 μm. (F) Summary of the effect of CD-specific ILK expression on renal P-Akt/Akt levels. (G) Percentage of cytosolic P-S6 positive cells, normalized to the total nuclei in DBA-positive collecting ducts. Data are mean ± S.E. for kidneys from three mice per group. *P<0.05 and **P<0.01 compared to WT, #P <0.05 and ##P <0.01 compared to Ilk+/+ PKD.
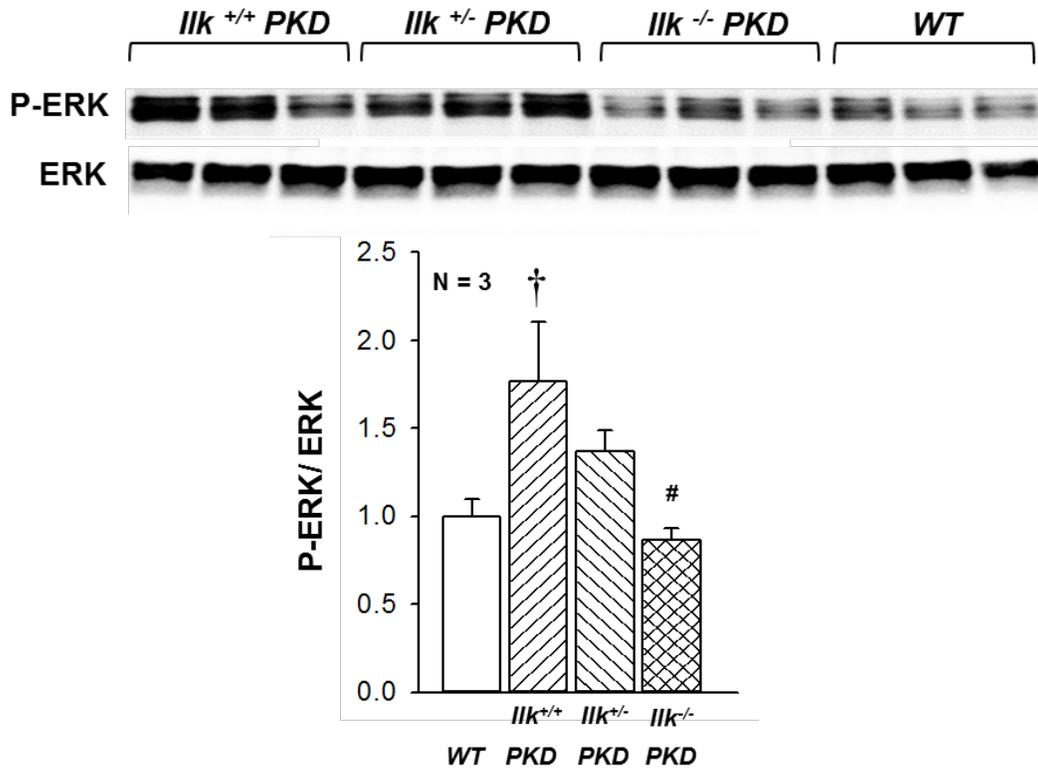
Figure 3-10. Effect of ILK expression on renal P-ERK levels in PKD mice. Immunoblot analysis was used to compare phosphorylated levels of renal ERK (P-ERK) in $Ilk^{+/+};Pkd1^{fl/fl};Pkhd1-Cre$ ($Ilk^{+/+}$ *PKD*), $Ilk^{fl/+};Pkd1^{fl/fl};Pkhd1-Cre$ ($Ilk^{+/-}$ *PKD*), $Ilk^{fl/fl};Pkd1^{fl/fl};Pkhd1-Cre$ ($Ilk^{-/-}$ *PKD*) and wildtype (*WT*) mice. Each lane represents a single mouse kidney lysate (N = 3 per group). Summary of the effect of CD-specific ILK expression on renal P-ERK/ERK levels. Data are means ± S.E. for kidneys from three mice per group †P= 0.05, compared to *WT*. #P <0.05, compared to $Ilk^{+/+}$ *PKD*.
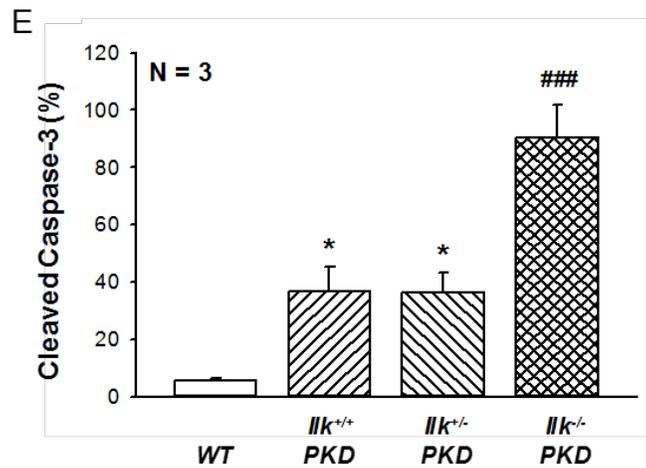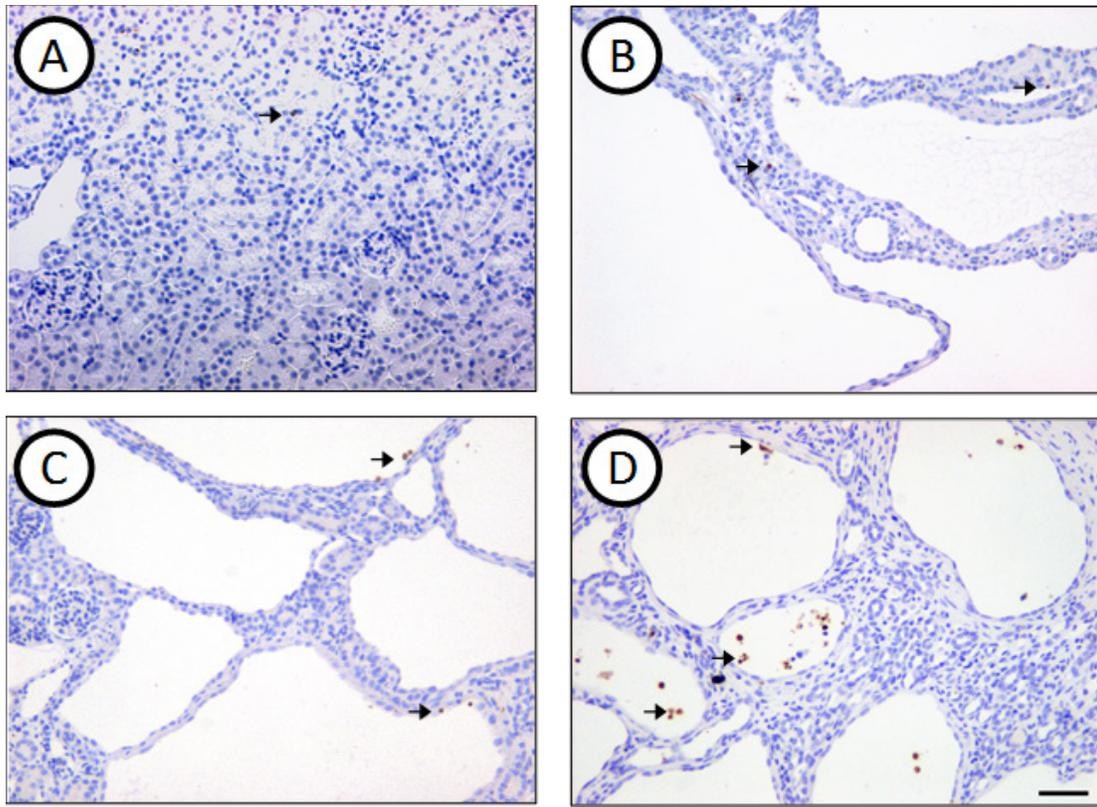
Figure 3-11. Effect of ILK expression on caspase-3-mediated apoptosis in *PKD* mice. Representative kidney sections from (A) wild type, WT, (B) *Ilk$^{+/+}$;Pkd1$^{fl/fl}$;Pkhd1-Cre* (*Ilk$^{+/+}$ PKD*), (C) *Ilk$^{fl/+}$;Pkd1$^{fl/fl}$;Pkhd1-Cre* (*Ilk$^{+/-}$PKD*) and (D) *Ilk$^{fl/fl}$;Pkd1$^{fl/fl}$;Pkhd1-Cre* (*Ilk$^{-/-}$ PKD*) mice were stained with an antibody to cleaved caspase-3 to visualize apoptotic cells (brown staining; arrows). All images were taken at the same magnification. Scale bar = 50 μm. (E) Total number of cleaved caspase-3 positive cells in the entire section was counted and normalized to the non-cystic surface area of the kidney (represented as % cleaved caspase). Data are means ± S.E. for kidneys from three mice per group. *P<0.05 compared to WT, $^{###}$P <0.001 compared to *Ilk$^{+/+}$ PKD*.

3.4.4. Effect of ILK on interstitial fibrosis, renal function and survival in *PKD* kidneys

Pkd1$^{fl/fl}$*;Pkhd1-Cre* mice develop extensive interstitial damage involving fibrosis and edema, a precursor for collagen deposition and fibrosis. At PN day 25, there was massive fibrosis/edema in *Ilk*$^{+/+}$ *PKD* kidneys with 91% of the interstitial space showing pathologic damage (**Figure 3-12**). *Ilk*$^{+/+}$ *PKD* mice showed a marked increase in BUN (132.8±7.7 mg/dl; normal range is 8-33 mg/dl). Loss of one or both alleles of ILK in CD cells caused a reduction in fibrosis. Decreased expression of ILK in *Ilk*$^{+/-}$*PKD* mice reduced BUN levels, compared to *Ilk*$^{+/+}$ *PKD* mice. By contrast, BUN levels of *Ilk* $^{-/-}$ *PKD* mice were similar to *Ilk*$^{+/+}$ *PKD* mice, suggesting that renal injury due to loss of ILK confounds the improved cystic phenotype.

Next, we determined if knockdown of ILK alters the lifespan of the PKD mice. *Pkd1*$^{fl/fl}$*;Pkhd1-Cre* mice expressing normal ILK lived to ~33 days (**Figure 3-13**). PKD mice heterozygous at the ILK locus (*Ilk*$^{+/-}$ *PKD*) survived to 42 days, displaying a 27% increase in lifespan. Complete ILK knockout increased survival to 40 days; however, this was not significant. These data indicate that a reduction in ILK decreased cyst growth by inhibiting mitogenic pathways, leading to improved renal function and survival. By contrast, complete loss of ILK induced cell death, contributing, in part, to the decrease in cyst burden.
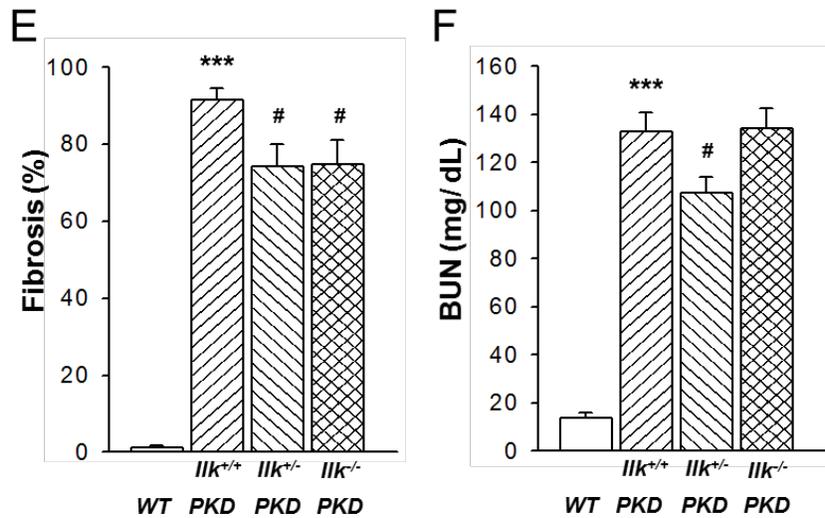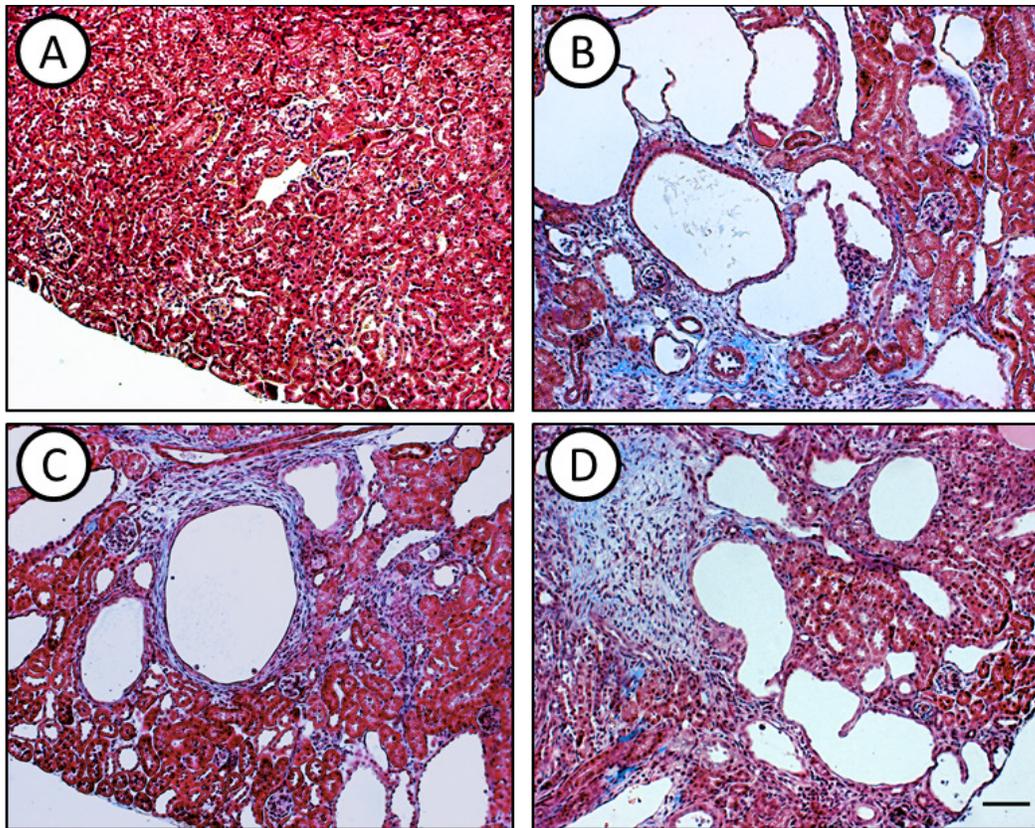
Figure 3-12. Effect of ILK expression on interstitial fibrosis and renal function in *PKD* mice. Representative kidney sections from (A) wild type (WT), (B) *Ilk$^{+/+}$;Pkd1$^{fl/fl}$;Pkhd1-Cre* (*Ilk$^{+/+}$ PKD*), (C) *Ilk$^{fl/+}$;Pkd1$^{fl/fl}$;Pkhd1-Cre* (*Ilk$^{+/-}$PKD*) and (D) *Ilk$^{fl/fl}$;Pkd1$^{fl/fl}$;Pkhd1-Cre* (*Ilk$^{-/-}$ PKD*) mice were stained with Masson trichrome to visualize pathogenic collagen deposition (stained blue). All images were taken at the same magnification. Scale bar = 50 µm. (E) Tissue sections were coded to conceal the group assignment prior to being visually scored for percentage of interstitial fibrosis and edema per total area of the tissue section Data are means ± S.E. for kidneys from seven mice per group. (F) Serum was isolated from WT (N = 5), *Ilk$^{+/+}$ PKD* (N = 10), *Ilk$^{+/-}$ PKD* (N = 10), *Ilk$^{-/-}$ PKD* (N = 7) and blood urea nitrogen (BUN) was determined to assess renal function. ***P<0.001 compared to WT, #P <0.05 compared to *Ilk$^{+/+}$ PKD*.

63
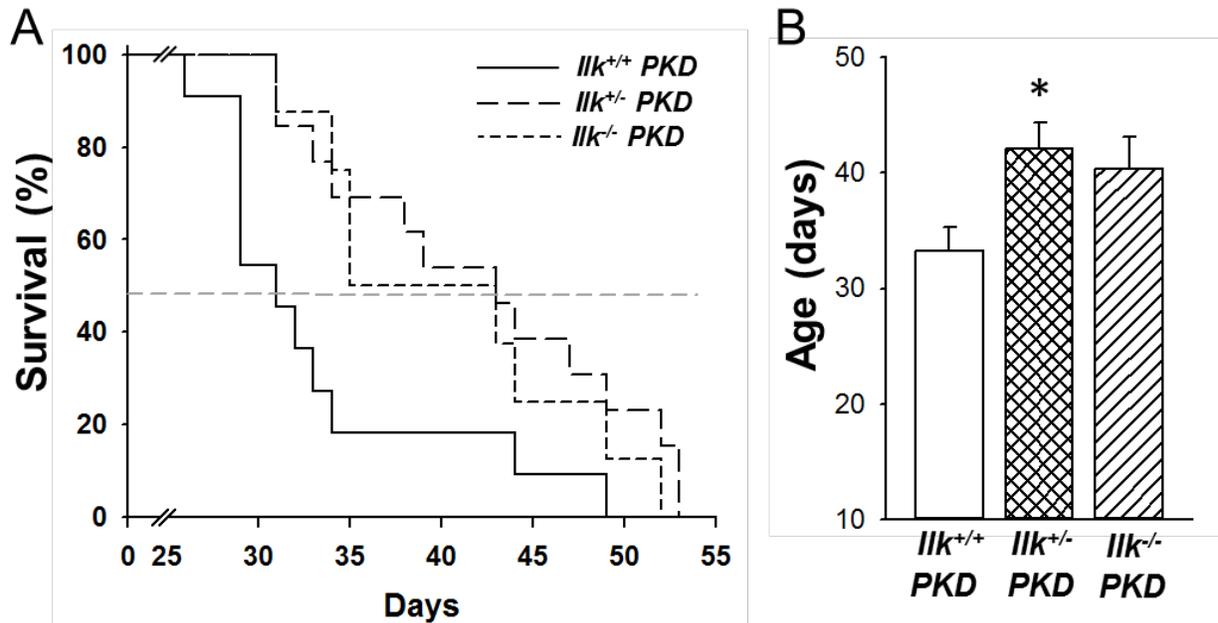
Figure 3-13. Effect of ILK expression on survival of *PKD* mice. (A) Kaplan-Meier survival curve for *Ilk$^{+/+}$;Pkd1$^{fl/fl}$;Pkhd1-Cre* (*Ilk$^{+/+}$ PKD,* N = 11), *Ilk$^{fl/+}$;Pkd1$^{fl/fl}$;Pkhd1-Cre* (*Ilk$^{+/-}$PKD*, N = 13) and *Ilk$^{fl/fl}$;Pkd1$^{fl/fl}$;Pkhd1-Cre* (*Ilk$^{-/-}$ PKD*, N = 8) mice. The dotted line represents the time point at which 50% of the mice had died. ILK knockdown in CD cells extended the survival of PKD mice. (B) Heterozygous loss of ILK significantly increased mean survival age from 33 ± 2 for the *Ilk$^{+/+}$ PKD* mice to 42 ± 2 days for the *Ilk$^{+/-}$ PKD* mice, *P< 0.05. Complete loss of ILK (*Ilk $^{-/-}$ PKD*) appeared to extend survival; however, the difference did not reach statistical significance.

3.4.5. Effect of ILK on PKD progression in *pcy/pcy* mice

Next, we examined the role of ILK in *pcy/pcy (pcy)* mice, a well-characterized slowly progressive model of PKD [235, 236]. We crossed *Ilk* $^{fl/+}$ and *Pkhd1-Cre* mice to *pcy* mice to generate *Ilk$^{+/+}$;pcy/pcy* (*Ilk$^{+/+}$ pcy*) and *Ilk$^{fl/+}$;Pkhd1-Cre;pcy/pcy* (*Ilk$^{+/-}$ pcy*) mice. Male *Ilk$^{+/+}$ pcy* and *Ilk$^{+/-}$ pcy* mice were euthanized at 10 weeks, and BW, KW(%BW), cystic index and fibrosis were measured (**Figure 3-14**). We found that *Ilk$^{+/-}$ pcy* mice had a pronounced reduction in KW(%BW), with no effect on body weight. There was a pronounced reduction in cystic area and cyst number compared to *Ilk$^{+/+}$ pcy* mice. Measurement of Ki-67 positive cells showed a 59% reduction in proliferating cells in the *Ilk$^{+/-}$ pcy* kidneys. There was prominent interstitial fibrosis in *pcy* mice, and reduced ILK decreased fibrotic area by more than 50%. mTOR signaling is elevated in *pcy* kidneys [4] and reduced ILK expression downregulated both P-S6K and total S6K (**Figure 3-15**). We found that the average BUN for *Ilk$^{+/+}$ pcy* mice at 25 weeks was 57.4 mg/dl, demonstrating a decline in renal function (**Figure 3-16 A**). These mice lived to an average age of 40 weeks (**Figure 3-16 B**) [5]. By comparison, BUN for *Ilk$^{+/-}$ pcy* littermates was significantly lower (42.0 mg/dl) and the mice survived to 48 weeks, indicating a 20% increase in lifespan. Taken together, these data demonstrate that ILK plays an important role in renal cyst growth and fibrosis in PKD.
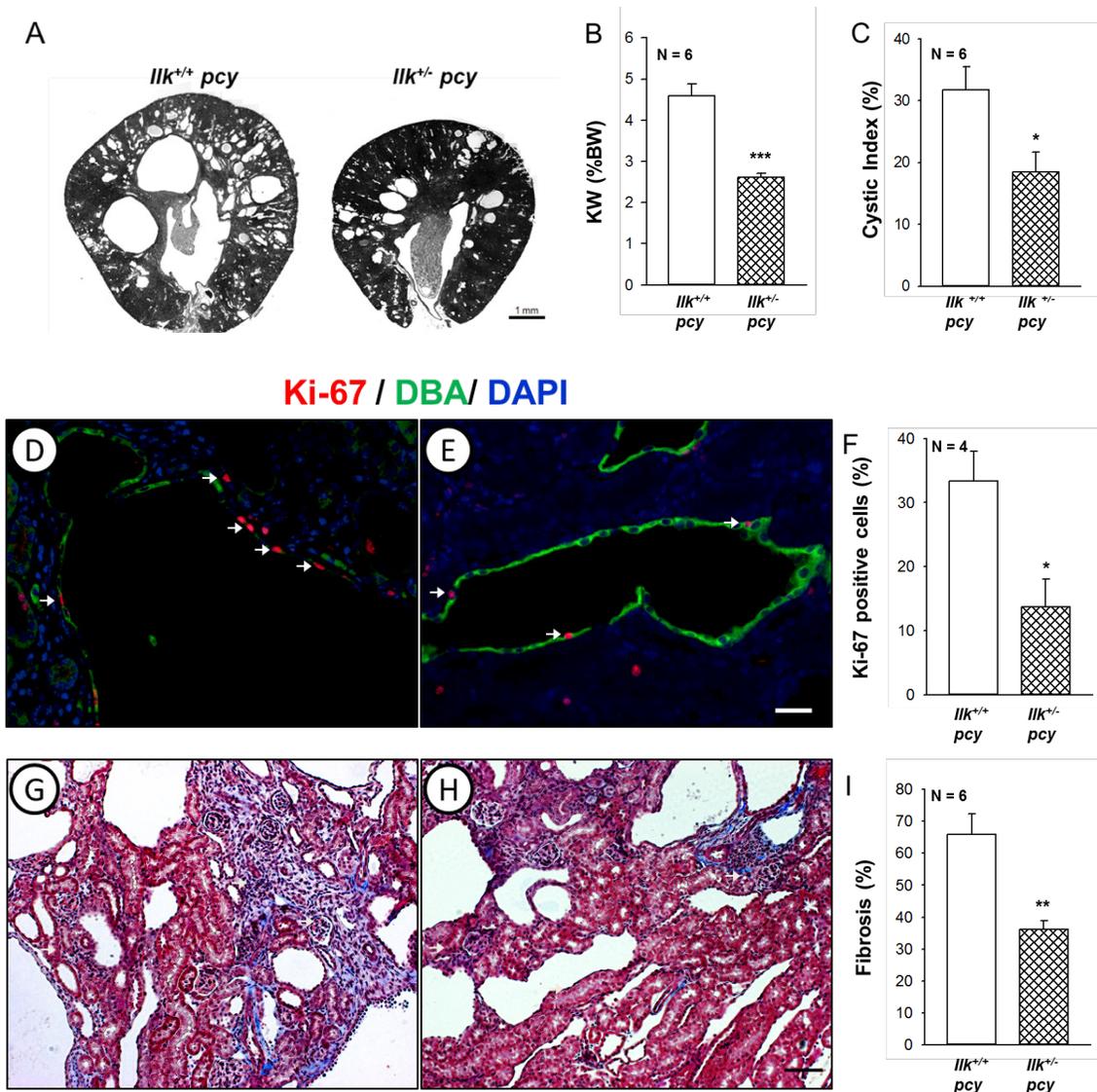
Figure 3-14. Effect of ILK expression on renal cyst development in *pcy* mice. (A) Representative images of kidney cross-sections of *Ilk*$^{+/+}$*;pcy/pcy* (*Ilk*$^{+/+}$ *pcy*) and *Ilk*$^{fl/+}$*;Pkhd1-Cre;pcy/pcy* (*Ilk*$^{+/-}$ *pcy*) mice at 10 weeks of age. Images were taken at the same magnification. Scale Bar = 1 mm. There was a dramatic reduction in (B) kidney weight (% BW), (C) cystic index in *Ilk*$^{+/-}$*pcy* mice compared to *Ilk*$^{+/+}$ *pcy* mice. compared to *Ilk*$^{+/+}$ *pcy* mice. Proliferating cells were determined in kidney sections from (D) *Ilk*$^{+/+}$ *pcy* and (E) *Ilk*$^{+/-}$ *pcy* mice that were stained for Ki-67 (red), DBA (green) and DAPI (blue). Arrows indicate Ki-67 positive cells. Images were taken at the same magnification. Scale bar = 5 µm. (F) Comparison of nuclear Ki-67 staining in *Ilk*$^{+/+}$ *pcy* and *Ilk*$^{+/-}$ *pcy* sections, normalized to total nuclei. Representative kidney sections from (G) *Ilk*$^{+/+}$ *pcy* and (H) *Ilk*$^{+/-}$ *pcy* mice were stained with Masson's trichrome to visualize interstitial fibrosis. Scale bar = 50 µm. (I) Tissue sections stained with Masson's trichrome were coded to conceal the group assignment and visually scored for percentage of interstitial edema and fibrosis. *P <0.05, **P <0.01, and ***P < 0.001 compared to *Ilk*$^{+/+}$ *pcy*.
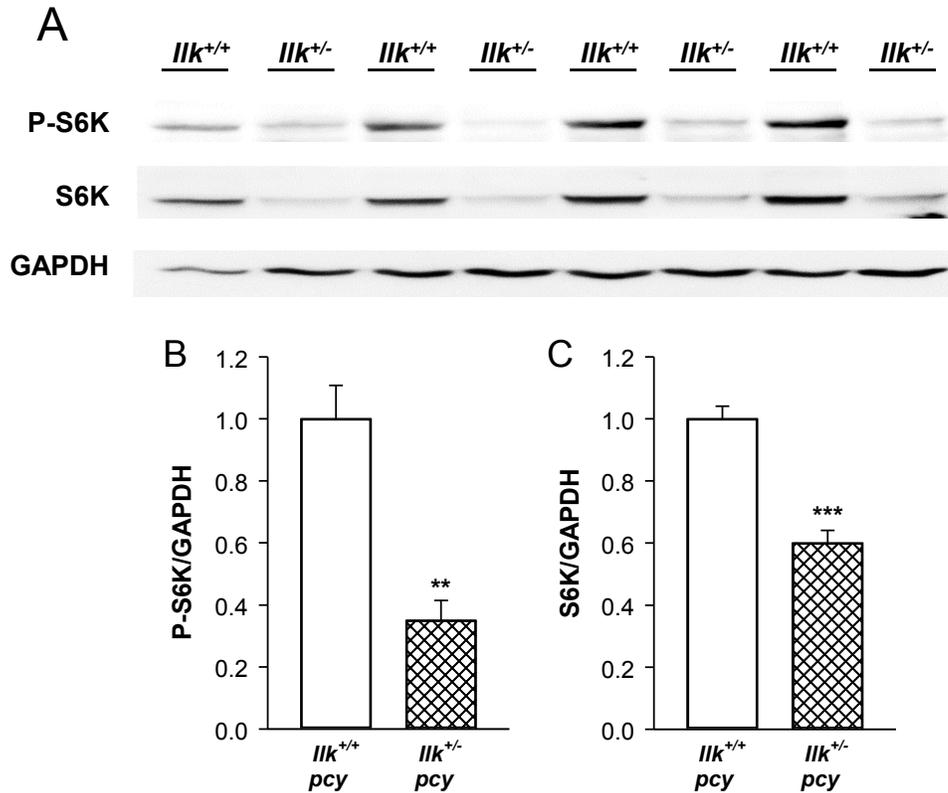
Figure 3-15. Effect of ILK expression on renal mTOR signaling in *pcy* kidneys. (A) Immunoblot analysis was used to compare phosphorylated S6 kinase (P-S6K) and total S6K in kidneys of 10-week old *Ilk*^{+/+}*;pcy/pcy* (*Ilk*^{+/+}), and *Ilk*^{fl/+}*;Pkhd1-Cre;pcy/pcy* (*Ilk*^{+/-}) mice. P-S6K and S6K were normalized to GAPDH, a reference protein. The bar graphs are mean ± SE for the effect of ILK expression on renal (B) P-S6K and (C) total S6K, normalized to GAPDH (N = 4 per group). Previously, total S6K and P-S6K were shown to be upregulated in *pcy* mice, relative to total protein[4]. These data show that reduced ILK expression in CDs of *pcy* mice significantly reduced P-S6K and total S6K, demonstrating that ILK is central for the aberrant mTOR activity in cystic disease. $^{**}P < 0.01$ and $^{***}P < 0.001$, compared to *Ilk*^{+/+} *pcy*.
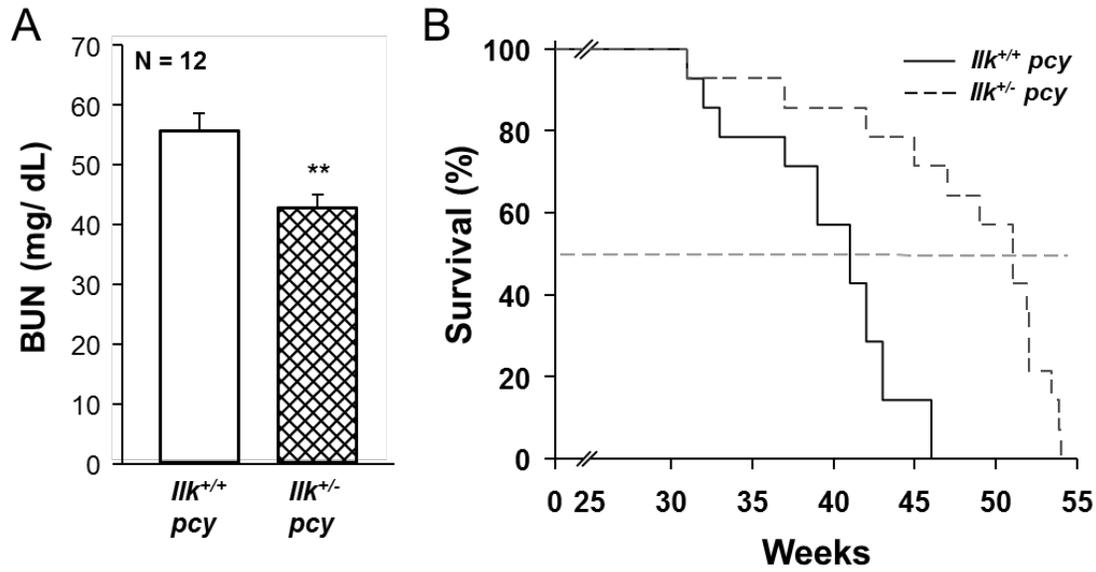
Figure 3-16. Effect of ILK knockdown on renal function and survival in *pcy* mice. *Ilk$^{+/+}$;pcy/pcy* (*Ilk$^{+/+}$ pcy*) and *Ilk$^{fl/+}$;Pkhd1-Cre;pcy/pcy* (*Ilk$^{+/-}$ pcy*) mice were given standard chow and water *ad libitum* and monitored regularly until moribund. (A) At 25 weeks, blood was collected from the tail vein and BUN was measured to assess renal function (N = 12 mice per group). $^{**}P <0.01$, compared to *Ilk$^{+/+}$ pcy*. (B) Kaplan-Meier survival curve indicates that heterozygous loss of ILK significantly increased the average lifespan of the *pcy* mice (N = 14 mice per group). Average survival age increased from 40 ± 2 weeks for the *Ilk$^{+/+}$ pcy* mice to 48 ± 2 weeks for the *Ilk$^{+/-}$ pcy* mice, $P < 0.001$.

3.5. Discussion

Our results demonstrate that 1) ILK is a central intermediate for periostin activation of the Akt/mTOR pathway and proliferation of human ADPKD cells, 2) pharmacological inhibition of ILK blocked periostin-induced Akt/mTOR signaling and cell proliferation, 3) heterozygous knockdown of ILK in CDs of WT mice had no effect on renal morphology or function, whereas complete ILK knockout caused caspase-3-mediated anoikis, dilated cortical tubules with apoptotic cells in the lumens, interstitial fibrosis, and death of the mice by 10 weeks of age, 4) reduced ILK expression in *Pkd1^fl/fl^;Pkhd1-Cre* and *pcy/pcy* mice decreased renal Akt/mTOR activity, cell proliferation, cyst growth, and interstitial fibrosis and significantly extended the survival of PKD mice and 5) homozygous deletion of ILK in the CDs of *Pkd1^fl/fl^;Pkhd1-Cre* mice decreased cystic index, in part, due to apoptosis of the cystic cells.

In PKD, aberrant cell proliferation is responsible for the formation and growth of renal cysts; however, the mechanisms remain unclear. One hypothesis is that mutations in the PKD genes incite a maladaptive repair mechanism, involving pathways that activate cell proliferation [106]. Abnormal and extensive expression of ECM molecules, including laminins, collagens, and matricellular proteins, accelerate cyst growth through activation of integrin signaling [2, 23, 118, 143, 155]. Recently, we discovered that periostin, a tissue repair molecule, was highly overexpressed in ADPKD, ARPKD and animal models of cystic disease [2]. Periostin binding to α_V-integrins activates mTOR and promotes the proliferation of human ADPKD cells. Global knockout of periostin in *pcy* mice led to a striking reduction in renal mTOR activity, cell proliferation, cystic area and tubulointerstitial fibrosis [5].

ECM and matricellular proteins regulate gene expression by integrin signaling through ILK, which has been shown to be necessary for embryonic development of the kidneys. Deletion

of ILK in the ureteric bud of *Ilk^{fl/fl};HoxB7-Cre* mice caused tubule obstruction, and the mice died at 8 weeks of age [211]. Conditional knockout of ILK using a tamoxifen-inducible Cre caused a urinary concentrating defect which the authors attribute to a disruption of AQP2 expression and localization; however, a compensatory increase in V2 receptor activation or cAMP expression was not observed. Morphological changes in the kidneys were not reported [232]. Here, we show that postnatal ablation of ILK in CDs caused a urinary concentrating defect, a decline in body weight and the mice died by 10 weeks of age. Loss of ILK caused anoikis and tubule dilations in the kidneys. Thus, complete knockout of ILK appeared to disrupt the connection between the ECM and cell cytoskeleton, leading to detachment of CD cells into the lumen and tubule obstruction.

Pkd1^{fl/fl};Pkhd1-Cre mice die at ~33 days of age due to renal failure. Complete knockout of ILK caused apoptosis of the cystic epithelial cells, contributing to a reduction in the cyst area and size of the cystic kidneys. Mice with heterozygous knockout of ILK in CDs had normal kidneys, urinary concentrating ability, BUN and lived beyond one year. Importantly, reduction in ILK expression in the *Pkd1^{fl/fl};Pkhd1-Cre* mice and *pcy* mice decreased Akt/mTOR signaling, cell proliferation, cyst number, cystic index and fibrosis. There was improved renal function and increased lifespan of the PKD mice. Previously, a small molecule ILK inhibitor was shown to reduce renal fibrosis in a model of obstructive nephropathy [237], suggesting that ILK inhibition may be an effective approach for the treatment of ADPKD. Since complete knockout of ILK in CD cells caused renal injury, long-term use of an ILK inhibitor would need to be considered with caution.

In summary, aberrant secretion of periostin by cystic epithelial cells activates the ILK-Akt-mTOR pathway, promoting cyst growth and fibrosis **(Figure 3-17)**. We propose that

targeting the periostin-integrin-ILK axis may be a potential therapeutic approach to slow cyst growth and fibrosis in PKD.
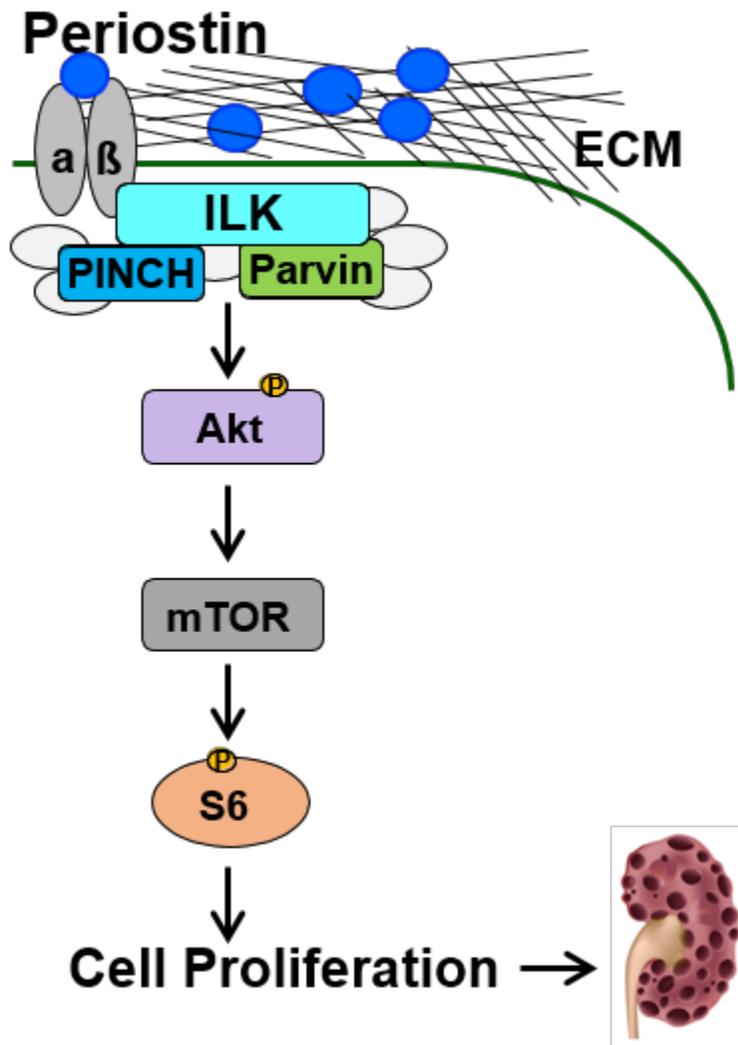
Figure 3-17. ILK promotes periostin-induced ADPKD cell proliferation and cyst growth. Binding of periostin to α_V-integrins stimulates integrin-linked kinase (ILK), a scaffold protein that is essential for linking the extracellular matrix to the actin cytoskeleton, leading to Akt/mTOR pathway-mediated cell proliferation and cyst growth in ADPKD.

CHAPTER 4. PERIOSTIN ACTIVATES PATHWAYS INVOLVED IN TISSUE REPAIR AND ACCELERATES PKD PROGRESSION

4.1. Abstract

In polycystic kidney disease (PKD), persistent activation of the Akt/mTOR pathway, cell proliferation and matrix production by cystic epithelial cells appears to be consistent with the activation of a futile repair response that contributes to cyst growth and tubulointerstitial fibrosis. Periostin is a matricellular protein involved in tissue repair and is aberrantly expressed in PKD. Previously, we showed that periostin binds to $\alpha_V\beta_3$- and $\alpha_V\beta_5$-integrins and activates integrin-linked kinase (ILK) leading to Akt/mTOR-mediated ADPKD cell proliferation. Here, we found that periostin activates focal adhesion kinase, Rho GTPase, cytoskeletal reorganization, actin stress fiber formation, and cell migration. Periostin also stimulates the expression of genes involved integrin signaling and ECM production in human PKD cells. These *in vitro* data are consistent with periostin activation of cellular pathways involved in tissue repair. To determine if overexpression of periostin in the cyst-lining cells accelerates PKD progression, we generated *pcy/pcy* mice with conditional overexpression of periostin selectively in collecting duct (CD) cells. CD-specific periostin overexpression significantly increased renal mTOR activity, cell proliferation, cyst growth and interstitial fibrosis. Taken together, our results suggest that aberrant expression of periostin could contribute to a futile repair program, leading to increased mTOR-mediated cell proliferation, cytoskeletal remodeling, and fibrosis, promoting PKD progression.

4.2. Introduction

Autosomal dominant polycystic kidney disease (ADPKD) is a commonly inherited renal disorder [238]. In ADPKD, renal cyst formation begins *in utero* and is caused by the aberrant proliferation of tubular epithelial cells and accumulation of fluid in the newly formed cysts due to transepithelial fluid secretion [76, 79]. Several signaling pathways aberrantly regulated in ADPKD, have been shown to play a role in cyst growth [116-118, 239]. This altered regulation appears consistent with transcriptional reprogramming typically seen during tissue repair and perhaps, further accelerates the disease [240, 241].

Periostin, 90-kDa matricellular protein, is typically expressed in tissues involved in mechanical stress, such as periodontal ligaments, periosteum, skin, and bone. Atypical expression of periostin is also observed in carcinomas, and in the ECM of tissues following acute injury to tissues such as the heart, lung and skin [135, 157, 158, 242-244]. In addition to modulating biomechanical properties of tissues, periostin binds α_V-integrins on the cell surface and activates cellular pathways involved in cell proliferation, survival, and profibrotic TGF-β signaling [2, 8, 137, 164, 169-171].

We found that periostin is aberrantly expressed in human ADPKD, human autosomal recessive PKD (ARPKD) and several mouse models of renal cystic disease, while it is not expressed in a normal adult kidney [2, 5]. Periostin binding to $\alpha_V\beta_3$- and $\alpha_V\beta_5$-integrins promotes ADPKD cell proliferation by activating integrin-linked kinase (ILK) and stimulating downstream Akt/mTOR signaling [245]. Further, genetic deletion of periostin in *pcy/pcy* (*pcy*) mice decreased renal mTOR activity and delayed the progression of the cystic disease, demonstrating that periostin is an important modifier of PKD [5]. Several human and murine renal injury models including, diabetic nephropathy, hypertensive nephropathy, and glomerulosclerosis show

aberrant periostin expression. In fact, urinary periostin may be a potential biomarker for chronic kidney diseases [136, 243, 244, 246], suggesting that unchecked periostin-integrin signaling may be involved in tissue repair in renal pathologies.

Here, we determined if periostin stimulates pathways involved in tissue repair in human ADPKD cells and if overexpression of periostin activates mTOR signaling, promoting proliferation and cyst growth, and fibrosis in PKD mice.

4.3. Materials and Methods

Human ADPKD and normal human kidney cells. Primary cultures of ADPKD and normal human kidneys (NHK) cells were generated by the PKD Biomarkers and Biomaterials Core in the Kansas PKD Center at the Kansas University Medical Center (KUMC) as described [245]. Cells were grown in DMEM/F12 supplemented with 5% FBS, penicillin G and streptomycin (P/S), and a cocktail of insulin, transferrin, and sodium selenite (ITS). Upon reaching 70-80% confluence, the cells were trypsinized using a trypsin-EDTA solution (Sigma Chemical, Saint Louis, MO) and re-plated for experiments. Primary ADPKD and NHK cells were not passaged more than two times before use in experiments. We tested the effect of 75 kDa (Biovendor, Asheville, NC) and full-length 91.7 kDa (R&D Systems, Minneapolis, MN) periostin and found that had similar effects on *in vitro* experiments, consistent with our earlier findings [2, 245], and have been used interchangeably.

Cell migration assay. ADPKD cells (1×10^5) were seeded into individual wells of 12-well plates containing DMEM/F12, ITS, 1% FBS and P/S. After cells reach approximately 80% confluency,

the serum was reduced to 0.05%. 24 h later, a 200 μm pipette tip was used to create a uniform scratch in the cell layer near the middle of the well. Immediately after the scratch, cells were treated with control media, 250 ng/ml human recombinant periostin or 25 ng/ml hepatocyte growth factor (HGF; Sigma Chemical), which was used as a positive control for cell migration [247]. The scratched area was imaged using Nikon Eclipse Ti microscope (Nikon Instruments, Melville, NY) with a motorized stage that was controlled by computer software. This allowed repeated measurements to be made at the same location within each well. Plates were allowed to equilibrate for 4 h in the incubation after setting up the imaging parameters, and images were captured for measurements 4 h and 8 h post-wounding. The extent of closure was determined relative to the area of the initial wound, using Metamorph Image Analysis software (Molecular Devices, Sunnyvale, CA). Percent closure for each treatment was determined from 4 h to 8 h and normalized to control. Treatments were carried out in triplicates, and two picture fields per well were examined.

Quantitative RT-PCR. NHK and ADPKD cells (0.5×10^6) were plated on transwells (Costar, Kennebunk, ME; 34320) and grown in media containing 1% FBS until they formed tight epithelial monolayers. Control media or media containing periostin (250 ng/ml) was added to the both sides of the monolayer for 24 hours. RNA was isolated using RNeasy isolation kit (Qiagen), and its integrity was verified using an Agilent Bioanalyzer (Santa Clara, CA). cDNA was synthesized from 1 μg of total RNA, using the iScript™ advanced cDNA synthesis kit for RT-qPCR (Biorad, Munich, Germany) according to manufacturer instructions. Real-time PCR reactions were set up by preparing a master mix of cDNA samples (1.92 μg/ 96-well plate) and the SsoAdvanced™ Universal SYBR® Green Supermix (Biorad; 960 μl/ 96-well plate). We

used the Biorad PrimePCR array plates for integrin outside-in signaling, collagen diseases, wounds and injuries, and transcription factors (tier 1) to screen 220 genes, many of which are markers for tissue repair. GAPDH, HPRT1, and TBP were used as reference genes, and results were analyzed with the PrimePCR™ Analysis Software (Biorad). Changes greater than 1.5-fold and $p < 0.05$ were considered significant. Three different cell preps were used for the screen, and results were validated by qPCR in a separate study with primers purchased from SuperArray (Frederick, MD) or Genecopoeia (Rockville, MD).

Measurement of activated Rho. ADPKD and NHK cells were plated onto plastic petri dishes (100 mm diameter) and grown in media containing 1% FBS. Serum was reduced to 0.002% when the cells reached 75% confluency. Treatments were carried out as indicated, and lysates were prepared in Triton lysis buffer at the specified time points. Rho was immunoprecipitated from cell lysates using GST-RBD beads that have a high affinity for GTP-bound Rho. For negative control, GDP was loaded before immunoprecipitation to inactivate endogenous Rho. The immunoprecipitate and the whole cell lysates were immunoblotted using a Rho antibody. Rho activity was defined as GTP-bound Rho to total Rho, normalized to control treatment.

Western blot analysis. ADPKD and NHK cells were plated on petri dishes or transwell supports, in DMEM/F12 medium as described above. Treatments were as indicated and lysates were prepared in Triton lysis buffer at the specified time points. Tissue lysates were also prepared from mice kidneys as described previously [229]. Total protein concentration was determined using BCA protein assay (Pierce, Rockford, IL) and 75 µg of protein was used for immunoblot analysis [224]. The following antibodies were used: P-FAK (Cell Signaling Technology, Beverly,

MA [CS]; 3283), FAK (ThermoFisher Scientific, AHO0502), GAPDH (CS 2118), integrin β_1 (Abcam [ab] Inc., Cambridge, MA; 529751), integrin α_v (ab 179475), integrin β_3 (CS 4702), and periostin (ab 14041). The blots were then incubated with an HRP-linked secondary antibody against rabbit or mouse (NA934, NA931; GE Healthcare). Bands were detected with ECL (RPN2232, GE Healthcare), imaged using an AI 600 imager (GE Healthcare) and quantified with Biorad Quantity One program.

Generation of transgenic mice with conditional overexpression of periostin. A cDNA encoding mouse *Postn* and a 3' bovine growth hormone polyadenylation signal were subcloned into pBT378-mCherry-LSL-MCS. An attB-flanked targeting construct was co-injected with RNA encoding the PhiC31 integrase (Applied Stem Cell, Milpitas, CA) into pronuclei of homozygous Rosa26-P3 mice [248] by the University of Kansas Medical Center Transgenic and Gene-Targeting Institutional Facility. Embryos were implanted in pseudopregnant females and the pups were genotyped by PCR to identify a founder with the transgene integrated into the attP sites at the Rosa26 locus via PhiC31 mediated integration. This founder line was expanded for further analysis. The resulting transgenic strain (*Postn^{tg}*) harbors the *Postn* coding sequences downstream of a splice acceptor and loxP-flanked-mCherry STOP cassette under the transcriptional control of the endogenous Rosa26 transcriptional regulatory elements (**Figure 4-6**). In the absence of Cre recombinase expression, mCherry (but not *Postn*) is expressed under the control of the broadly expressed Rosa26 promoter. Cre-mediated excision of the floxed-mCherry STOP results in *Postn* expression under the transcriptional control of Rosa26.

Characterization of mice with collecting duct-specific overexpression of periostin. Postn^{tg} mice were crossed to *Pkhd1-Cre* mice, which express cre-recombinase specifically in the collecting

ducts (CD [226] to generate *Postn^{tg};Pkhd1-Cre* (*Postn^{TG}*) and littermates that lacked the cre (*Postn^{tg}*) or the transgene (*Pkhd1-Cre*). Both genotypes will be referred to as wild type (WT) since appeared normal and were indistinguishable from each other. To determine the effect of CD-specific overexpression of periostin in PKD, we crossed *Postn^{tg}* mice to *pcy/pcy* (*pcy*) mice, a slowly progressive PKD model [5, 228], orthologous to human nephronophthisis type 3 (NPHP3). The course of disease progression in *pcy* mice phenocopies human ADPKD, with cystic enlargement of the kidney, interstitial fibrosis, and progressive decline in renal function by 48 weeks of age [228]. We generated *Postn^{tg};Pkhd1-Cre;pcy/pcy* (*Postn^{TG} pcy*) and littermate *Postn^{tg};pcy/pcy* or *Pkhd1-Cre;pcy/pcy* mice (both genotypes were indistinguishable and will be referred to as *pcy* mice). We observed normal Mendelian inheritance. Mice were monitored daily and provided food and water *ad libitum*. One group of mice were euthanized at 10 wk of age and cardiac puncture was performed to collect blood for measurement of blood urea nitrogen (BUN) followed by removal of the kidneys, as described previously [245]. The second group of mice was euthanized at 30 wk. The third group of mice was set aside for survival study where they received food and water *ad libitum* and were monitored every day until their death. In some cases, these mice were euthanized when they showed signs of imminent death, as described previously [245]. The Animal Care and Use Committee at KUMC approved the protocols for the use of these mice. All the mice used for breeding and experiments were 5-6 generations backcrossed to *pcy/pcy* mice.

Genotyping. We genotyped for the presence of the *Postn^{tg}* using PCR. The forward primer sequence was 5′- GCCATCATCAAGGAGTTCATGCGCTTC -3′ and the reverse sequence was 5′- GGAGGTGATGTCCAACTTGATGTTGACG -3′. For genotyping for Cre alleles, the

forward sequence was 5′- GCGGTCTGGCAGTAAAAACTATC -3′ and the reverse primer was 5′- GTGAAACAGCATTGCTGTCACTT -3′. Cre-mediated excision of the floxed-mCherry STOP was validated using the forward primer sequence 5'-GCGCAGTAGTCCAGGGTTTCCTTGATGATG -3' and the reverse primer sequence 5'-AGAATTTGCTGGAGGGCACAGACGTTTGGG -3' and gave a ~ 400 bp product (data not shown).

Histology, immunofluorescence, and immunocytochemistry. Kidney sections fixed in 4% paraformaldehyde overnight, were embedded in paraffin blocks and sectioned onto microscope glass slides. For immunofluorescence, tissues were deparaffinized, rehydrated, and subject to antigen retrieval with Antigen Unmasking Solution (Vector Laboratories, Burlingame, CA). Tissues were incubated with primary antibodies overnight at 4°C and secondary antibodies for one hour at room temperature. For immunocytochemistry, ADPKD and NHK cells were grown on 25 mm glass coverslips (Fisher Scientific, PA). At 75% confluency, cells were serum-deprived for 24 h and treated as indicated. Cells are then fixed in 4% paraformaldehyde and stained with the $\alpha_V\beta_3$ (Merk Millipore, MA; MAB1976) and corresponding anti-mouse IGG (H+L) - CS 4408; or with phalloidin to stain actin fibers (ThermoFisher Scientific; A12379). The following primary antibodies were used to stain renal tissues: Ki-67 (ab15880 and blocking peptide ab15881), periostin (Origene, Rockville, MD; TA500070,), P-S6 (CS 4858), and corresponding secondary antibodies (ab 150084, CS 4408). Sections were co-stained with FITC or rhodamine-conjugated Dolichos *biflorus* agglutinin (DBA; FL-1031 or RL-1032, Vector) to label CD cells and mounted with a mounting agent that contained DAPI (ThermoFisher Scientific; P36931). Slides were coded to deindentify the genotype and three non-overlapping

fields were imaged per section using a Nikon Eclipse Ti microscope. Nuclear Ki-67 and cytoplasmic P-S6 staining were quantified using the multi-wavelength cell scoring application in Metamorph Image Analysis software.

Measurement of renal cystic area. Slides mounted with tissue sections were coded, stained with hematoxylin and eosin, and imaged using a dissecting microscope (Leica Microsystems, Buffalo Grove, IL) connected to a digital color camera. A tubule dilation of 0.002 mm^2 was considered as a cyst. The total number of cysts, cystic area, and the total area of the kidney were measured using Image Pro Premiere (Media Cybernetics Inc, Silverspring, MD) as described previously [5].

Measurement of tissue fibrosis. Masson's trichrome was used on tissue sections to visualize collagen fibers (blue) [5] and pre-fibrotic edematous areas characterized by an increase in spacing between tubules (pale blue). Representative images were captured post-analysis using a Nikon T-DH microscope attached to a digital color camera. Tissues sections were scored by a naïve observer assigning a percentage of fibrotic/edematous cortical area per total area of the cortex. $Postn^{TG} pcy$ mice develop modest fibrosis by 10 wk.

Measurement of blood urea nitrogen (BUN). Blood was collected by cardiac puncture from experimental mice at the time of euthanasia. Serum was isolated by centrifugation at 10,000 RPM for 10 min. A colorimetric QuantiChrom urea assay kit (DIUR 100; Bioassay Systems, Hayward, CA) was used to quantitate urea concentration, and BUN was calculated using the formula BUN = (Urea/2.14).

Statistics. Data are expressed as mean ± standard error (SE). Statistical significance was determined by unpaired t-test for comparisons between two experimental groups. For comparisons between multiple experimental conditions, one-way analysis of variance (ANOVA) followed by Student-Newman-Keuls (SNK) post-test was used. The Gehan-Breslow analysis was performed to determine statistical significance for survival studies. Pairwise analysis of the survival curves was performed using the Bonferroni method.

4.4. Results

4.4.1. The role of periostin in cytoskeletal reorganization in ADPKD cells.

Previously, we showed that periostin promotes the proliferation of human ADPKD cells, but not normal human kidney cells. This difference in the response is likely due to differences in the expression of α_V-integrin, the receptor for periostin[2]. To determine if periostin induces structural changes in the actin cytoskeleton, ADPKD cells were treated with periostin for 1 h and actin was visualized using phalloidin conjugated to green fluorescent protein. Periostin caused stress fiber formation and bundling of actin filaments into transverse and ventral stress fibers. (**Figure 4-1**). We also found integrin-clustering with an accumulation of α_V-integrins at focal adhesion junctions [249]. The formation of mature focal adhesions is responsible for ECM-integrin interaction to the actin cytoskeleton. Activation of focal adhesion kinase (FAK) is a rapid event in mature focal adhesions and promotes cell motility and actin cytoskeletal changes by activating Rho-family GTPases [250, 251]. Periostin induced tyrosine phosphorylation of FAK (**Figure 4-2**) and activation of RhoA, a small Rho-family GTPase. To examine cell motility, we measured the

migration of ADPKD cells following a scratch in the monolayer. Periostin accelerated wound healing by increasing the rate of cell migration in ADPKD cells by 42% (**Figure 4-3**); however, periostin had no effect on NHK cells (**Figure 4-4**). HGF was used as a positive control and accelerated the migration of both ADPKD and NHK cells. These results suggest that periostin mediates changes in the actin cytoskeleton and ADPKD cell motility by activation of FAK and RhoA.

Actin / DAPI

α_V-Integrin / DAPI
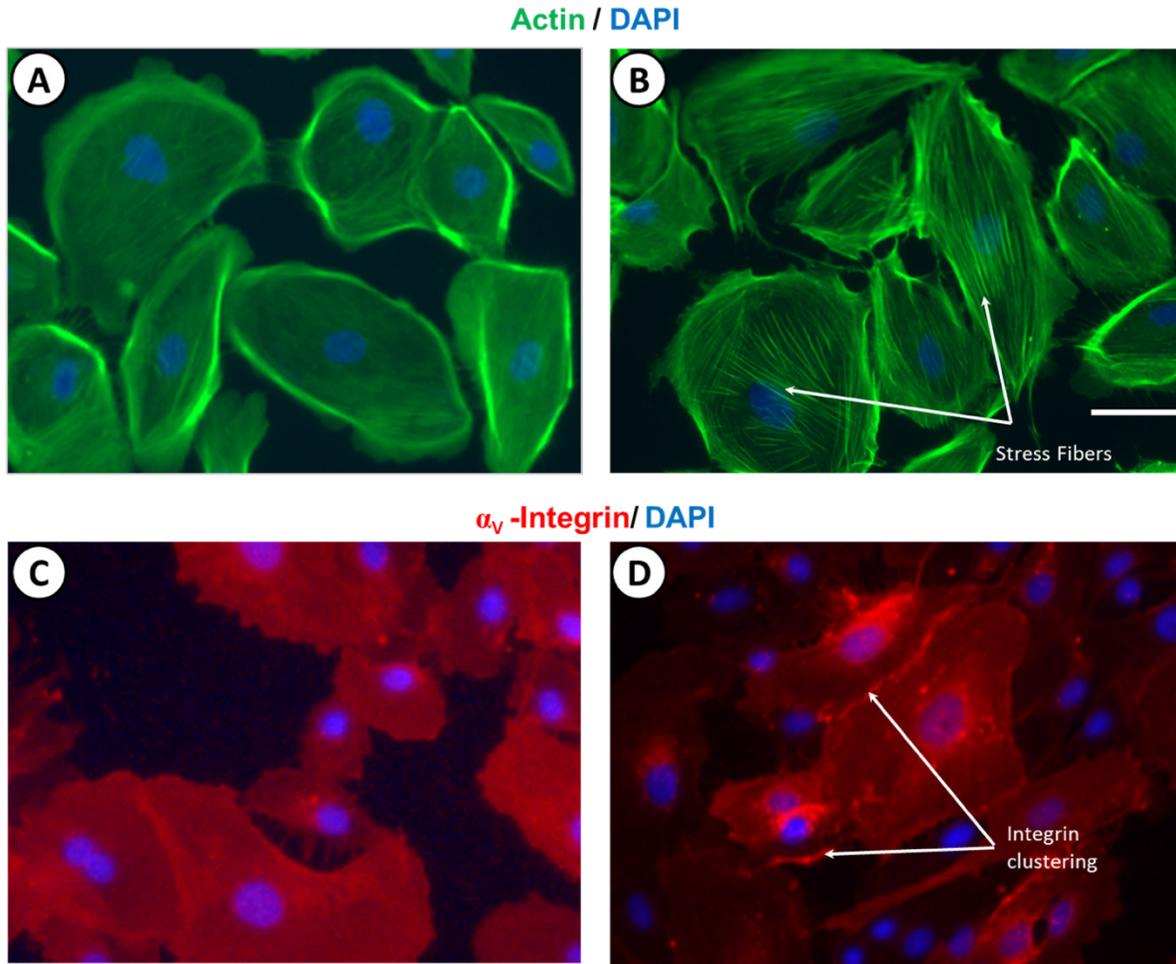
Figure 4-1. Effect of periostin on actin stress fiber formation and $\alpha_V\beta_3$-integrin clustering. Primary cells derived from human ADPKD kidneys were treated with control media (A, C) or 250 ng/ml recombinant periostin (B, D) for 1 h. (A, B) Cells were stained with phalloidin to visualize F-Actin fibers (green), and nuclei were stained with DAPI (blue). Arrows indicate the formation of the actin stress fibers. (C, D) Integrin clustering was determined by staining with $\alpha_V\beta_3$-integrin antibody (red). Arrows indicate integrin clustering at the cell membrane. Scale bar = 5 µm.
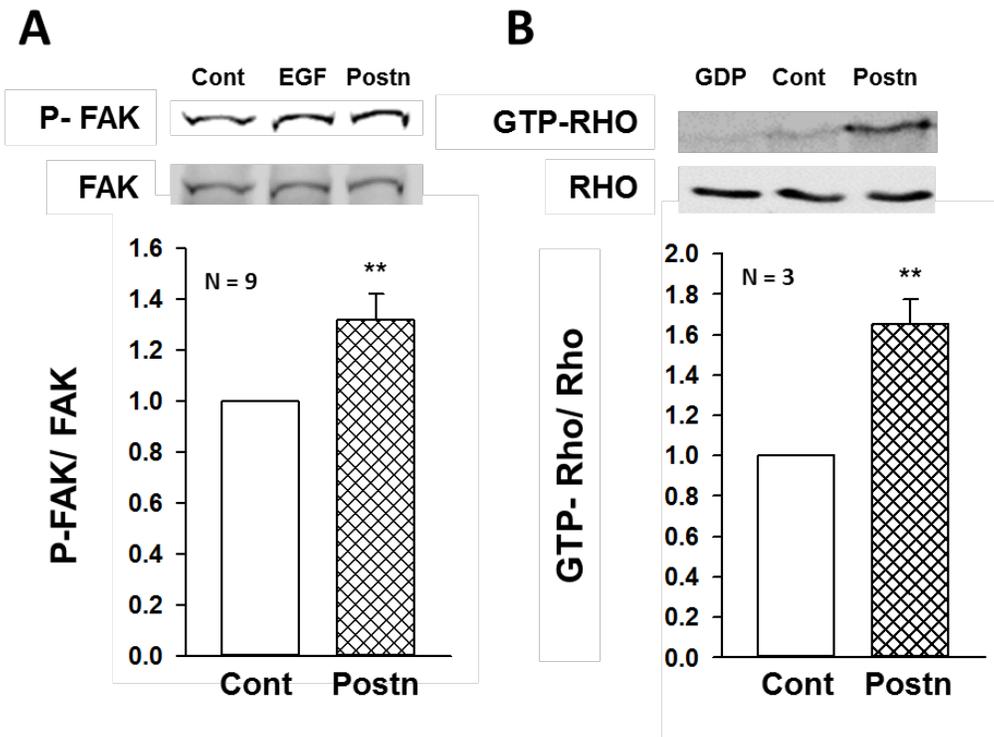
Figure 4-2. Effect of periostin on the activation of FAK and Rho signaling in ADPKD cells. Human ADPKD cells were incubated in media containing periostin for 15 min. Immunoblot analysis was used to measure the levels of phosphorylated FAK to total FAK. A representative immunoblot is shown. Bar graph represents mean and standard error (S.E) of phosphorylated FAK (P-FAK)/ total FAK, normalized to control (set to 1.0). Rho was immunoprecipitated from cell lysates using GST-RBD beads that have a high affinity for GTP-bound Rho. For negative control, GDP was loaded before immunoprecipitation to inactivate endogenous Rho. The immunoprecipitate and the whole cell lysates were immunoblotted for Rho. Bar graph represents mean and S.E of GTP-bound Rho to total Rho, normalized to control (set to 1.0). *P < 0.05 and **P < 0.01, versus control treatment.
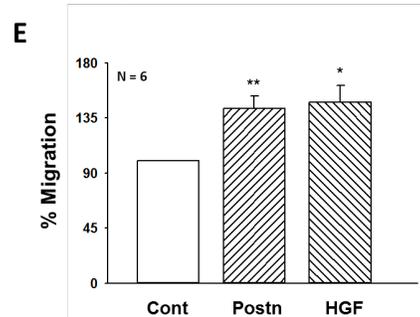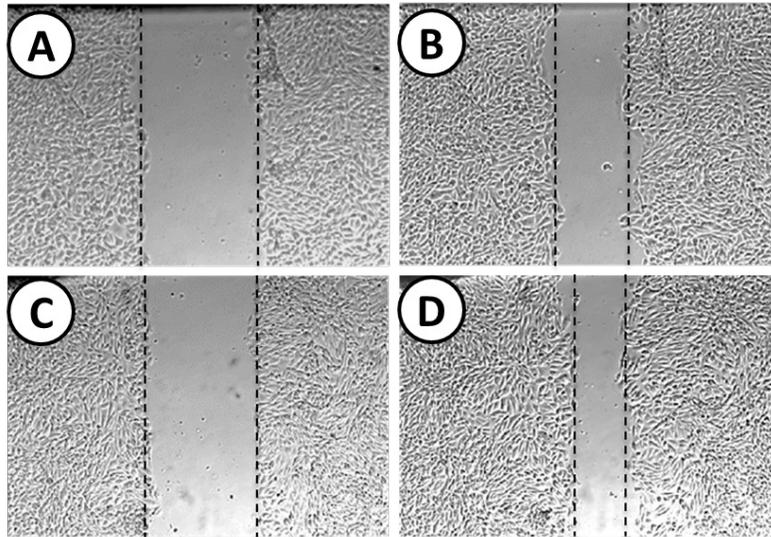
Figure 4-3. Effect of periostin on ADPKD cell migration. Confluent cell monolayers were scratched and then treated with control media (A and B), periostin (C and D) or 40 ng/ml HGF (images not shown). Representative images of ADPKD cell migration 4 h (A and C) and 8 h (B and D) post-wounding. (E) The graph represents the quantification of the cell migration between 4 h and 8 h post-wounding. **P < 0.01, *P< 0.05, versus control treatment.
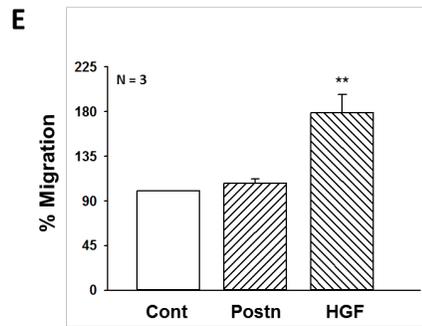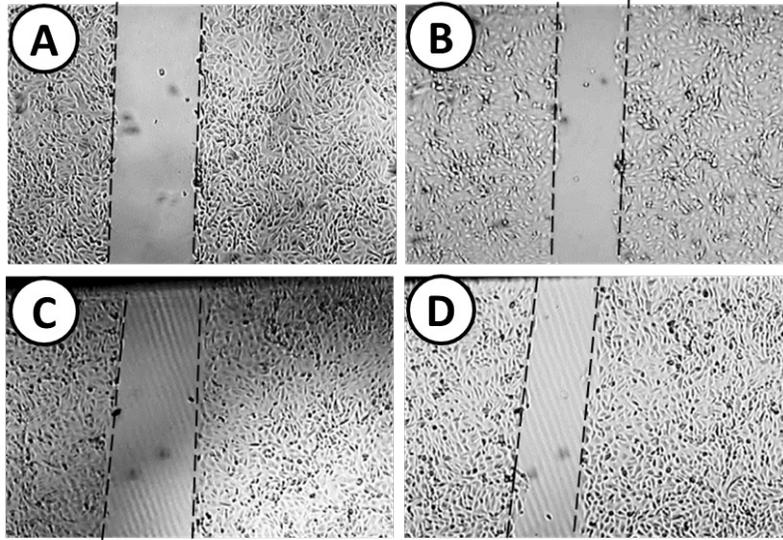
Figure 4-4. Effect of periostin on NHK cell migration. Confluent NHK cell monolayers were scratched, and then treated with control media (A and B), 250 ng/ml periostin (C and D) or 40 ng/ml HGF (images not shown). Representative images of NHK cell migration 4 h (A and C) and 8 h (B and D) post-wounding. (E) Graph represents the quantification of the cell migration between 4 h and 8 h post-wounding. N = 3 NHK cell preparations. **$P < 0.01$; *$P<0.05$, versus control treatment.

4.4.2. Periostin-induced gene expression changes in ADPKD cells.

We sought to determine if periostin changes genes involved in tissue repair. We grew ADPKD cell monolayers grown on transwell supports were treated with periostin or control media for 24 h. Changes in the expression of 220 genes for integrin signaling, cytoskeletal remodeling and growth factor signaling were determined by quantitative real-time PCR analysis using Biorad PrimePCR array panels and gene changes were analyzed by the BioRad CFX manager. Periostin differentially regulated genes (**Table 4-1**) involved in ECM production (collagens type I and IV), cytoskeletal remodelling, including integrins (α_V and β_3 ; **Figure 4-5**) and elements of actin cytoskeleton (β- Actin, Actinins, and Filamin), focal adhesion proteins (ILK, AKT and β- catenin), and some molecules involved in growth factor signaling (SRC, GRB2, ATF1, RAF1 and MAP3K1), consistent with periostin-mediated activation of pathways involved in tissue repair. Interestingly, there was a significant decrease in the expression of NR1H4, a gene that encodes the farnesoid X receptor (FXR), a member of the nuclear receptor subfamily.

Upregulated genes	Gene name	Fold regulation
ECM		
COL1A1	Collagen I Alpha 1	4.0
COL4A4	Collagen IV Alpha 4	1.8
Actin cytoskeleton		
FLNA	Filamin A	2.1
ACTB	Actin Beta	2.0
ACTN1	Actinin Alpha 1	1.7
ACTN4	Actinin Alpha 4	1.6
Integrins		
ITGAV	Integrin Alpha V	2.0
ITGA5	Integrin Alpha 5	1.5
Focal adhesion / Integrin signaling		
AKT1	AKT Serine/Threonine Kinase 1	1.6
ILK	Integrin Linked Kinase	1.6
CTNNB1	Beta-Catenin	1.6
Growth factor signaling		
SRC	SRC Proto-Oncogene	2.5
GRB2	Growth Factor Receptor Bound Protein 2	1.8

Downregulated genes	Gene name	Fold regulation
Renal injury signaling/nuclear receptor		
NR1H4	Farnesoid X-Activated Receptor	-4.3
Growth factor signaling		
ATF1	Activating Transcription Factor 1	-3.2
MAP3K1	MEK Kinase 1	-2.3
RAF1	Raf Proto-Oncogene	-1.6

Table 4-1. Periostin-induced gene regulation in ADPKD cells. Human primary ADPKD cells (N = 3 kidney preparations) were grown on transwells to form polarized epithelial monolayers. Cells were treated with or periostin for 24 h. Total cellular RNA was isolated and reverse transcribed. mRNA levels of 220 genes involved integrin outside-in signaling were detected using pre-designed PrimePCR arrays. The results were analyzed using Bio-Rad CFX Manager software. The genes that showed greater than ± 1.5-fold change in gene regulation, with a p-value less than 0.05 are represented here. The expression changes for these genes have also been validated in a separate study using qPCR.
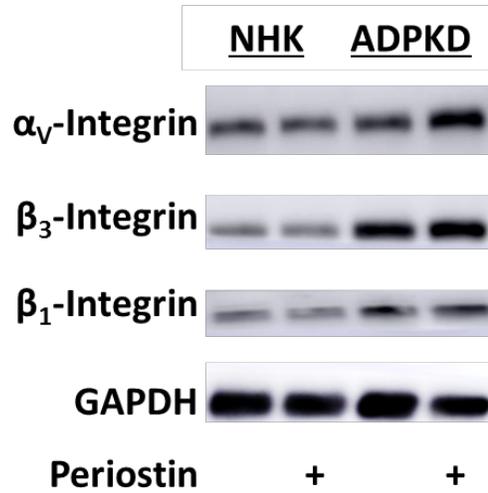
Figure 4-5. Effect of periostin on the expression of integrins α_V, β_1 and β_3 in ADPKD and NHK cells. 2 ADPKD and NHK cell preparations were grown on transwells and were treated with or without periostin for 24 h. The protein levels of α_V, β_1 and β_3 integrins were estimated by immunoblot analysis and normalized to relative levels of GAPDH. N = 2 ADPKD kidneys.

4.4.3. Generation of mice with CD-specific overexpression of periostin.

We generated periostin transgenic mice (*Postn^{tg}*), which allow tissue-specific overexpression of periostin (**Figure 4-6**). To obtain CD-specific expression of periostin, we crossed the *Postn^{tg}* mice to *Pkhd1-Cre* mice [226]. We confirmed periostin overexpression by immunoblot analysis of 10-wk-old mouse kidneys from *Postn^{tg};Pkhd1-Cre* (*Postn^{TG}*) mice (**Figure 4-6 B**). The littermate wildtype (WT) mice (*Postn^{tg}* and *Pkhd1-Cre* mice) did not express periostin, consistent with our previous observations [5]. CD-specific expression of the *Postn^{TG}* mice was visualized by immunofluorescence (**Figure 4-6 C, D**) using antibodies to periostin (green, ECM staining) and AQP-2 (red; a CD marker). Kidney sections from *Postn^{TG}* mice expressed periostin in the ECM adjacent to the CD cells. By contrast, WT kidneys did not display periostin expression, consistent with earlier observations [5]. At 10 weeks, we did not see cysts or the development of interstitial fibrosis in *Postn^{TG}* mice, suggesting that periostin overexpression was not sufficient to induce cell proliferation or cause injury.

A

lox — mCherry — lox — Postn
Rosa26

✕

Cre
Pkhd1*

↓

lox — Postn
Rosa26

Collecting ducts

B

Postn^{tg} mice

| mPostn CM | Pkhd1 -Cre | No Cre |

90-kDa Postn →

Actin →

Periostin / **DAPI** / **AQP-2**

C **D**
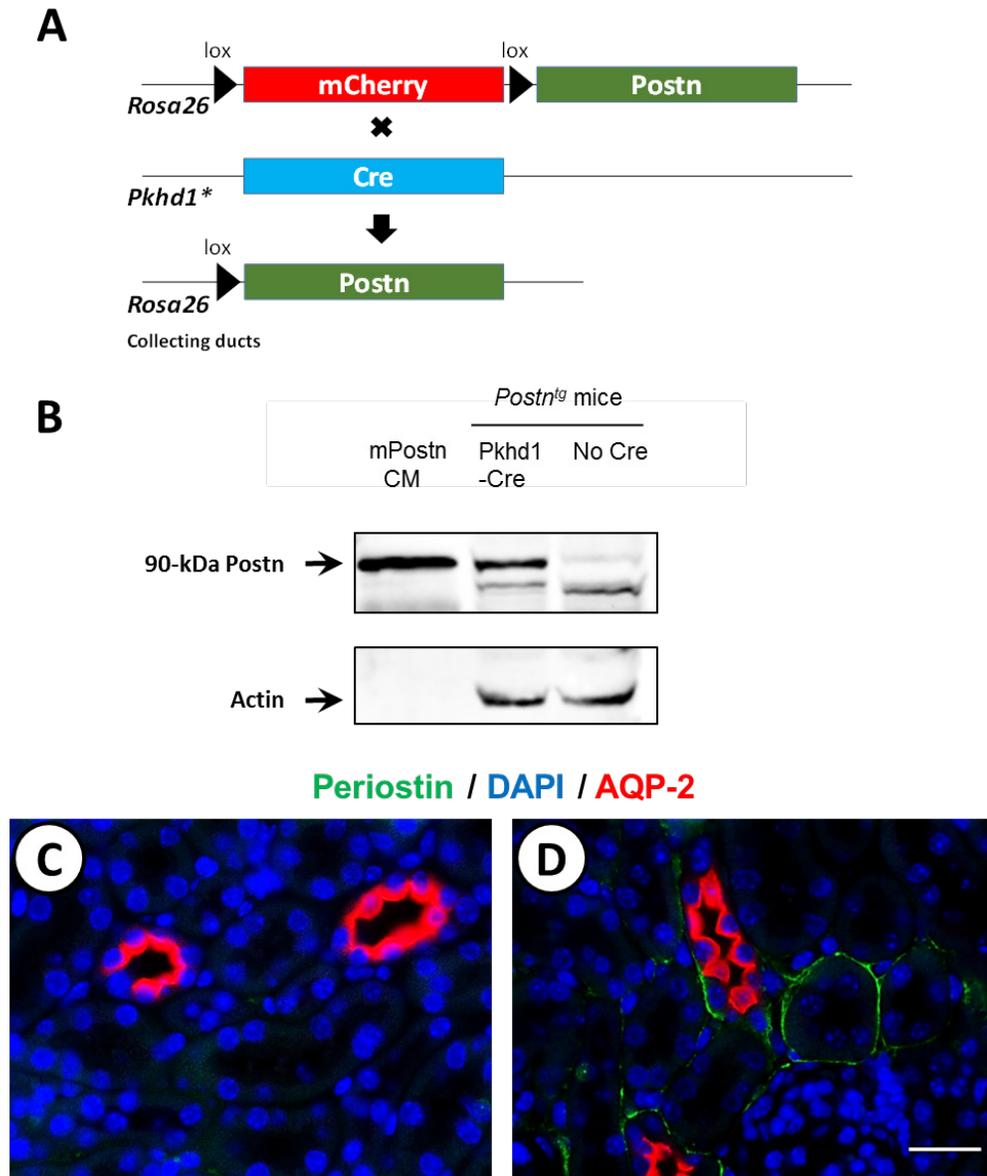
Figure 4-6. Collecting duct (CD)-specific overexpression of periostin. (A) We generated a transgenic mouse carrying a full-length periostin cDNA construct adjacent to a floxed mCherry stop cassette, downstream of the *Rosa26* promoter. These mice were bred to Pkhd1-Cre mice to selectively express periostin in the CD. (B) To confirm Cre-mediated transgene expression, protein lysates from WT and *Postn^{TG}* mice were immunoblotted for periostin. Conditional media (CM) from M1 cells transfected with full-length mouse periostin cDNA (mPostn) was used as positive control for periostin expression. Sections were stained for periostin (green), AQP-2 (CD marker) and DAPI (nuclear stain). (C) WT, (D) *Postn^{TG}*. Scale bar = 5 µm.

4.4.4. Effect of periostin overexpression in the cyst-lining cells of *pcy* mice

To determine if persistent overexpression of periostin in the cyst-lining cells accelerates PKD progression in *pcy* mice, we crossed *Postn^tg and Pkhd1-Cre* mice to *pcy* mice to obtain *Postn^tg;Pkhd1-Cre;pcy/pcy* (*Postn^TG pcy*) mice and littermate *pcy* mice. At 10 and 30 wk, male *Postn^TG pcy* and *pcy* mice were euthanized, and body weight, KW(%BW) and cystic index were measured (**Figure 4-7**, **Figure 4-10**). Periostin overexpression was visualized by immunofluorescence using an antibody to periostin (green), and CD cells were indicated by AQP-2 (red). *Pcy* mice have elevated expression of periostin compared to WT mice (**Figure 4-7**). In the *Postn^tg pcy* mice, there was a much higher expression of periostin in the renal cystic epithelia compared to *pcy* mice lacking the transgene. At 10 wk, *Postn^TG pcy* mice had a 38% increase in KW(%BW), compared to the kidneys of *pcy* littermates, with no effect on body weight. There was also a significant increase in cystic area and number of cysts in *Postn^TG pcy* mice compared to littermate *pcy* kidneys.
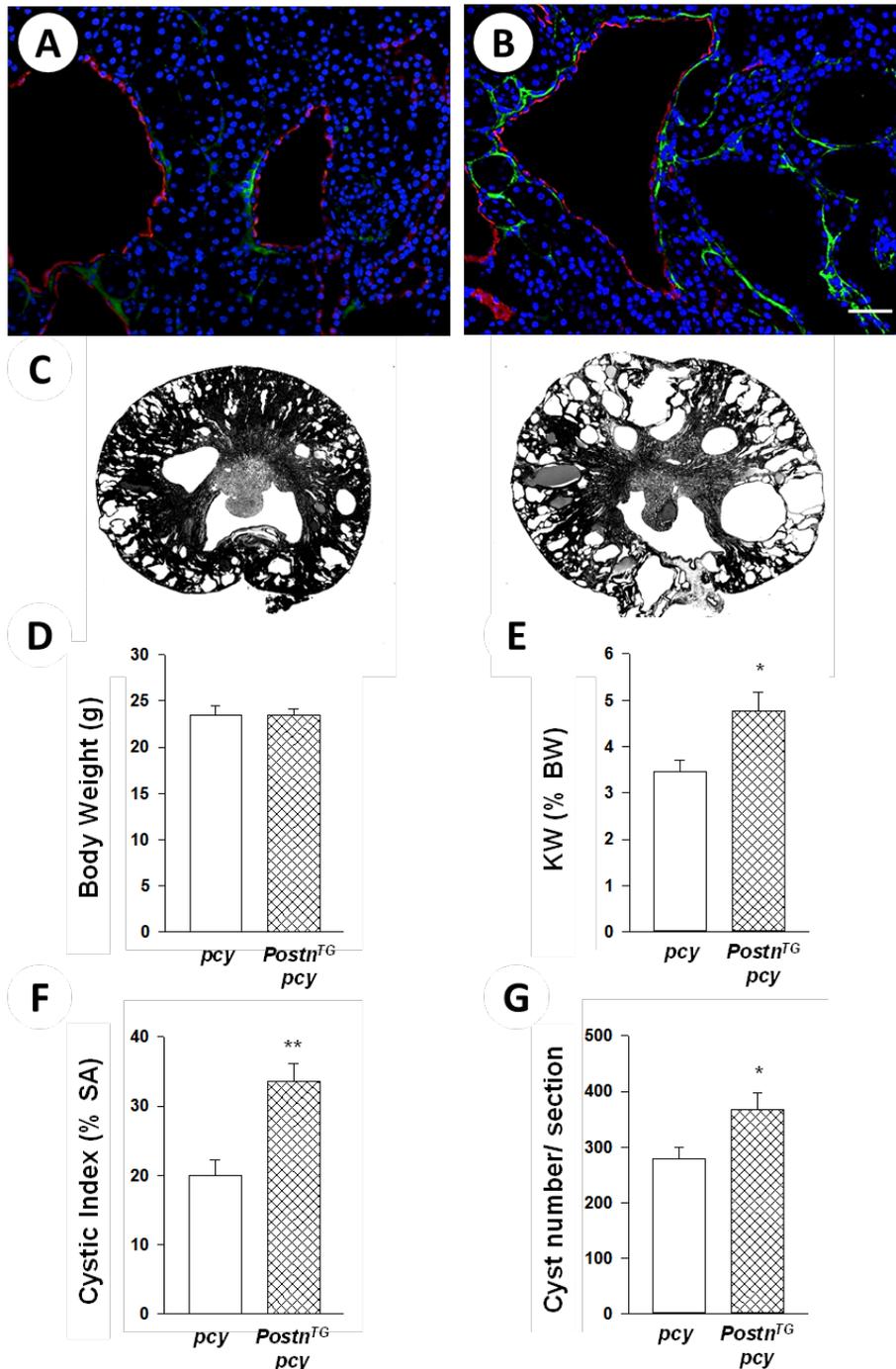
Figure 4-7. Effect of CD-specific periostin overexpression on kidney weight and cystic index in *pcy* mice. At 10 weeks, sections were stained for periostin (green), AQP-2 (CD marker) and DAPI (nuclear stain). (A) *pcy*, (B) *Postn^{TG}pcy*. Scale bar = 5 μm. (C) Representative images of kidney cross-sections from 10 wk old *pcy* and *Postn^{TG} pcy*. Images were taken at the same magnification. Scale Bar = 1 mm. (D) Overexpression of periostin in CD cells had no effect on body weight. However, there was a significant increase in (E) kidney weight (% BW), (F) cystic index and (G) cyst number per section in *Postn^{TG} pcy* (N = 8) mice compared to *pcy* (N = 6) mice. *P < 0.05, **P < 0.01 compared to *pcy* mice.

Next, we determined if CD-specific periostin overexpression increased cell proliferation. The number of Ki-67 positive cells per total nuclei was evaluated by immunofluorescence (**Figure 4-8 A, B**). Overexpression of periostin in the *Postn*^{TG} *pcy* mice increased renal cell by 2.1-fold. (**Figure 4-8 C**). Tissue sections from *Postn*^{TG} *pcy* and *pcy* mice were stained with Masson Trichrome to visualize the collagen fibers and were scored for interstitial fibrosis (**Figure 4-8 D, E**). *pcy* mice that overexpressed periostin showed a 60% increase in interstitial damage (**Figure 4-8 F**) with more pathologic fibrosis (blue color), compared to littermate *pcy* mice.

Previously, we found that periostin-induced cell proliferation and cyst growth was mediated by ILK signaling to the Akt/mTOR signaling pathway [245]. In the current study, *pcy* mice displayed increased renal levels of P-S6 [5], consistent with previous studies. Further, the level of phosphorylated S6 (P-S6) was two-fold higher in the *Postn*^{TG} *pcy* mice compared to *pcy* littermates demonstrating that periostin overexpression further increased mTOR signaling in cystic kidneys (**Figure 4-9**).

Ki-67 / **DBA** / **DAPI**
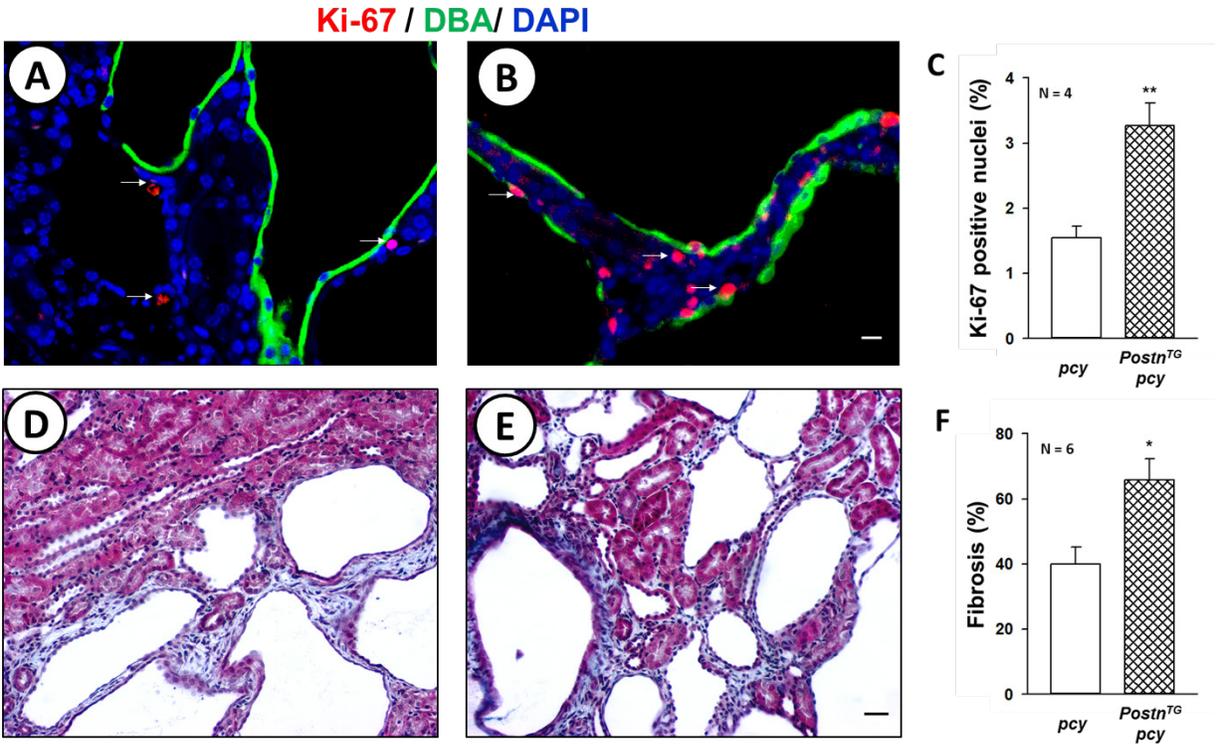
Figure 4-8. Effect of CD-specific periostin overexpression on renal cell proliferation and fibrosis in *pcy* mice. Proliferating cells were measured in kidney sections from (A) *pcy* and (B) *Postn^{tg};Pkhd1-Cre;pcy* (*Postn^{TG} pcy*) mice that were stained for Ki-67 (red), DBA (green) and DAPI (blue). Arrows indicate Ki-67 positive cells. Images (A, B) were taken at the same magnification. Scale bar = 5 µm. (C) Comparison of nuclear Ki-67 staining in *pcy* and *Postn^{TG} pcy* sections, normalized to total nuclei. Representative kidney sections from (D) *pcy* and (E) *Postn^{TG} pcy* mice were stained with Masson's trichrome to visualize edema and interstitial fibrosis. Scale bar = 50 µm. (F) Percentage of interstitial edema and fibrosis. $^*P < 0.05$ and $^{**}P < 0.01$, compared to *pcy*.

P-S6 / DAPI
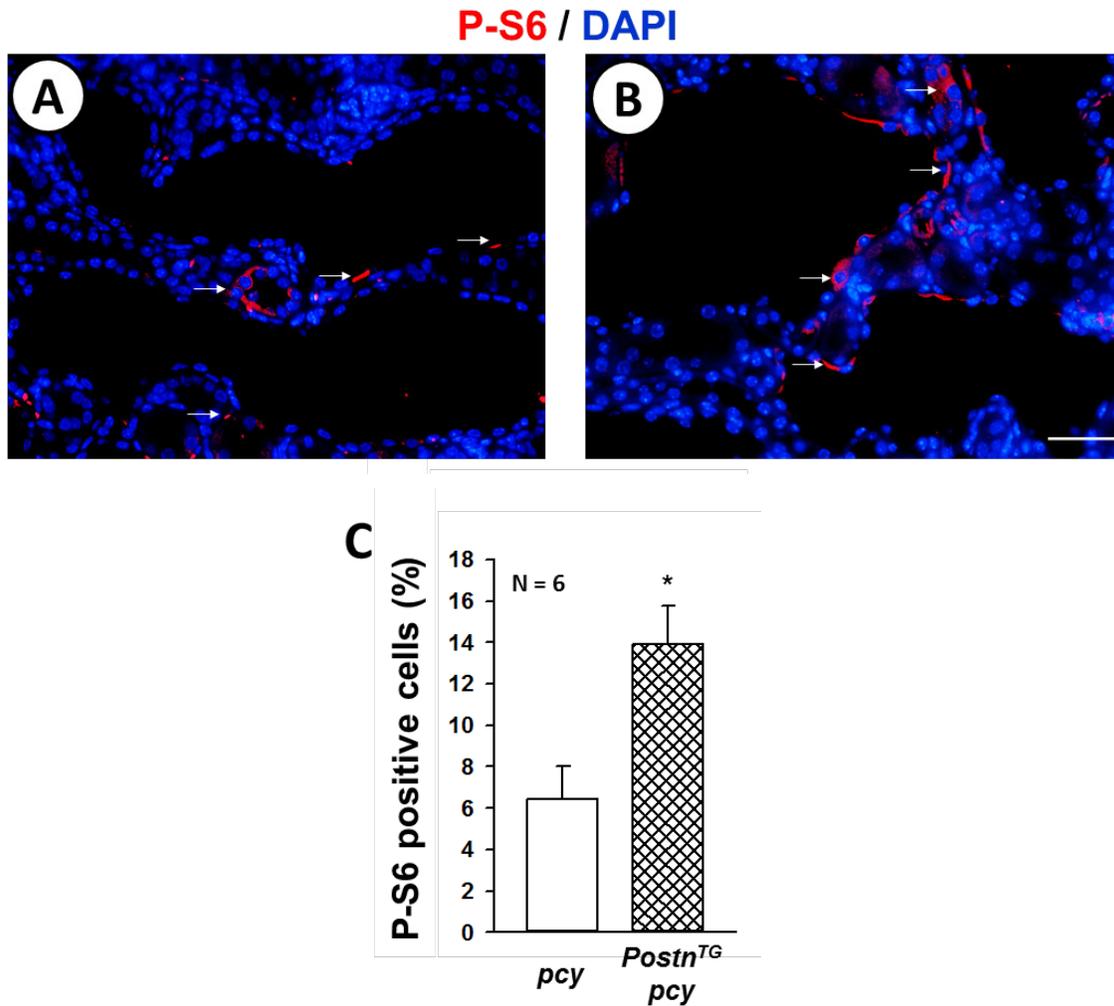
Figure 4-9. Effect of CD-specific overexpression of periostin on mTOR signaling in *pcy* kidneys.

Representative sections from (A) *pcy* and (B) *Postn^{tg};Pkhd1-Cre;pcy* (*Postn^{TG} pcy*) sections mice stained with an antibody to P-S6 (red). Tissues were also stained with DAPI nuclear stain (blue). Arrows indicate cytoplasmic P-S6 in cyst-lining cells. All images were taken at the same magnification. Scale bar = 5 μm. (C) Percentage of cytosolic P-S6 positive cells normalized to the total nuclei. $^{*}P < 0.05$ compared to *pcy* mice.

At 30 wk of age, $Postn^{TG}$ pcy mice showed a remarkable increase in KW(%BW) and a significant increase in the cystic index, compared to pcy mice (**Figure 4-10**). Previously, we showed that KW(%BW) of pcy mice plateaus by 20 wk due to fibrosis [228]; however, overexpression of periostin causes the kidneys to continue to enlarge despite elevated fibrosis. This indicates that overexpression of periostin maintains the cystic cells in a state of proliferation. Renal function was assessed at 10 and 30 wk by measuring blood urea nitrogen (BUN) levels from the serum samples collected (**Figure 4-10 D**). At 10 wk, pcy mice have relatively normal BUN. Overexpression of periostin in the CD of pcy mice caused an increase in BUN; however, this trend was not significant. At 30 wk, BUN levels of pcy mice are elevated consistent with the decline in normal parenchyma. Overexpression of periostin caused a significant elevation in BUN compared to pcy mice, indicating that overexpression of periostin worsened renal function.

Furthermore, we found that overexpression of periostin reduced the lifespan of pcy mice by 3 wk and the mice survived only ~ 45 wk, compared to littermate pcy mice, which survived to about 48 wk (**Figure 4-11**). These data suggest that CD-specific overexpression of periostin induces mTOR-mediated cell proliferation, increases the number of cysts and cystic area, accelerates interstitial fibrosis and the decline in renal function and shortens the lifespan of pcy mice.
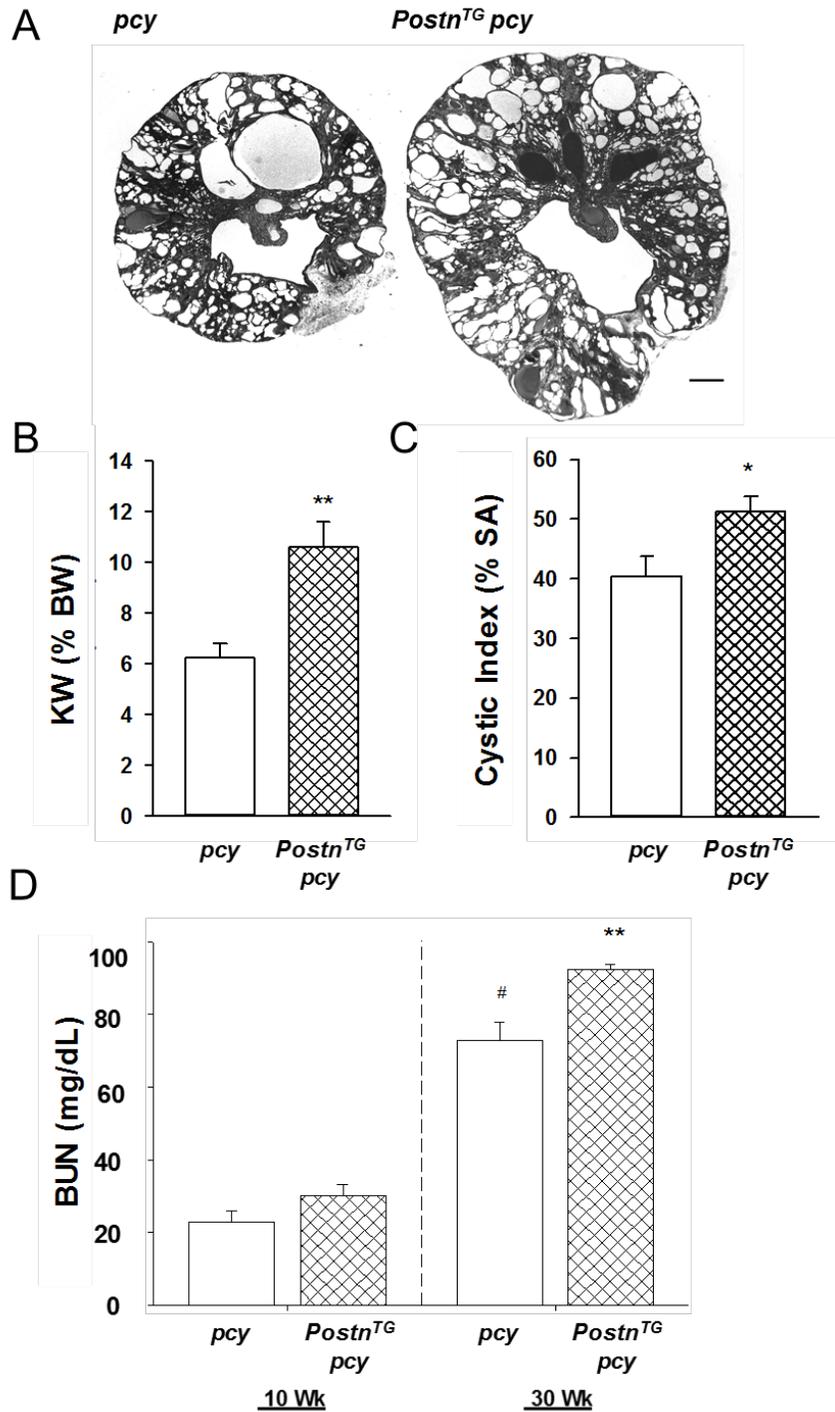
Figure 4-10. Effect of CD-specific periostin overexpression on kidney weight and cystic index in *pcy* mice at 30 wk. At 30 weeks, mice were euthanized, and kidneys were harvested. (A) Representative images of kidney cross-sections from 30 wk old *pcy* and *Postn^tg;Pkhd1-Cre;pcy* (*Postn^TG pcy*) mice. Images were taken at the same magnification. Scale Bar = 5 mm. Overexpression of periostin in CD cells had no effect on body weight (data not shown). However, there was a significant increase in (B) kidney weight (% BW), and (C) cystic index in *Postn^TG pcy* mice compared to *pcy* mice. N = 4 mice per group. (D) At 10 and 30 wk, blood was collected by cardiac puncture before euthanasia, and BUN was measured to assess renal function. BUN was not elevated in the *pcy* mice at 10 wk due to significantly preserved renal parenchyma at this age. $^*P < 0.05$, $^{**}P < 0.01$, compared to 30 wk *pcy* mice, and $^{\#}P < 0.05$, compared to 10 wk pcy mice.
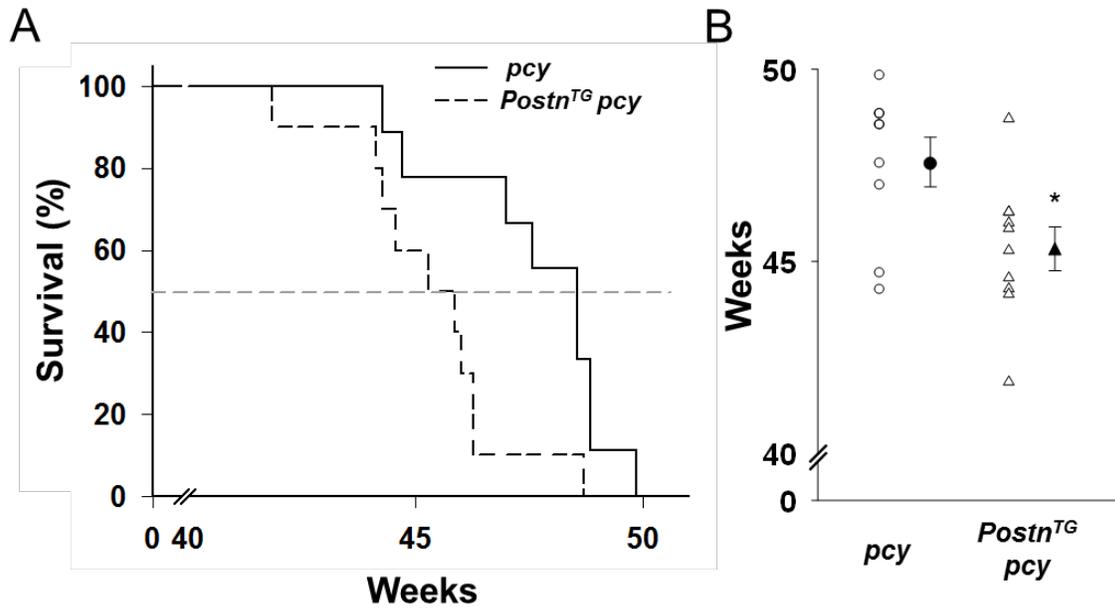
Figure 4-11. Effect of periostin overexpression on the survival of *pcy* mice. (A) *pcy* mice and *Postn^tg^;Pkhd1-Cre;pcy* (*Postn^TG^ pcy*) mice were given standard chow and water *ad libitum* and regularly monitored until moribund. The graph shows Gehan-Breslow survival curves of mice. (B) The graph represents a summary of the ages of *pcy* mice (N = 9), and *Postn^TG^ pcy* (N = 10), at the time of death. *P < 0.05 compared to *pcy* mice.

4.5. Discussion

In PKD, cystic epithelial cells are characterized as being incompletely differentiated with elevated expression of c-myc proto-oncogene and Akt/mTOR activity, contributing to aberrant cell proliferation and cyst growth [107, 115, 116, 118]. It has been hypothesized that functional loss of the polycystins induces a cellular repair response to rectify the cystic phenotype [120]. Due to the underlying gene mutation, this effort becomes futile, and the activation of these pathways accelerates the progression of disease. We found that aberrant expression of periostin, a repair molecule, by cystic epithelial cells increases the ILK-Akt-mTOR signaling pathway and cell proliferation, and contributes to cyst growth and fibrosis in PKD mice [2, 5, 245].

Periostin is expressed in several tissues following injury and promotes tissue remodeling and repair [8, 131, 135, 165, 242, 252-254]. In this study, we found that periostin caused actin stress fiber formation, integrin clustering, activation of FAK and Rho signaling, and cell migration. This is consistent with previous evidence for aberrant activation of Rho and FAK signaling in PKD [95, 118]. Moreover, periostin induced gene expression of ECM molecules, integrins, components of focal adhesion and the actin cytoskeleton, and molecules involved in growth factor signaling, consistent with cellular responses in tissue repair.

Studies have shown that renal injury accelerates disease progression in slowly progressive models of PKD [121-125]; however, the mechanism remains unclear. We found that persistent overexpression of periostin increased mTOR-mediated cell proliferation, cyst growth, fibrosis, and reduced the survival of PKD mice. Recently, periostin expression was found to be highly elevated in models of kidney injury [136, 243, 244, 246]. We propose that the expression of periostin activates tissue repair mechanisms that promote cyst growth and fibrosis, further exacerbating the disease.

Overexpression of periostin did not result in any abnormal renal phenotype in wildtype mice. Similarly, periostin had no effect on mTOR activity or the proliferation of normal human kidney cells [2]. We determined that ADPKD cells had a 9-fold higher expression of α_V-integrin, the receptor for periostin, thus accounting for the difference in the periostin response. In fact, several integrin receptors including α_v, β_3, β_1, and β_4 have been shown to be upregulated in PKD and, therefore, may be involved in predisposing the cells to misregulated signals from the ECM [2, 143, 154]. Consistent with our hypothesis that aberrant expression of ECM contributes to cystic disease, laminin-332 (laminin-5), an ECM molecule overexpressed in PKD, promotes cell proliferation, adhesion and migration [143, 155].

In summary, periostin overexpression in PKD exacerbates cyst growth and fibrosis by regulating genes and pathways involved in tissue repair, including cell proliferation, cytoskeletal remodeling, and matrix production (**Figure 4-12**). We propose that blockade of ECM-integrin signaling may slow cyst growth and fibrosis in PKD.
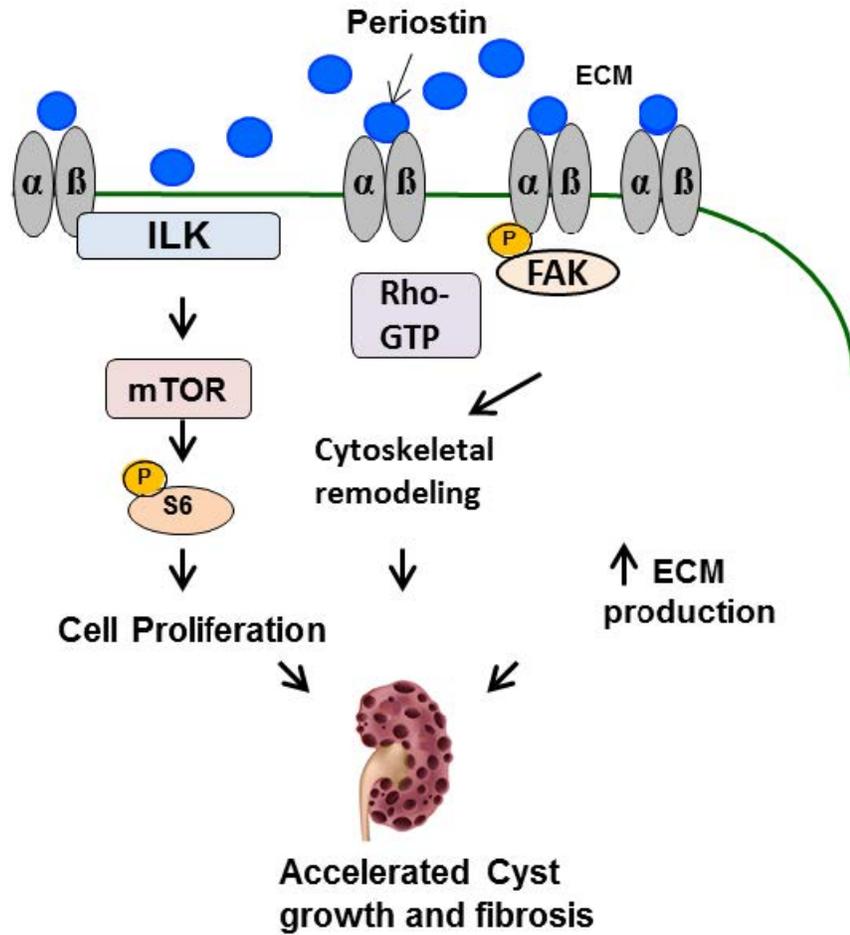
Figure 4-12. Periostin promotes futile repair in PKD. Matricellular molecules including periostin, bind integrin receptors to activate pathways involved in futile repair. Integrin engagement activates ILK signaling to Akt and mTOR, leading to ADPKD cell proliferation. Alternatively, integrin engagement leads to activation of FAK and Rho mediated cytoskeletal remodeling and ADPKD cell migration. These tissue repair pathways are persistently activated by matricellular molecules including periostin.

CHAPTER 5. SUMMARY, CONCLUSIONS, AND FUTURE DIRECTIONS

5.1. Summary

ADPKD affects over 150,000 people in the US and 12.5 million worldwide and has a devastating effect on the families as well as the national health care system [20]. Therapeutic strategies for the treatment of ADPKD must consider the balance between drug efficacy and potential adverse effects due to long-term treatment [87, 255]. A better understanding of the disease is necessary to develop novel targeted therapies to alter the course of the disease.

Extracellular matrix (ECM) proteins not only make up components of the fibrotic scar but are also active regulators of tissue remodeling via cell-matrix signaling and may be involved in unchecked repair mechanisms that contribute to aberrant cell proliferation, cyst expansion, and fibrosis, ultimately leading to renal failure. Periostin, a tissue repair molecule, is persistently upregulated in PKD [2], leading to increased cyst growth and fibrosis. Gene knockout of periostin significantly improved renal function and survival of *pcy/pcy* mice, a slowly progressive murine model of PKD [5]. Based on these observations, we reasoned that periostin and its associated signaling pathways are potentially viable targets for therapy.

We demonstrated that treatment of human primary ADPKD cells with periostin increased the activity of integrin-linked kinase (ILK), a key mediator of integrin signaling, by 1.5-fold. There was also an increase in periostin-induced phosphorylation of Akt and S6 kinase (S6K), a downstream target of mTOR. The proliferative effect of periostin on PKD cells was blocked in the presence of an αv-integrin blocking antibody [2]. From these results, we hypothesized that periostin-induced cell proliferation and cyst growth in PKD is mediated by activation of ILK and its downstream signaling targets, Akt, and mTOR. We reasoned that targeting ILK signaling will effectively block aberrant signals from ECM molecules including periostin, and delay PKD

progression. Pharmacological inhibition of ILK and shRNA knockdown of ILK blocked periostin-induced phosphorylation of Akt and S6K and prevented periostin-induced ADPKD cell proliferation. In contrast to ILK inhibition, shRNA knockdown of ILK also decreased EGF-induced ADPKD cell proliferation. We reasoned that shRNA knockdown of ILK disrupted the interaction between receptor tyrosine kinase (RTK) and the ILK-Pinch-Parvin (IPP) complex [192, 230, 231].

Postnatal ablation of ILK in collecting ducts (CDs) caused a urinary concentrating defect, a decline in body weight, and the mice died by ten weeks of age. Complete loss of ILK ($Ilk^{-/-}$) appeared to disrupt the connection between the ECM and cell cytoskeleton, a process called anoikis, leading to shedding of CD cells into the lumen, tubule obstruction, and dilation. By contrast, mice with a heterozygous deletion of ILK in the CDs ($Ilk^{+/-}$) seemed normal with no apparent renal deficiency. Our results indicate that ILK is crucial for renal development, maintenance, and function, and corroborates previous findings that ILK is essential for renal development and function [205, 211].

Next, we determined if CD-specific knockdown or knockout of ILK reduced cystic disease progression in ADPKD mice. We used 1) $Pkd1^{fl/fl};Pkhd1$-Cre mice, an aggressive orthologous model of ADPKD with a survival age of ~ 33 days and 2) pcy/pcy (pcy) mice, a slowly progressive model of PKD with a survival age of about 45 wk. Since mice with complete loss of ILK in the CDs died by 10 weeks, we did not generate $Ilk^{-/-}$ pcy mice. $Pkd1^{fl/fl};Pkhd1$-Cre mice with complete ablation of ILK ($Ilk^{-/-}$) had a significant reduction in cystic burden. Upon examination, these mice showed increased apoptosis (anoikis) of the CD cells, causing the cells to be shed into the lumen. However, the renal function of these mice remained compromised due to the loss of ILK. Therefore, the reduction in cystic burden did not translate into an

improvement in survival. More importantly, we observed that deletion of one allele of ILK ($Ilk^{+/-}$) in the CDs was sufficient to decrease cyst growth, renal Akt/mTOR activity, and interstitial fibrosis, and significantly extended the survival of both models of PKD. ILK inhibitors have been shown to reduce carcinogenic cell proliferation and were also effective in reducing renal fibrosis [213, 237]. However, due to the important role of ILK in the maintenance of normal renal function, pre-clinical studies should carefully document and monitor the effects of long-term use of ILK inhibitors.

The work outlined in the first part of the dissertation demonstrates that 1) ILK is an important intermediate of periostin-induced cell proliferation and cyst growth in PKD and that 2) the ECM-ILK- mTOR pathway plays a crucial role in promoting cyst growth and fibrosis in PKD.

Periostin is involved in a multitude of functions in different cellular contexts. Predominantly, periostin binds α_V-integrins on the cell surface and activates cellular pathways involved in cell proliferation, survival, and profibrotic TGF-β signaling [2, 8, 137, 164, 169-171]. Periostin also interacts with and regulates components of the ECM, including collagen and fibronectin, and promotes collagen cross-linking, which is important for tissue integrity [167, 168]. Our lab was the first to demonstrate the involvement of periostin in a kidney disease. Considering that ADPKD cells have a cellular phenotype consistent with tissue repair and that periostin is expressed during tissue repair, we hypothesized that persistent expression of periostin by the cyst-lining epithelia, triggers tissue repair pathways in PKD, accelerating cyst growth and fibrosis.

We found that periostin induced, signature molecular patterns pertaining to cytoskeletal rearrangement, including actin stress fiber formation, and integrin clustering. Integrin clustering

promotes the formation of mature focal adhesions responsible for ECM-integrin interaction and cell migration [249-251]. Periostin induced tyrosine phosphorylation of focal adhesion kinase (FAK) and activated the Rho-family GTPases (Rho). Further, periostin promoted cell migration in ADPKD cells, but not NHK cells. Next, we determined if periostin regulated genes involved in renal repair. In ADPKD cells, periostin treatment induced the expression of molecules involved in actin assembly, focal adhesion formation, ECM production and integrin signaling.

Finally, we determined if the overexpression of periostin in the CDs accelerates PKD progression. To this end, we generated *pcy* mice with ectopic expression of periostin in the CDs. Periostin overexpression accelerated the progression of the cystic disease by significantly increasing renal mTOR activity, cell proliferation, cyst growth and interstitial fibrosis. By contrast, wild-type mice with CD-specific periostin overexpression did not display any phenotype, supporting the idea that a prior genetic insult in the kidney is required for periostin pathogenesis. Preliminary immunoblot analysis indicated that the renal levels of periostin expression in the transgenic mice were equivalent to the physiological levels of periostin expression in mice hearts. While this indicates that physiological levels of periostin is sufficient to accelerate disease, it could also explain why we do not see a dramatic increase in disease progression at ten weeks in *pcy* mice. By 20 weeks of age, *pcy* mice already have a 20-fold overexpression of periostin compared to control mice [5]. We speculate that the already elevated expression of periostin accelerates the disease progression and masks the effect of the transgene expression since there was only a small decline in survival with periostin overexpression.

Our work demonstrates that aberrant expression of periostin in PKD appears to promote pathways involved in tissue repair, including proliferation, cytoskeletal remodeling and ECM deposition, leading to increased mTOR-mediated cell proliferation, and fibrosis.

5.2. Future Directions

Our long-term goals are to delineate the cellular and molecular mechanisms underlying the mitogenic and fibrotic effects of matricellular molecules including periostin, in renal cystic diseases. This work has led us to several potential future directions.

- TGF-β, the master cytokine responsible for ECM production [137] is elevated in the cystic epithelia of most human and rodent forms of PKD and is heavily implicated in accelerating PKD progression [147]. Previously, we found that TGF-β increases periostin expression in renal epithelial cells [2]. In addition to being involved in periostin activation of ILK and its downstream pathways, αv-integrin appears to regulate the release of the active form of TGF-β [256, 257]. We can determine the interplay between periostin, αv-integrin, and TGF-β in ADPKD. We could also determine if periostin is involved in the direct activation of the TGF-β signaling pathway.

- We generated periostin transgenic mice (*Postn^tg*), which allow tissue-specific overexpression of periostin (Figure 4-6). We observed that CD-specific overexpression of periostin in wild-type mice did not cause any pathologies. Recently, periostin was also shown to be overexpressed in glomerular injury, hypertensive nephropathy and diabetic nephropathy [136, 243, 244], supporting the idea that aberrant expression of periostin is an injury response. Our work was the first to identify a role for periostin in renal pathology. However, currently, there is very little known about periostin in the pathogenesis of other chronic kidney diseases. Our *Postn^tg* mice is a highly useful tool to study the effects of aberrant periostin expression in CKD.

- Recently, Morra et al. have identified about eight splice variants of periostin from fetal kidneys and tissue samples of renal cell carcinoma patients [166]. While the splice variants in the C-terminus might not affect integrin binding, it has been speculated that they may play a role in tumor metastasis in cancers by influencing the ECM composition. Despite the massive enlargement of the kidneys due to cysts, there is surprisingly very few cases of kidney cancers in PKD patients [258]. Identifying periostin splice variants in PKD uncover a better understanding of its pathogenic functions, such as proliferation, fibrosis, and metastasis. Identifying periostin splice variants in PKD holds potential since it is possible that different splice variants may be responsible for various pathogenic functions, such as proliferation and fibrosis.

- We have demonstrated that periostin binds to the integrin receptors and activates ILK signaling to the Akt/ mTOR pathway in PKD. Based on these observations, we have identified some potential therapeutic targets (**Figure 5-1**) 1) ILK: Recently, Li et al. showed that ILK inhibitors could be effectively used in a mouse model of obstructive nephropathy to reduce TGF-β-induced renal fibrosis [237]. However, ILK may be a difficult therapeutic target for long-term treatment, since it is critical for maintaining the renal parenchyma [205, 211, 245]. 2) Integrin antagonists: We showed that α_V-integrins are upregulated in PKD and can remain persistently upregulated due to the aberrant repair signals from the ECM. Cilengitide, an α_V-integrin antagonist, has been extensively studied in cancer and may be a potential therapeutic target for PKD [259]. 3) ECM molecules: We have demonstrated that targeting aberrant periostin expression in PKD could significantly reduce cyst growth and fibrosis. Ma *et al.*[260], recently showed that abrogation of fibronectin reduced the progression of PKD. ECM molecules such as laminin are also aberrantly expressed in PKD and contribute to increased cell adhesion,

migration and proliferation [143, 155]. The use of antisense oligonucleotides to target secreted molecules in PKD is intriguing. Recently, Mael-Ainin *et al.* successfully used periostin oligonucleotides to treat L-NAME-induced tubular injury in mice [261].

5.3. Conclusions

Our data elucidates certain molecular mechanisms involved in periostin-mediated PKD progression, highlighting the role of ILK signaling in PKD. Our results indicate that aberrant expression of periostin stimulates integrin-ILK signaling and promotes cell proliferation, cytoskeletal rearrangement and migration, and ECM production. Targeting ECM-integrin signaling may hold significant therapeutic potential in PKD. Our results also provide a framework for future studies to investigate periostin and ILK in other renal diseases.
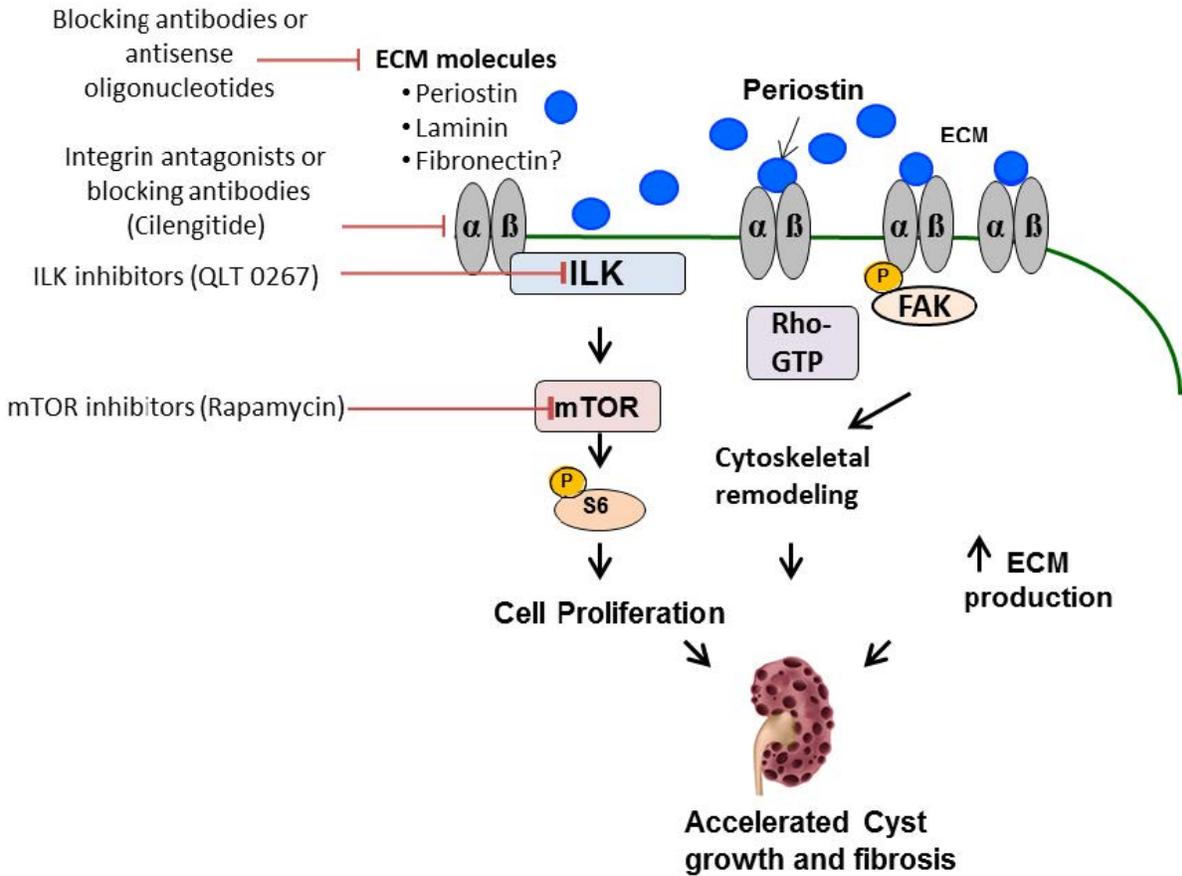
Figure 5-1. The role of matricellular signaling in PKD. ECM molecules including periostin, bind integrin receptors to activate pathways involved in futile repair. Integrin engagement activates ILK signaling to Akt and mTOR, leading to ADPKD cell proliferation. Integrin engagement also leads to activation of FAK and Rho mediated cytoskeletal remodeling, ADPKD cell migration and ECM production. Red arrows (flat ends) indicate potential therapeutic targets for PKD that we gleaned from this study.

REFERENCES

1. Wallace, DP: Cyclic AMP-mediated cyst expansion. *Biochim Biophys Acta,* 1812**:** 1291-1300, 2011.

2. Wallace, DP, Quante, MT, Reif, GA, Nivens, E, Ahmed, F, Hempson, SJ, Blanco, G, Yamaguchi, T: Periostin induces proliferation of human autosomal dominant polycystic kidney cells through alphaV-integrin receptor. *Am J Physiol Renal Physiol,* 295**:** F1463-1471, 2008.

3. Ong, AC, Harris, PC: A polycystin-centric view of cyst formation and disease: the polycystins revisited. *Kidney Int,* 88**:** 699-710, 2015.

4. Gattone, VH, 2nd, Sinders, RM, Hornberger, TA, Robling, AG: Late progression of renal pathology and cyst enlargement is reduced by rapamycin in a mouse model of nephronophthisis. *Kidney Int,* 76**:** 178-182, 2009.

5. Wallace, DP, White, C, Savinkova, L, Nivens, E, Reif, GA, Pinto, CS, Raman, A, Parnell, SC, Conway, SJ, Fields, TA: Periostin promotes renal cyst growth and interstitial fibrosis in polycystic kidney disease. *Kidney Int,* 85**:** 845-854, 2014.

6. Chebib, FT, Sussman, CR, Wang, X, Harris, PC, Torres, VE: Vasopressin and disruption of calcium signalling in polycystic kidney disease. *Nat Rev Nephrol,* 11**:** 451-464, 2015.

7. Grantham, JJ, Mulamalla, S, Swenson-Fields, KI: Why kidneys fail in autosomal dominant polycystic kidney disease. *Nat Rev Nephrol,* 7**:** 556-566, 2011.

8. Kudo, A: Periostin in fibrillogenesis for tissue regeneration: periostin actions inside and outside the cell. *Cell Mol Life Sci,* 68**:** 3201-3207, 2011.

9. Cabodi, S, del Pilar Camacho-Leal, M, Di Stefano, P, Defilippi, P: Integrin signalling adaptors: not only figurants in the cancer story. *Nat Rev Cancer,* 10**:** 858-870, 2010.

10. Attwell, S, Roskelley, C, Dedhar, S: The integrin-linked kinase (ILK) suppresses anoikis. *Oncogene,* 19**:** 3811-3815, 2000.

11. Cano-Penalver, JL, Griera, M, Serrano, I, Rodriguez-Puyol, D, Dedhar, S, de Frutos, S, Rodriguez-Puyol, M: Integrin-linked kinase regulates tubular aquaporin-2 content and intracellular location: a link between the extracellular matrix and water reabsorption. *FASEB journal : official publication of the Federation of American Societies for Experimental Biology*, 2014.

12. Brakebusch, C, Fassler, R: The integrin-actin connection, an eternal love affair. *EMBO J,* 22**:** 2324-2333, 2003.

13. Grantham, JJ: Polycystic kidney disease: huge kidneys, huge problems, huge progress. *Trans Am Clin Climatol Assoc,* 108**:** 165-170; discussion 170-162, 1997.

14. Mochizuki, T, Wu, G, Hayashi, T, Xenophontos, SL, Veldhuisen, B, Saris, JJ, Reynolds, DM, Cai, Y, Gabow, PA, Pierides, A, Kimberling, WJ, Breuning, MH, Deltas, CC, Peters, DJ, Somlo, S: PKD2, a gene for polycystic kidney disease that encodes an integral membrane protein. *Science,* 272**:** 1339-1342, 1996.

15. Consortium, EPKD: The polycystic kidney disease 1 gene encodes a 14 kb transcript and lies within a duplicated region on chromosome 16. *Cell,* 77**:** 881-894, 1994.

16. Guay-Woodford, LM: Autosomal recessive polycystic kidney disease: the prototype of the hepato-renal fibrocystic diseases. *J Pediatr Genet,* 3**:** 89-101, 2014.

17. Sweeney, WE, Jr., Avner, ED: Pathophysiology of childhood polycystic kidney diseases: new insights into disease-specific therapy. *Pediatr Res,* 75**:** 148-157, 2014.

18. Ward, CJ, Hogan, MC, Rossetti, S, Walker, D, Sneddon, T, Wang, X, Kubly, V, Cunningham, JM, Bacallao, R, Ishibashi, M, Milliner, DS, Torres, VE, Harris, PC: The gene mutated in autosomal recessive polycystic kidney disease encodes a large, receptor-like protein. *Nature genetics,* 30**:** 259-269, 2002.

19. Onuchic, LF, Furu, L, Nagasawa, Y, Hou, X, Eggermann, T, Ren, Z, Bergmann, C, Senderek, J, Esquivel, E, Zeltner, R, Rudnik-Schoneborn, S, Mrug, M, Sweeney, W, Avner, ED, Zerres, K, Guay-Woodford, LM, Somlo, S, Germino, GG: PKHD1, the polycystic kidney and hepatic disease 1 gene, encodes a novel large protein containing multiple immunoglobulin-like plexin-transcription-factor domains and parallel beta-helix 1 repeats. *Am J Hum Genet,* 70**:** 1305-1317, 2002.

20. Torres, VE, Harris, PC: Autosomal dominant polycystic kidney disease: the last 3 years. *Kidney Int,* 76**:** 149-168, 2009.

21. Baert, L: Hereditary polycystic kidney disease (adult form): a microdissection study of two cases at an early stage of the disease. *Kidney Int,* 13**:** 519-525, 1978.

22. Calvet, JP, Grantham, JJ: The genetics and physiology of polycystic kidney disease. *Semin Nephrol,* 21**:** 107-123, 2001.

23. Wilson, PD, Hreniuk, D, Gabow, PA: Abnormal extracellular matrix and excessive growth of human adult polycystic kidney disease epithelia. *Journal of Cellular Physiology,* 150**:** 360-369, 1992.

24. Harris, PC, Torres, VE: Polycystic kidney disease, autosomal dominant. 2015.

25. Cornec-Le Gall, E, Audrezet, MP, Chen, JM, Hourmant, M, Morin, MP, Perrichot, R, Charasse, C, Whebe, B, Renaudineau, E, Jousset, P, Guillodo, MP, Grall-Jezequel, A, Saliou, P, Ferec, C, Le Meur, Y: Type of PKD1 mutation influences renal outcome in ADPKD. *Journal of the American Society of Nephrology : JASN,* 24**:** 1006-1013, 2013.

26. Heyer, CM, Sundsbak, JL, Abebe, KZ, Chapman, AB, Torres, VE, Grantham, JJ, Bae, KT, Schrier, RW, Perrone, RD, Braun, WE, Steinman, TI, Mrug, M, Yu, AS, Brosnahan, G, Hopp, K, Irazabal, MV, Bennett, WM, Flessner, MF, Moore, CG, Landsittel, D, Harris, PC, Halt, PKD, Investigators, C: Predicted Mutation Strength of Nontruncating PKD1 Mutations Aids Genotype-Phenotype Correlations in Autosomal Dominant Polycystic Kidney Disease. *Journal of the American Society of Nephrology : JASN,* 27**:** 2872-2884, 2016.

27. Brunelli, SM, Blanchette, CM, Claxton, AJ, Roy, D, Rossetti, S, Gutierrez, B: End-stage renal disease in autosomal dominant polycystic kidney disease: a comparison of dialysis-related utilization and costs with other chronic kidney diseases. *Clinicoecon Outcomes Res,* 7**:** 65-72, 2015.

28. Bogdanova, N, Markoff, A, Gerke, V, McCluskey, M, Horst, J, Dworniczak, B: Homologues to the first gene for autosomal dominant polycystic kidney disease are pseudogenes. *Genomics,* 74**:** 333-341, 2001.

29. Igarashi, P, Somlo, S: Genetics and pathogenesis of polycystic kidney disease. *Journal of the American Society of Nephrology : JASN,* 13**:** 2384-2398, 2002.

30. Qian, F, Watnick, TJ, Onuchic, LF, Germino, GG: The molecular basis of focal cyst formation in human autosomal dominant polycystic kidney disease type I. *Cell,* 87**:** 979-987, 1996.

31. Wu, G, D'Agati, V, Cai, Y, Markowitz, G, Park, JH, Reynolds, DM, Maeda, Y, Le, TC, Hou, H, Jr., Kucherlapati, R, Edelmann, W, Somlo, S: Somatic inactivation of Pkd2 results in polycystic kidney disease. *Cell,* 93**:** 177-188, 1998.

32. Lantinga-van Leeuwen, IS, Dauwerse, JG, Baelde, HJ, Leonhard, WN, van de Wal, A, Ward, CJ, Verbeek, S, Deruiter, MC, Breuning, MH, de Heer, E, Peters, DJ: Lowering of Pkd1 expression is sufficient to cause polycystic kidney disease. *Hum Mol Genet,* 13**:** 3069-3077, 2004.

33. Jiang, ST, Chiou, YY, Wang, E, Lin, HK, Lin, YT, Chi, YC, Wang, CK, Tang, MJ, Li, H: Defining a link with autosomal-dominant polycystic kidney disease in mice with congenitally low expression of Pkd1. *Am J Pathol,* 168**:** 205-220, 2006.

34. Rossetti, S, Kubly, VJ, Consugar, MB, Hopp, K, Roy, S, Horsley, SW, Chauveau, D, Rees, L, Barratt, TM, van't Hoff, WG, Niaudet, P, Torres, VE, Harris, PC: Incompletely penetrant PKD1 alleles suggest a role for gene dosage in cyst initiation in polycystic kidney disease. *Kidney Int,* 75**:** 848-855, 2009.

35. Hopp, K, Ward, CJ, Hommerding, CJ, Nasr, SH, Tuan, HF, Gainullin, VG, Rossetti, S, Torres, VE, Harris, PC: Functional polycystin-1 dosage governs autosomal dominant polycystic kidney disease severity. *J Clin Invest,* 122**:** 4257-4273, 2012.

36. Vujic, M, Heyer, CM, Ars, E, Hopp, K, Markoff, A, Orndal, C, Rudenhed, B, Nasr, SH, Torres, VE, Torra, R, Bogdanova, N, Harris, PC: Incompletely penetrant PKD1 alleles mimic the renal manifestations of ARPKD. *Journal of the American Society of Nephrology : JASN,* 21**:** 1097-1102, 2010.

37. Piontek, K, Menezes, LF, Garcia-Gonzalez, MA, Huso, DL, Germino, GG: A critical developmental switch defines the kinetics of kidney cyst formation after loss of Pkd1. *Nat Med,* 13**:** 1490-1495, 2007.

38. Parnell, SC, Magenheimer, BS, Maser, RL, Rankin, CA, Smine, A, Okamoto, T, Calvet, JP: The polycystic kidney disease-1 protein, polycystin-1, binds and activates heterotrimeric G-proteins in vitro. *Biochem Biophys Res Commun,* 251**:** 625-631, 1998.

39. Sandford, R, Sgotto, B, Aparicio, S, Brenner, S, Vaudin, M, Wilson, RK, Chissoe, S, Pepin, K, Bateman, A, Chothia, C, Hughes, J, Harris, P: Comparative analysis of the polycystic kidney disease 1 (PKD1) gene reveals an integral membrane glycoprotein with multiple evolutionary conserved domains. *Hum Mol Genet,* 6**:** 1483-1489, 1997.

40. Ponting, CP, Hofmann, K, Bork, P: A latrophilin/CL-1-like GPS domain in polycystin-1. *Curr Biol,* 9**:** R585-588, 1999.

41. Arac, D, Boucard, AA, Bolliger, MF, Nguyen, J, Soltis, SM, Sudhof, TC, Brunger, AT: A novel evolutionarily conserved domain of cell-adhesion GPCRs mediates autoproteolysis. *EMBO J,* 31**:** 1364-1378, 2012.

42. Yu, S, Hackmann, K, Gao, J, He, X, Piontek, K, Garcia-Gonzalez, MA, Menezes, LF, Xu, H, Germino, GG, Zuo, J, Qian, F: Essential role of cleavage of Polycystin-1 at G protein-coupled receptor proteolytic site for kidney tubular structure. *Proc Natl Acad Sci U S A,* 104**:** 18688-18693, 2007.

43. Kurbegovic, A, Kim, H, Xu, H, Yu, S, Cruanes, J, Maser, RL, Boletta, A, Trudel, M, Qian, F: Novel functional complexity of polycystin-1 by GPS cleavage in vivo: role in polycystic kidney disease. *Mol Cell Biol,* 34**:** 3341-3353, 2014.

44. Bateman, A, Sandford, R: The PLAT domain: a new piece in the PKD1 puzzle. *Curr Biol,* 9**:** R588-590, 1999.

45. Xu, Y, Ong, AC, Williamson, MP, Hounslow, AM: Backbone assignment and secondary structure of the PLAT domain of human polycystin-1. *Biomol NMR Assign,* 9**:** 369-373, 2015.

46. Moy, GW, Mendoza, LM, Schulz, JR, Swanson, WJ, Glabe, CG, Vacquier, VD: The sea urchin sperm receptor for egg jelly is a modular protein with extensive homology to the human polycystic kidney disease protein, PKD1. *J Cell Biol,* 133**:** 809-817, 1996.

47. Parnell, SC, Magenheimer, BS, Maser, RL, Zien, CA, Frischauf, AM, Calvet, JP: Polycystin-1 activation of c-Jun N-terminal kinase and AP-1 is mediated by heterotrimeric G proteins. *J Biol Chem,* 277**:** 19566-19572, 2002.

48. Shillingford, JM, Murcia, NS, Larson, CH, Low, SH, Hedgepeth, R, Brown, N, Flask, CA, Novick, AC, Goldfarb, DA, Kramer-Zucker, A, Walz, G, Piontek, KB, Germino, GG, Weimbs, T: The mTOR pathway is regulated by polycystin-1, and its inhibition reverses renal cystogenesis in polycystic kidney disease. *Proc Natl Acad Sci U S A,* 103**:** 5466-5471, 2006.

49. Lal, M, Song, X, Pluznick, JL, Di Giovanni, V, Merrick, DM, Rosenblum, ND, Chauvet, V, Gottardi, CJ, Pei, Y, Caplan, MJ: Polycystin-1 C-terminal tail associates with beta-catenin and inhibits canonical Wnt signaling. *Hum Mol Genet,* 17**:** 3105-3117, 2008.

50. Bhunia, AK, Piontek, K, Boletta, A, Liu, L, Qian, F, Xu, PN, Germino, FJ, Germino, GG: PKD1 induces p21(waf1) and regulation of the cell cycle via direct activation of the JAK-STAT signaling pathway in a process requiring PKD2. *Cell,* 109**:** 157-168, 2002.

51. Parnell, SC, Magenheimer, BS, Maser, RL, Calvet, JP: Identification of the major site of in vitro PKA phosphorylation in the polycystin-1 C-terminal cytosolic domain. *Biochem Biophys Res Commun,* 259**:** 539-543, 1999.

52. Streets, AJ, Wessely, O, Peters, DJ, Ong, AC: Hyperphosphorylation of polycystin-2 at a critical residue in disease reveals an essential role for polycystin-1-regulated dephosphorylation. *Hum Mol Genet,* 22**:** 1924-1939, 2013.

53. Parnell, SC, Puri, S, Wallace, DP, Calvet, JP: Protein phosphatase-1alpha interacts with and dephosphorylates polycystin-1. *PLoS One,* 7**:** e36798, 2012.

54. Chauvet, V, Tian, X, Husson, H, Grimm, DH, Wang, T, Hiesberger, T, Igarashi, P, Bennett, AM, Ibraghimov-Beskrovnaya, O, Somlo, S, Caplan, MJ: Mechanical stimuli induce cleavage and nuclear translocation of the polycystin-1 C terminus. *J Clin Invest,* 114**:** 1433-1443, 2004.

55. Koulen, P, Cai, Y, Geng, L, Maeda, Y, Nishimura, S, Witzgall, R, Ehrlich, BE, Somlo, S: Polycystin-2 is an intracellular calcium release channel. *Nature cell biology,* 4**:** 191-197, 2002.

56. Giamarchi, A, Feng, S, Rodat-Despoix, L, Xu, Y, Bubenshchikova, E, Newby, LJ, Hao, J, Gaudioso, C, Crest, M, Lupas, AN, Honore, E, Williamson, MP, Obara, T, Ong, AC, Delmas, P: A polycystin-2 (TRPP2) dimerization domain essential for the function of heteromeric polycystin complexes. *EMBO J,* 29**:** 1176-1191, 2010.

57. Gonzalez-Perrett, S, Kim, K, Ibarra, C, Damiano, AE, Zotta, E, Batelli, M, Harris, PC, Reisin, IL, Arnaout, MA, Cantiello, HF: Polycystin-2, the protein mutated in autosomal dominant polycystic kidney disease (ADPKD), is a Ca2+-permeable nonselective cation channel. *Proc Natl Acad Sci U S A,* 98**:** 1182-1187, 2001.

58. Wilkes, M, Madej, MG, Kreuter, L, Rhinow, D, Heinz, V, De Sanctis, S, Ruppel, S, Richter, RM, Joos, F, Grieben, M, Pike, AC, Huiskonen, JT, Carpenter, EP, Kuhlbrandt, W, Witzgall, R, Ziegler, C: Molecular insights into lipid-assisted Ca2+ regulation of the TRP channel Polycystin-2. *Nat Struct Mol Biol,* 24**:** 123-130, 2017.

59. Zhang, P, Luo, Y, Chasan, B, Gonzalez-Perrett, S, Montalbetti, N, Timpanaro, GA, Cantero Mdel, R, Ramos, AJ, Goldmann, WH, Zhou, J, Cantiello, HF: The multimeric structure of polycystin-2 (TRPP2): structural-functional correlates of homo- and hetero-multimers with TRPC1. *Hum Mol Genet,* 18**:** 1238-1251, 2009.

60. Cantero Mdel, R, Cantiello, HF: Calcium transport and local pool regulate polycystin-2 (TRPP2) function in human syncytiotrophoblast. *Biophys J,* 105**:** 365-375, 2013.

61. Grieben, M, Pike, AC, Shintre, CA, Venturi, E, El-Ajouz, S, Tessitore, A, Shrestha, L, Mukhopadhyay, S, Mahajan, P, Chalk, R, Burgess-Brown, NA, Sitsapesan, R, Huiskonen, JT, Carpenter, EP: Structure of the polycystic kidney disease TRP channel Polycystin-2 (PC2). *Nat Struct Mol Biol,* 24**:** 114-122, 2017.

62. Shen, PS, Yang, X, DeCaen, PG, Liu, X, Bulkley, D, Clapham, DE, Cao, E: The Structure of the Polycystic Kidney Disease Channel PKD2 in Lipid Nanodiscs. *Cell,* 167**:** 763-773 e711, 2016.

63. Geng, L, Segal, Y, Pavlova, A, Barros, EJ, Lohning, C, Lu, W, Nigam, SK, Frischauf, AM, Reeders, ST, Zhou, J: Distribution and developmentally regulated expression of murine polycystin. *Am J Physiol,* 272**:** F451-459, 1997.

64. Zhou, J: Polycystins and primary cilia: primers for cell cycle progression. *Annu Rev Physiol,* 71**:** 83-113, 2009.

65. Hogan, MC, Manganelli, L, Woollard, JR, Masyuk, AI, Masyuk, TV, Tammachote, R, Huang, BQ, Leontovich, AA, Beito, TG, Madden, BJ, Charlesworth, MC, Torres, VE, LaRusso, NF, Harris, PC, Ward, CJ: Characterization of PKD protein-positive exosome-like vesicles. *Journal of the American Society of Nephrology : JASN,* 20**:** 278-288, 2009.

66. Ong, AC, Harris, PC: Molecular pathogenesis of ADPKD: the polycystin complex gets complex. *Kidney Int,* 67**:** 1234-1247, 2005.

67. Cahalan, MD: The ins and outs of polycystin-2 as a calcium release channel. *Nature cell biology,* 4**:** E56-57, 2002.

68. Hanaoka, K, Qian, F, Boletta, A, Bhunia, AK, Piontek, K, Tsiokas, L, Sukhatme, VP, Guggino, WB, Germino, GG: Co-assembly of polycystin-1 and -2 produces unique cation-permeable currents. *Nature,* 408**:** 990-994, 2000.

69. Delling, M, Indzhykulian, AA, Liu, X, Li, Y, Xie, T, Corey, DP, Clapham, DE: Primary cilia are not calcium-responsive mechanosensors. *Nature,* 531**:** 656-660, 2016.

70. Orhon, I, Dupont, N, Zaidan, M, Boitez, V, Burtin, M, Schmitt, A, Capiod, T, Viau, A, Beau, I, Kuehn, EW, Friedlander, G, Terzi, F, Codogno, P: Primary-cilium-dependent autophagy controls epithelial cell volume in response to fluid flow. *Nature cell biology,* 18**:** 657-667, 2016.

71. Grantham, JJ: The Jeremiah Metzger Lecture. Polycystic kidney disease: old disease in a new context. *Trans Am Clin Climatol Assoc,* 113**:** 211-224; discussion 224-216, 2002.

72. Yamaguchi, T, Hempson, SJ, Reif, GA, Hedge, AM, Wallace, DP: Calcium restores a normal proliferation phenotype in human polycystic kidney disease epithelial cells. *Journal of the American Society of Nephrology : JASN,* 17**:** 178-187, 2006.

73. Yamaguchi, T, Nagao, S, Kasahara, M, Takahashi, H, Grantham, JJ: Renal accumulation and excretion of cyclic adenosine monophosphate in a murine model of slowly progressive polycystic kidney disease. *Am J Kidney Dis,* 30**:** 703-709, 1997.

74. Nagao, S, Nishii, K, Katsuyama, M, Kurahashi, H, Marunouchi, T, Takahashi, H, Wallace, DP: Increased water intake decreases progression of polycystic kidney disease in the PCK rat. *Journal of the American Society of Nephrology : JASN,* 17**:** 2220-2227, 2006.

75. Torres, VE, Wang, X, Qian, Q, Somlo, S, Harris, PC, Gattone, VH, 2nd: Effective treatment of an orthologous model of autosomal dominant polycystic kidney disease. *Nat Med,* 10**:** 363-364, 2004.

76. Belibi, FA, Reif, G, Wallace, DP, Yamaguchi, T, Olsen, L, Li, H, Helmkamp, GM, Jr., Grantham, JJ: Cyclic AMP promotes growth and secretion in human polycystic kidney epithelial cells. *Kidney Int,* 66**:** 964-973, 2004.

77. Yamaguchi, T, Nagao, S, Wallace, DP, Belibi, FA, Cowley, BD, Jr., Pelling, JC, Grantham, JJ: Cyclic AMP activates B-Raf and ERK in cyst epithelial cells from autosomal-dominant polycystic kidneys. *Kidney Int,* 63**:** 1983-1994, 2003.

78. Yamaguchi, T, Reif, GA, Calvet, JP, Wallace, DP: Sorafenib inhibits cAMP-dependent ERK activation, cell proliferation, and in vitro cyst growth of human ADPKD cyst epithelial cells. *Am J Physiol Renal Physiol,* 299**:** F944-951, 2010.

79. Yamaguchi, T, Wallace, DP, Magenheimer, BS, Hempson, SJ, Grantham, JJ, Calvet, JP: Calcium restriction allows cAMP activation of the B-Raf/ERK pathway, switching cells to a cAMP-dependent growth-stimulated phenotype. *J Biol Chem,* 279**:** 40419-40430, 2004.

80. Davidow, CJ, Maser, RL, Rome, LA, Calvet, JP, Grantham, JJ: The cystic fibrosis transmembrane conductance regulator mediates transepithelial fluid secretion by human autosomal dominant polycystic kidney disease epithelium in vitro. *Kidney Int,* 50**:** 208-218, 1996.

81. Lu, M, Dong, K, Egan, ME, Giebisch, GH, Boulpaep, EL, Hebert, SC: Mouse cystic fibrosis transmembrane conductance regulator forms cAMP-PKA-regulated apical chloride channels in cortical collecting duct. *Proc Natl Acad Sci U S A,* 107**:** 6082-6087, 2010.

82. Magenheimer, BS, St John, PL, Isom, KS, Abrahamson, DR, De Lisle, RC, Wallace, DP, Maser, RL, Grantham, JJ, Calvet, JP: Early embryonic renal tubules of wild-type and polycystic kidney disease kidneys respond to cAMP stimulation with cystic fibrosis transmembrane

conductance regulator/Na(+),K(+),2Cl(-) Co-transporter-dependent cystic dilation. *Journal of the American Society of Nephrology : JASN,* 17**:** 3424-3437, 2006.

83. Gattone, VH, 2nd, Wang, X, Harris, PC, Torres, VE: Inhibition of renal cystic disease development and progression by a vasopressin V2 receptor antagonist. *Nat Med,* 9**:** 1323-1326, 2003.

84. Gattone, VH, 2nd, Maser, RL, Tian, C, Rosenberg, JM, Branden, MG: Developmental expression of urine concentration-associated genes and their altered expression in murine infantile-type polycystic kidney disease. *Dev Genet,* 24**:** 309-318, 1999.

85. Wang, X, Wu, Y, Ward, CJ, Harris, PC, Torres, VE: Vasopressin directly regulates cyst growth in polycystic kidney disease. *Journal of the American Society of Nephrology : JASN,* 19**:** 102-108, 2008.

86. Wang, X, Gattone, V, 2nd, Harris, PC, Torres, VE: Effectiveness of vasopressin V2 receptor antagonists OPC-31260 and OPC-41061 on polycystic kidney disease development in the PCK rat. *Journal of the American Society of Nephrology : JASN,* 16**:** 846-851, 2005.

87. Torres, VE, Chapman, AB, Devuyst, O, Gansevoort, RT, Grantham, JJ, Higashihara, E, Perrone, RD, Krasa, HB, Ouyang, J, Czerwiec, FS: Tolvaptan in Patients with Autosomal Dominant Polycystic Kidney Disease. *New England Journal of Medicine,* 367**:** 2407-2418, 2012.

88. Pinto, CS, Reif, GA, Nivens, E, White, C, Wallace, DP: Calmodulin-sensitive adenylyl cyclases mediate AVP-dependent cAMP production and Cl- secretion by human autosomal dominant polycystic kidney cells. *Am J Physiol Renal Physiol,* 303**:** F1412-1424, 2012.

89. Rees, S, Kittikulsuth, W, Roos, K, Strait, KA, Van Hoek, A, Kohan, DE: Adenylyl cyclase 6 deficiency ameliorates polycystic kidney disease. *Journal of the American Society of Nephrology : JASN,* 25**:** 232-237, 2014.

90. Pinto, CS, Raman, A, Reif, GA, Magenheimer, BS, White, C, Calvet, JP, Wallace, DP: Phosphodiesterase Isoform Regulation of Cell Proliferation and Fluid Secretion in Autosomal Dominant Polycystic Kidney Disease. *Journal of the American Society of Nephrology*, 2015.

91. Kakade, VR, Tao, S, Rajagopal, M, Zhou, X, Li, X, Yu, AS, Calvet, JP, Pandey, P, Rao, R: A cAMP and CREB-mediated feed-forward mechanism regulates GSK3beta in polycystic kidney disease. *J Mol Cell Biol,* 8**:** 464-476, 2016.

92. Rao, R, Patel, S, Hao, C, Woodgett, J, Harris, R: GSK3beta mediates renal response to vasopressin by modulating adenylate cyclase activity. *Journal of the American Society of Nephrology : JASN,* 21**:** 428-437, 2010.

93. Tao, S, Kakade, VR, Woodgett, JR, Pandey, P, Suderman, ED, Rajagopal, M, Rao, R: Glycogen synthase kinase-3beta promotes cyst expansion in polycystic kidney disease. *Kidney Int,* 87**:** 1164-1175, 2015.

94. Orellana, SA, Sweeney, WE, Neff, CD, Avner, ED: Epidermal growth factor receptor expression is abnormal in murine polycystic kidney. *Kidney Int,* 47**:** 490-499, 1995.

95. Torres, VE, Harris, PC: Polycystic kidney disease: genes, proteins, animal models, disease mechanisms and therapeutic opportunities. *Journal of internal medicine,* 261**:** 17-31, 2007.

96. Richards, WG, Sweeney, WE, Yoder, BK, Wilkinson, JE, Woychik, RP, Avner, ED: Epidermal growth factor receptor activity mediates renal cyst formation in polycystic kidney disease. *J Clin Invest,* 101**:** 935-939, 1998.

97. Sweeney, WE, Chen, Y, Nakanishi, K, Frost, P, Avner, ED: Treatment of polycystic kidney disease with a novel tyrosine kinase inhibitor. *Kidney Int,* 57**:** 33-40, 2000.

98. Sweeney, WE, Futey, L, Frost, P, Avner, ED: In vitro modulation of cyst formation by a novel tyrosine kinase inhibitor. *Kidney Int,* 56**:** 406-413, 1999.

99. Torres, VE, Sweeney, WE, Jr., Wang, X, Qian, Q, Harris, PC, Frost, P, Avner, ED: EGF receptor tyrosine kinase inhibition attenuates the development of PKD in Han:SPRD rats. *Kidney Int,* 64**:** 1573-1579, 2003.

100. Omori, S, Hida, M, Fujita, H, Takahashi, H, Tanimura, S, Kohno, M, Awazu, M: Extracellular signal-regulated kinase inhibition slows disease progression in mice with polycystic kidney disease. *Journal of the American Society of Nephrology : JASN,* 17**:** 1604-1614, 2006.

101. Shibazaki, S, Yu, Z, Nishio, S, Tian, X, Thomson, RB, Mitobe, M, Louvi, A, Velazquez, H, Ishibe, S, Cantley, LG, Igarashi, P, Somlo, S: Cyst formation and activation of the extracellular regulated kinase pathway after kidney specific inactivation of Pkd1. *Hum Mol Genet,* 17**:** 1505-1516, 2008.

102. Sandford, R, Sgotto, B, Burn, T, Brenner, S: The tuberin (TSC2), autosomal dominant polycystic kidney disease (PKD1), and somatostatin type V receptor (SSTR5) genes form a synteny group in the Fugu genome. *Genomics,* 38**:** 84-86, 1996.

103. Sampson, JR, Maheshwar, MM, Aspinwall, R, Thompson, P, Cheadle, JP, Ravine, D, Roy, S, Haan, E, Bernstein, J, Harris, PC: Renal cystic disease in tuberous sclerosis: role of the polycystic kidney disease 1 gene. *Am J Hum Genet,* 61**:** 843-851, 1997.

104. Kleymenova, E, Ibraghimov-Beskrovnaya, O, Kugoh, H, Everitt, J, Xu, H, Kiguchi, K, Landes, G, Harris, P, Walker, C: Tuberin-dependent membrane localization of polycystin-1: a functional link between polycystic kidney disease and the TSC2 tumor suppressor gene. *Mol Cell,* 7**:** 823-832, 2001.

105. Pema, M, Drusian, L, Chiaravalli, M, Castelli, M, Yao, Q, Ricciardi, S, Somlo, S, Qian, F, Biffo, S, Boletta, A: mTORC1-mediated inhibition of polycystin-1 expression drives renal cyst formation in tuberous sclerosis complex. *Nat Commun,* 7**:** 10786, 2016.

106. Weimbs, T: Regulation of mTOR by polycystin-1: is polycystic kidney disease a case of futile repair? *Cell Cycle,* 5**:** 2425-2429, 2006.

107. Tao, Y, Kim, J, Schrier, RW, Edelstein, CL: Rapamycin markedly slows disease progression in a rat model of polycystic kidney disease. *Journal of the American Society of Nephrology : JASN,* 16**:** 46-51, 2005.

108. Wahl, PR, Serra, AL, Le Hir, M, Molle, KD, Hall, MN, Wuthrich, RP: Inhibition of mTOR with sirolimus slows disease progression in Han:SPRD rats with autosomal dominant polycystic kidney disease (ADPKD). *Nephrol Dial Transplant,* 21**:** 598-604, 2006.

109. Shillingford, JM, Piontek, KB, Germino, GG, Weimbs, T: Rapamycin ameliorates PKD resulting from conditional inactivation of Pkd1. *Journal of the American Society of Nephrology : JASN,* 21**:** 489-497, 2010.

110. Zafar, I, Ravichandran, K, Belibi, FA, Doctor, RB, Edelstein, CL: Sirolimus attenuates disease progression in an orthologous mouse model of human autosomal dominant polycystic kidney disease. *Kidney Int,* 78**:** 754-761, 2010.

111. Ravichandran, K, Zafar, I, Ozkok, A, Edelstein, CL: An mTOR kinase inhibitor slows disease progression in a rat model of polycystic kidney disease. *Nephrol Dial Transplant,* 30**:** 45-53, 2015.

112. Shillingford, JM, Leamon, CP, Vlahov, IR, Weimbs, T: Folate-conjugated rapamycin slows progression of polycystic kidney disease. *Journal of the American Society of Nephrology : JASN,* 23**:** 1674-1681, 2012.

113. Zafar, I, Belibi, FA, He, Z, Edelstein, CL: Long-term rapamycin therapy in the Han:SPRD rat model of polycystic kidney disease (PKD). *Nephrol Dial Transplant,* 24**:** 2349-2353, 2009.

114. Grantham, JJ, Bennett, WM, Perrone, RD: mTOR inhibitors and autosomal dominant polycystic kidney disease. *N Engl J Med,* 364**:** 286-287; author reply 287-289, 2011.

115. Rankin, CA, Grantham, JJ, Calvet, JP: C-fos expression is hypersensitive to serum-stimulation in cultured cystic kidney cells from the C57BL/6J-cpk mouse. *J Cell Physiol,* 152**:** 578-586, 1992.

116. Calvet, JP: Polycystic kidney disease: primary extracellular matrix abnormality or defective cellular differentiation? *Kidney Int,* 43**:** 101-108, 1993.

117. Tran, PV, Sharma, M, Li, X, Calvet, JP: Developmental signaling: does it bridge the gap between cilia dysfunction and renal cystogenesis? *Birth Defects Res C Embryo Today,* 102**:** 159-173, 2014.

118. Song, X, Di Giovanni, V, He, N, Wang, K, Ingram, A, Rosenblum, ND, Pei, Y: Systems biology of autosomal dominant polycystic kidney disease (ADPKD): computational identification of gene expression pathways and integrated regulatory networks. *Hum Mol Genet,* 18**:** 2328-2343, 2009.

119. Weimbs, T: Polycystic kidney disease and renal injury repair: common pathways, fluid flow, and the function of polycystin-1. *Am J Physiol Renal Physiol,* 293**:** F1423-1432, 2007.

120. Weimbs, T, Olsan, EE, Talbot, JJ: Regulation of STATs by polycystin-1 and their role in polycystic kidney disease. *JAKSTAT,* 2**:** e23650, 2013.

121. Patel, V, Li, L, Cobo-Stark, P, Shao, X, Somlo, S, Lin, F, Igarashi, P: Acute kidney injury and aberrant planar cell polarity induce cyst formation in mice lacking renal cilia. *Hum Mol Genet,* 17**:** 1578-1590, 2008.

122. Takakura, A, Contrino, L, Zhou, X, Bonventre, JV, Sun, Y, Humphreys, BD, Zhou, J: Renal injury is a third hit promoting rapid development of adult polycystic kidney disease. *Hum Mol Genet,* 18**:** 2523-2531, 2009.

123. Happe, H, Leonhard, WN, van der Wal, A, van de Water, B, Lantinga-van Leeuwen, IS, Breuning, MH, de Heer, E, Peters, DJ: Toxic tubular injury in kidneys from Pkd1-deletion mice accelerates cystogenesis accompanied by dysregulated planar cell polarity and canonical Wnt signaling pathways. *Hum Mol Genet,* 18**:** 2532-2542, 2009.

124. Bell, PD, Fitzgibbon, W, Sas, K, Stenbit, AE, Amria, M, Houston, A, Reichert, R, Gilley, S, Siegal, GP, Bissler, J, Bilgen, M, Chou, PC, Guay-Woodford, L, Yoder, B, Haycraft, CJ, Siroky, B: Loss of primary cilia upregulates renal hypertrophic signaling and promotes cystogenesis. *Journal of the American Society of Nephrology : JASN,* 22**:** 839-848, 2011.

125. Leonhard, WN, Zandbergen, M, Veraar, K, van den Berg, S, van der Weerd, L, Breuning, M, de Heer, E, Peters, DJ: Scattered Deletion of PKD1 in Kidneys Causes a Cystic Snowball Effect and Recapitulates Polycystic Kidney Disease. *Journal of the American Society of Nephrology : JASN,* 26**:** 1322-1333, 2015.

126. Daley, WP, Peters, SB, Larsen, M: Extracellular matrix dynamics in development and regenerative medicine. *J Cell Sci,* 121**:** 255-264, 2008.

127. Pozzi, A, Zent, R: Integrins, extracellular matrix, and terminal differentiation of renal epithelial cells. *Journal of the American Society of Nephrology : JASN,* 19**:** 1043-1044, 2008.

128. Walker, JT, McLeod, K, Kim, S, Conway, SJ, Hamilton, DW: Periostin as a multifunctional modulator of the wound healing response. *Cell Tissue Res,* 365**:** 453-465, 2016.

129. Eddy, AA: Overview of the cellular and molecular basis of kidney fibrosis. *Kidney Int Suppl (2011),* 4**:** 2-8, 2014.

130. Bornstein, P, Sage, EH: Matricellular proteins: extracellular modulators of cell function. *Curr Opin Cell Biol,* 14**:** 608-616, 2002.

131. Norris, RA, Moreno-Rodriguez, R, Hoffman, S, Markwald, RR: The many facets of the matricelluar protein periostin during cardiac development, remodeling, and pathophysiology. *J Cell Commun Signal,* 3**:** 275-286, 2009.

132. Hannigan, G, Troussard, AA, Dedhar, S: Integrin-linked kinase: a cancer therapeutic target unique among its ILK. *Nat Rev Cancer,* 5**:** 51-63, 2005.

133. Canel, M, Serrels, A, Frame, MC, Brunton, VG: E-cadherin-integrin crosstalk in cancer invasion and metastasis. *J Cell Sci,* 126**:** 393-401, 2013.

134. Pozzi, A, Zent, R: Integrins in kidney disease. *Journal of the American Society of Nephrology : JASN,* 24**:** 1034-1039, 2013.

135. Conway, SJ, Molkentin, JD: Periostin as a heterofunctional regulator of cardiac development and disease. *Curr Genomics,* 9**:** 548-555, 2008.

136. Sen, K, Lindenmeyer, MT, Gaspert, A, Eichinger, F, Neusser, MA, Kretzler, M, Segerer, S, Cohen, CD: Periostin is induced in glomerular injury and expressed de novo in interstitial renal fibrosis. *Am J Pathol,* 179**:** 1756-1767, 2011.

137. Sidhu, SS, Yuan, S, Innes, AL, Kerr, S, Woodruff, PG, Hou, L, Muller, SJ, Fahy, JV: Roles of epithelial cell-derived periostin in TGF-beta activation, collagen production, and collagen gel elasticity in asthma. *Proc Natl Acad Sci U S A,* 107**:** 14170-14175, 2010.

138. Chiodoni, C, Colombo, MP, Sangaletti, S: Matricellular proteins: from homeostasis to inflammation, cancer, and metastasis. *Cancer metastasis reviews,* 29**:** 295-307, 2010.

139. Cuppage, FE, Huseman, RA, Chapman, A, Grantham, JJ: Ultrastructure and function of cysts from human adult polycystic kidneys. *Kidney Int,* 17**:** 372-381, 1980.

140. Wilson, PD, Burrow, CR: Cystic diseases of the kidney: role of adhesion molecules in normal and abnormal tubulogenesis. *Exp Nephrol,* 7**:** 114-124, 1999.

141. Schafer, K, Bader, M, Gretz, N, Oberbaumer, I, Bachmann, S: Focal overexpression of collagen IV characterizes the initiation of epithelial changes in polycystic kidney disease. *Exp Nephrol,* 2**:** 190-195, 1994.

142. Candiano, G, Gusmano, R, Altieri, P, Bertelli, R, Ginevri, F, Coviello, DA, Sessa, A, Caridi, G, Ghiggeri, GM: Extracellular matrix formation by epithelial cells from human polycystic kidney cysts in culture. *Virchows Arch B Cell Pathol Incl Mol Pathol,* 63**:** 1-9, 1992.

143. Dominique Joly D, MV, Hummel A, Ruello A, Nusbaum P, Patey N, Noël LH, Rousselle P, Knebelmann B.: β4 Integrin and Laminin 5 Are Aberrantly Expressed in Polycystic Kidney Disease.

144. Mangos, S, Lam, PY, Zhao, A, Liu, Y, Mudumana, S, Vasilyev, A, Liu, A, Drummond, IA: The ADPKD genes pkd1a/b and pkd2 regulate extracellular matrix formation. *Disease models & mechanisms,* 3**:** 354-365, 2010.

145. Schaefer, L, Han, X, Gretz, N, Hafner, C, Meier, K, Matzkies, F, Schaefer, RM: Tubular gelatinase A (MMP-2) and its tissue inhibitors in polycystic kidney disease in the Han:SPRD rat. *Kidney Int,* 49**:** 75-81, 1996.

146. Obermuller, N, Morente, N, Kranzlin, B, Gretz, N, Witzgall, R: A possible role for metalloproteinases in renal cyst development. *Am J Physiol Renal Physiol,* 280**:** F540-550, 2001.

147. Hassane, S, Leonhard, WN, van der Wal, A, Hawinkels, LJ, Lantinga-van Leeuwen, IS, ten Dijke, P, Breuning, MH, de Heer, E, Peters, DJ: Elevated TGFbeta-Smad signalling in experimental Pkd1 models and human patients with polycystic kidney disease. *J Pathol,* 222**:** 21-31, 2010.

148. Rankin, CA, Suzuki, K, Itoh, Y, Ziemer, DM, Grantham, JJ, Calvet, JP, Nagase, H: Matrix metalloproteinases and TIMPS in cultured C57BL/6J-cpk kidney tubules. *Kidney Int,* 50**:** 835-844, 1996.

149. Norman, J: Fibrosis and progression of autosomal dominant polycystic kidney disease (ADPKD). *Biochim Biophys Acta,* 1812**:** 1327-1336, 2011.

150. Nakamura, T, Ushiyama, C, Suzuki, S, Ebihara, I, Shimada, N, Koide, H: Elevation of serum levels of metalloproteinase-1, tissue inhibitor of metalloproteinase-1 and type IV collagen, and plasma levels of metalloproteinase-9 in polycystic kidney disease. *Am J Nephrol,* 20**:** 32-36, 2000.

151. Song, CJ, Zimmerman, KA, Henke, SJ, Yoder, BK: Inflammation and Fibrosis in Polycystic Kidney Disease. *Results Probl Cell Differ,* 60**:** 323-344, 2017.

152. Daikha-Dahmane, F, Narcy, F, Dommergues, M, Lacoste, M, Beziau, A, Gubler, MC: Distribution of alpha-integrin subunits in fetal polycystic kidney diseases. *Pediatr Nephrol,* 11**:** 267-273, 1997.

153. Zeltner, R, Hilgers, KF, Schmieder, RE, Porst, M, Schulze, BD, Hartner, A: A promoter polymorphism of the alpha 8 integrin gene and the progression of autosomal-dominant polycystic kidney disease. *Nephron Clin Pract,* 108**:** c169-175, 2008.

154. Lee, K, Boctor, S, Barisoni, LM, Gusella, GL: Inactivation of integrin-beta1 prevents the development of polycystic kidney disease after the loss of polycystin-1. *Journal of the American Society of Nephrology : JASN,* 26**:** 888-895, 2015.

155. Vijayakumar, S, Dang, S, Marinkovich, MP, Lazarova, Z, Yoder, B, Torres, VE, Wallace, DP: Aberrant expression of laminin-332 promotes cell proliferation and cyst growth in ARPKD. *Am J Physiol Renal Physiol,* 306**:** F640-654, 2014.

156. Takeshita, S, Kikuno, R, Tezuka, K, Amann, E: Osteoblast-specific factor 2: cloning of a putative bone adhesion protein with homology with the insect protein fasciclin I. *Biochem J,* 294 (Pt 1)**:** 271-278, 1993.

157. Horiuchi, K, Amizuka, N, Takeshita, S, Takamatsu, H, Katsuura, M, Ozawa, H, Toyama, Y, Bonewald, LF, Kudo, A: Identification and characterization of a novel protein, periostin, with restricted expression to periosteum and periodontal ligament and increased expression by transforming growth factor beta. *J Bone Miner Res,* 14**:** 1239-1249, 1999.

158. Ruan, K, Bao, S, Ouyang, G: The multifaceted role of periostin in tumorigenesis. *Cell Mol Life Sci,* 66**:** 2219-2230, 2009.

159. Hoersch, S, Andrade-Navarro, MA: Periostin shows increased evolutionary plasticity in its alternatively spliced region. *Bmc Evolutionary Biology,* 10**:** 30, 2010.

160. Kim, BY, Olzmann, JA, Choi, SI, Ahn, SY, Kim, TI, Cho, HS, Suh, H, Kim, EK: Corneal dystrophy-associated R124H mutation disrupts TGFBI interaction with Periostin and causes mislocalization to the lysosome. *J Biol Chem,* 284**:** 19580-19591, 2009.

161. Norris, RA, Damon, B, Mironov, V, Kasyanov, V, Ramamurthi, A, Moreno-Rodriguez, R, Trusk, T, Potts, JD, Goodwin, RL, Davis, J, Hoffman, S, Wen, X, Sugi, Y, Kern, CB, Mjaatvedt, CH, Turner, DK, Oka, T, Conway, SJ, Molkentin, JD, Forgacs, G, Markwald, RR: Periostin regulates collagen fibrillogenesis and the biomechanical properties of connective tissues. *J Cell Biochem,* 101**:** 695-711, 2007.

162. Takayama, G, Arima, K, Kanaji, T, Toda, S, Tanaka, H, Shoji, S, McKenzie, AN, Nagai, H, Hotokebuchi, T, Izuhara, K: Periostin: a novel component of subepithelial fibrosis of bronchial asthma downstream of IL-4 and IL-13 signals. *J Allergy Clin Immunol,* 118**:** 98-104, 2006.

163. Kim, JE, Kim, SJ, Lee, BH, Park, RW, Kim, KS, Kim, IS: Identification of motifs for cell adhesion within the repeated domains of transforming growth factor-beta-induced gene, betaig-h3. *J Biol Chem,* 275**:** 30907-30915, 2000.

164. Bao, S, Ouyang, G, Bai, X, Huang, Z, Ma, C, Liu, M, Shao, R, Anderson, RM, Rich, JN, Wang, XF: Periostin potently promotes metastatic growth of colon cancer by augmenting cell survival via the Akt/PKB pathway. *Cancer Cell,* 5**:** 329-339, 2004.

165. Cobo, T, Viloria, CG, Solares, L, Fontanil, T, Gonzalez-Chamorro, E, De Carlos, F, Cobo, J, Cal, S, Obaya, AJ: Role of Periostin in Adhesion and Migration of Bone Remodeling Cells. *PLoS One,* 11**:** e0147837, 2016.

166. Morra, L, Rechsteiner, M, Casagrande, S, Duc Luu, V, Santimaria, R, Diener, PA, Sulser, T, Kristiansen, G, Schraml, P, Moch, H, Soltermann, A: Relevance of periostin splice variants in renal cell carcinoma. *Am J Pathol,* 179**:** 1513-1521, 2011.

167. Maruhashi, T, Kii, I, Saito, M, Kudo, A: Interaction between periostin and BMP-1 promotes proteolytic activation of lysyl oxidase. *J Biol Chem,* 285**:** 13294-13303, 2010.

168. Laczko, R, Szauter, KM, Jansen, MK, Hollosi, P, Muranyi, M, Molnar, J, Fong, KS, Hinek, A, Csiszar, K: Active lysyl oxidase (LOX) correlates with focal adhesion kinase (FAK)/paxillin activation and migration in invasive astrocytes. *Neuropathol Appl Neurobiol,* 33**:** 631-643, 2007.

169. Lindner, V, Wang, Q, Conley, BA, Friesel, RE, Vary, CP: Vascular injury induces expression of periostin: implications for vascular cell differentiation and migration. *Arterioscler Thromb Vasc Biol,* 25**:** 77-83, 2005.

170. Litvin, J, Zhu, S, Norris, R, Markwald, R: Periostin family of proteins: therapeutic targets for heart disease. *Anat Rec A Discov Mol Cell Evol Biol,* 287**:** 1205-1212, 2005.

171. Shao, R, Bao, S, Bai, X, Blanchette, C, Anderson, RM, Dang, T, Gishizky, ML, Marks, JR, Wang, XF: Acquired expression of periostin by human breast cancers promotes tumor angiogenesis through up-regulation of vascular endothelial growth factor receptor 2 expression. *Molecular and cellular biology,* 24**:** 3992-4003, 2004.

172. Kuhn, B, del Monte, F, Hajjar, RJ, Chang, Y-S, Lebeche, D, Arab, S, Keating, MT: Periostin induces proliferation of differentiated cardiomyocytes and promotes cardiac repair. *Nat Med,* 13**:** 962-969, 2007.

173. Dorn, GW, 2nd: Periostin and myocardial repair, regeneration, and recovery. *N Engl J Med,* 357**:** 1552-1554, 2007.

174. Rios, H, Koushik, SV, Wang, H, Wang, J, Zhou, HM, Lindsley, A, Rogers, R, Chen, Z, Maeda, M, Kruzynska-Frejtag, A, Feng, JQ, Conway, SJ: periostin null mice exhibit dwarfism, incisor enamel defects, and an early-onset periodontal disease-like phenotype. *Mol Cell Biol,* 25**:** 11131-11144, 2005.

175. Baril, P, Gangeswaran, R, Mahon, PC, Caulee, K, Kocher, HM, Harada, T, Zhu, M, Kalthoff, H, Crnogorac-Jurcevic, T, Lemoine, NR: Periostin promotes invasiveness and resistance of pancreatic cancer cells to hypoxia-induced cell death: role of the beta4 integrin and the PI3k pathway. *Oncogene,* 26**:** 2082-2094, 2007.

176. Gillan, L, Matei, D, Fishman, DA, Gerbin, CS, Karlan, BY, Chang, DD: Periostin secreted by epithelial ovarian carcinoma is a ligand for alpha(V)beta(3) and alpha(V)beta(5) integrins and promotes cell motility. *Cancer research,* 62**:** 5358-5364, 2002.

177. Kudo, Y, Siriwardena, BS, Hatano, H, Ogawa, I, Takata, T: Periostin: novel diagnostic and therapeutic target for cancer. *Histol Histopathol,* 22**:** 1167-1174, 2007.

178. Morra, L, Moch, H: Periostin expression and epithelial-mesenchymal transition in cancer: a review and an update. *Virchows Arch,* 459**:** 465-475, 2011.

179. Sasaki, H, Dai, M, Auclair, D, Fukai, I, Kiriyama, M, Yamakawa, Y, Fujii, Y, Chen, LB: Serum level of the periostin, a homologue of an insect cell adhesion molecule, as a prognostic marker in nonsmall cell lung carcinomas. *Cancer,* 92**:** 843-848, 2001.

180. Sasaki, H, Yu, CY, Dai, M, Tam, C, Loda, M, Auclair, D, Chen, LB, Elias, A: Elevated serum periostin levels in patients with bone metastases from breast but not lung cancer. *Breast Cancer Res Treat,* 77**:** 245-252, 2003.

181. Naik, PK, Bozyk, PD, Bentley, JK, Popova, AP, Birch, CM, Wilke, CA, Fry, CD, White, ES, Sisson, TH, Tayob, N, Carnemolla, B, Orecchia, P, Flaherty, KR, Hershenson, MB, Murray, S, Martinez, FJ, Moore, BB, Investigators, C: Periostin promotes fibrosis and predicts progression in patients with idiopathic pulmonary fibrosis. *American journal of physiology Lung cellular and molecular physiology,* 303**:** L1046-1056, 2012.

182. Bible, E: Polycystic kidney disease: Periostin is involved in cell proliferation and interstitial fibrosis in polycystic kidney disease. *Nat Rev Nephrol,* 10**:** 66, 2014.

183. Frangogiannis, NG: Matricellular proteins in cardiac adaptation and disease. *Physiol Rev,* 92**:** 635-688, 2012.

184. Ito, T, Suzuki, A, Imai, E, Horimoto, N, Ohnishi, T, Daikuhara, Y, Hori, M: Tornado extraction: a method to enrich and purify RNA from the nephrogenic zone of the neonatal rat kidney. *Kidney Int,* 62**:** 763-769, 2002.

185. Hannigan, GE, Leung-Hagesteijn, C, Fitz-Gibbon, L, Coppolino, MG, Radeva, G, Filmus, J, Bell, JC, Dedhar, S: Regulation of cell adhesion and anchorage-dependent growth by a new beta 1-integrin-linked protein kinase. *Nature,* 379**:** 91-96, 1996.

186. McDonald, PC, Fielding, AB, Dedhar, S: Integrin-linked kinase--essential roles in physiology and cancer biology. *J Cell Sci,* 121**:** 3121-3132, 2008.

187. Wickstrom, SA, Lange, A, Montanez, E, Fassler, R: The ILK/PINCH/parvin complex: the kinase is dead, long live the pseudokinase! *EMBO J,* 29**:** 281-291, 2010.

188. Hannigan, GE, McDonald, PC, Walsh, MP, Dedhar, S: Integrin-linked kinase: not so 'pseudo' after all. *Oncogene,* 30**:** 4375-4385, 2011.

189. Fukuda, K, Gupta, S, Chen, K, Wu, C, Qin, J: The pseudoactive site of ILK is essential for its binding to alpha-Parvin and localization to focal adhesions. *Mol Cell,* 36**:** 819-830, 2009.

190. Tu, Y, Li, F, Goicoechea, S, Wu, C: The LIM-only protein PINCH directly interacts with integrin-linked kinase and is recruited to integrin-rich sites in spreading cells. *Mol Cell Biol,* 19**:** 2425-2434, 1999.

191. Tu, Y, Li, F, Wu, C: Nck-2, a novel Src homology2/3-containing adaptor protein that interacts with the LIM-only protein PINCH and components of growth factor receptor kinase-signaling pathways. *Mol Biol Cell,* 9**:** 3367-3382, 1998.

192. Legate, KR, Montanez, E, Kudlacek, O, Fassler, R: ILK, PINCH and parvin: the tIPP of integrin signalling. *Nature reviews Molecular cell biology,* 7**:** 20-31, 2006.

193. Delcommenne, M, Tan, C, Gray, V, Rue, L, Woodgett, J, Dedhar, S: Phosphoinositide-3-OH kinase-dependent regulation of glycogen synthase kinase 3 and protein kinase B/AKT by the integrin-linked kinase. *Proc Natl Acad Sci U S A,* 95**:** 11211-11216, 1998.

194. Leung-Hagesteijn, C, Mahendra, A, Naruszewicz, I, Hannigan, GE: Modulation of integrin signal transduction by ILKAP, a protein phosphatase 2C associating with the integrin-linked kinase, ILK1. *EMBO J,* 20**:** 2160-2170, 2001.

195. Graff, JR, Deddens, JA, Konicek, BW, Colligan, BM, Hurst, BM, Carter, HW, Carter, JH: Integrin-linked kinase expression increases with prostate tumor grade. *Clin Cancer Res,* 7**:** 1987-1991, 2001.

196. Marotta, A, Tan, C, Gray, V, Malik, S, Gallinger, S, Sanghera, J, Dupuis, B, Owen, D, Dedhar, S, Salh, B: Dysregulation of integrin-linked kinase (ILK) signaling in colonic polyposis. *Oncogene,* 20**:** 6250-6257, 2001.

197. Dai, DL, Makretsov, N, Campos, EI, Huang, C, Zhou, Y, Huntsman, D, Martinka, M, Li, G: Increased expression of integrin-linked kinase is correlated with melanoma progression and poor patient survival. *Clin Cancer Res,* 9**:** 4409-4414, 2003.

198. Takanami, I: Increased expression of integrin-linked kinase is associated with shorter survival in non-small cell lung cancer. *BMC Cancer,* 5**:** 1, 2005.

199. Edwards, LA, Thiessen, B, Dragowska, WH, Daynard, T, Bally, MB, Dedhar, S: Inhibition of ILK in PTEN-mutant human glioblastomas inhibits PKB/Akt activation, induces apoptosis, and delays tumor growth. *Oncogene,* 24**:** 3596-3605, 2005.

200. Maydan, M, McDonald, PC, Sanghera, J, Yan, J, Rallis, C, Pinchin, S, Hannigan, GE, Foster, LJ, Ish-Horowicz, D, Walsh, MP, Dedhar, S: Integrin-linked kinase is a functional Mn2+-dependent protein kinase that regulates glycogen synthase kinase-3beta (GSK-3beta) phosphorylation. *PLoS One,* 5**:** e12356, 2010.

201. Persad, S, Attwell, S, Gray, V, Mawji, N, Deng, JT, Leung, D, Yan, J, Sanghera, J, Walsh, MP, Dedhar, S: Regulation of protein kinase B/Akt-serine 473 phosphorylation by integrin-linked kinase: critical roles for kinase activity and amino acids arginine 211 and serine 343. *J Biol Chem,* 276**:** 27462-27469, 2001.

202. Troussard, AA, Mawji, NM, Ong, C, Mui, A, St -Arnaud, R, Dedhar, S: Conditional knock-out of integrin-linked kinase demonstrates an essential role in protein kinase B/Akt activation. *J Biol Chem,* 278**:** 22374-22378, 2003.

203. Lynch, DK, Ellis, CA, Edwards, PA, Hiles, ID: Integrin-linked kinase regulates phosphorylation of serine 473 of protein kinase B by an indirect mechanism. *Oncogene,* 18**:** 8024-8032, 1999.

204. Fukuda, K, Knight, JD, Piszczek, G, Kothary, R, Qin, J: Biochemical, proteomic, structural, and thermodynamic characterizations of integrin-linked kinase (ILK): cross-validation of the pseudokinase. *J Biol Chem,* 286**:** 21886-21895, 2011.

205. Lange, A, Wickstrom, SA, Jakobson, M, Zent, R, Sainio, K, Fassler, R: Integrin-linked kinase is an adaptor with essential functions during mouse development. *Nature,* 461**:** 1002-1006, 2009.

206. Tu, Y, Huang, Y, Zhang, Y, Hua, Y, Wu, C: A new focal adhesion protein that interacts with integrin-linked kinase and regulates cell adhesion and spreading. *J Cell Biol,* 153**:** 585-598, 2001.

207. Qin, J, Wu, C: ILK: a pseudokinase in the center stage of cell-matrix adhesion and signaling. *Curr Opin Cell Biol,* 24**:** 607-613, 2012.

208. Eke, I, Koch, U, Hehlgans, S, Sandfort, V, Stanchi, F, Zips, D, Baumann, M, Shevchenko, A, Pilarsky, C, Haase, M, Baretton, GB, Calleja, V, Larijani, B, Fassler, R, Cordes, N: PINCH1 regulates Akt1 activation and enhances radioresistance by inhibiting PP1alpha. *J Clin Invest,* 120**:** 2516-2527, 2010.

209. Persad, S, Attwell, S, Gray, V, Delcommenne, M, Troussard, A, Sanghera, J, Dedhar, S: Inhibition of integrin-linked kinase (ILK) suppresses activation of protein kinase B/Akt and induces cell cycle arrest and apoptosis of PTEN-mutant prostate cancer cells. *Proc Natl Acad Sci U S A,* 97**:** 3207-3212, 2000.

210. White, DE, Coutu, P, Shi, YF, Tardif, JC, Nattel, S, St Arnaud, R, Dedhar, S, Muller, WJ: Targeted ablation of ILK from the murine heart results in dilated cardiomyopathy and spontaneous heart failure. *Genes Dev,* 20**:** 2355-2360, 2006.

211. Smeeton, J, Zhang, X, Bulus, N, Mernaugh, G, Lange, A, Karner, CM, Carroll, TJ, Fassler, R, Pozzi, A, Rosenblum, ND, Zent, R: Integrin-linked kinase regulates p38 MAPK-dependent cell cycle arrest in ureteric bud development. *Development,* 137**:** 3233-3243, 2010.

212. Boppart, MD, Burkin, DJ, Kaufman, SJ: Activation of AKT signaling promotes cell growth and survival in alpha7beta1 integrin-mediated alleviation of muscular dystrophy. *Biochim Biophys Acta,* 1812**:** 439-446, 2011.

213. Koul, D, Shen, R, Bergh, S, Lu, Y, de Groot, JF, Liu, TJ, Mills, GB, Yung, WK: Targeting integrin-linked kinase inhibits Akt signaling pathways and decreases tumor progression of human glioblastoma. *Mol Cancer Ther,* 4**:** 1681-1688, 2005.

214. Watnick, T, Germino, GG: Molecular basis of autosomal dominant polycystic kidney disease. *Semin Nephrol,* 19**:** 327-343, 1999.

215. Wahl, PR, Le Hir, M, Vogetseder, A, Arcaro, A, Starke, A, Waeckerle-Men, Y, Serra, AL, Wuthrich, RP: Mitotic activation of Akt signalling pathway in Han:SPRD rats with polycystic kidney disease. *Nephrology (Carlton),* 12**:** 357-363, 2007.

216. Torres, VE, Boletta, A, Chapman, A, Gattone, V, Pei, Y, Qian, Q, Wallace, DP, Weimbs, T, Wuthrich, RP: Prospects for mTOR inhibitor use in patients with polycystic kidney disease and hamartomatous diseases. *Clinical journal of the American Society of Nephrology : CJASN,* 5**:** 1312-1329, 2010.

217. Cruet-Hennequart, S, Maubant, S, Luis, J, Gauduchon, P, Staedel, C, Dedhar, S: alpha(v) integrins regulate cell proliferation through integrin-linked kinase (ILK) in ovarian cancer cells. *Oncogene,* 22**:** 1688-1702, 2003.

218. Grashoff, C, Thievessen, I, Lorenz, K, Ussar, S, Fassler, R: Integrin-linked kinase: integrin's mysterious partner. *Curr Opin Cell Biol,* 16**:** 565-571, 2004.

219. Wu, C, Dedhar, S: Integrin-linked kinase (ILK) and its interactors: a new paradigm for the coupling of extracellular matrix to actin cytoskeleton and signaling complexes. *J Cell Biol,* 155**:** 505-510, 2001.

220. Piao, Z, Hong, CS, Jung, MR, Choi, C, Park, YK: Thymosin beta4 induces invasion and migration of human colorectal cancer cells through the ILK/AKT/beta-catenin signaling pathway. *Biochem Biophys Res Commun,* 452**:** 858-864, 2014.

221. McDonald, PC, Oloumi, A, Mills, J, Dobreva, I, Maidan, M, Gray, V, Wederell, ED, Bally, MB, Foster, LJ, Dedhar, S: Rictor and integrin-linked kinase interact and regulate Akt phosphorylation and cancer cell survival. *Cancer research,* 68**:** 1618-1624, 2008.

222. Wallace, DP, Grantham, JJ, Sullivan, LP: Chloride and fluid secretion by cultured human polycystic kidney cells. *Kidney Int,* 50**:** 1327-1336, 1996.

223. Lee, SL, Hsu, EC, Chou, CC, Chuang, HC, Bai, LY, Kulp, SK, Chen, CS: Identification and characterization of a novel integrin-linked kinase inhibitor. *J Med Chem,* 54**:** 6364-6374, 2011.

224. Reif, GA, Yamaguchi, T, Nivens, E, Fujiki, H, Pinto, CS, Wallace, DP: Tolvaptan inhibits ERK-dependent cell proliferation, Cl(-) secretion, and in vitro cyst growth of human ADPKD cells stimulated by vasopressin. *Am J Physiol Renal Physiol,* 301**:** F1005-1013, 2011.

225. Terpstra, L, Prud'homme, J, Arabian, A, Takeda, S, Karsenty, G, Dedhar, S, St-Arnaud, R: Reduced chondrocyte proliferation and chondrodysplasia in mice lacking the integrin-linked kinase in chondrocytes. *J Cell Biol,* 162**:** 139-148, 2003.

226. Ma, M, Tian, X, Igarashi, P, Pazour, GJ, Somlo, S: Loss of cilia suppresses cyst growth in genetic models of autosomal dominant polycystic kidney disease. *Nature genetics,* 45**:** 1004-1012, 2013.

227. Ray, MA, Johnston, NA, Verhulst, S, Trammell, RA, Toth, LA: Identification of markers for imminent death in mice used in longevity and aging research. *J Am Assoc Lab Anim Sci,* 49**:** 282-288, 2010.

228. Wallace, DP, Hou, YP, Huang, ZL, Nivens, E, Savinkova, L, Yamaguchi, T, Bilgen, M: Tracking kidney volume in mice with polycystic kidney disease by magnetic resonance imaging. *Kidney Int,* 73**:** 778-781, 2008.

229. Nagao, S, Nishii, K, Yoshihara, D, Kurahashi, H, Nagaoka, K, Yamashita, T, Takahashi, H, Yamaguchi, T, Calvet, JP, Wallace, DP: Calcium channel inhibition accelerates polycystic kidney disease progression in the Cy/+ rat. *Kidney Int,* 73**:** 269-277, 2008.

230. Malan, D, Elischer, A, Hesse, M, Wickstrom, SA, Fleischmann, BK, Bloch, W: Deletion of integrin linked kinase in endothelial cells results in defective RTK signaling caused by caveolin 1 mislocalization. *Development,* 140**:** 987-995, 2013.

231. Azimifar, SB, Böttcher, RT, Zanivan, S, Grashoff, C, Krüger, M, Legate, KR, Mann, M, Fässler, R: Induction of membrane circular dorsal ruffles requires co-signalling of integrin–ILK-complex and EGF receptor. *Journal of Cell Science,* 125**:** 435-448, 2012.

232. Cano-Peñalver, JL, Griera, M, Serrano, I, Rodríguez-Puyol, D, Dedhar, S, de Frutos, S, Rodríguez-Puyol, M: Integrin-linked kinase regulates tubular aquaporin-2 content and intracellular location: a link between the extracellular matrix and water reabsorption. *The FASEB Journal,* 28**:** 3645-3659, 2014.

233. Zhou, JX, Li, X: Apoptosis in Polycystic Kidney Disease: From Pathogenesis to Treatment. In: *Polycystic Kidney Disease.* edited by LI, X., Brisbane (AU), 2015.

234. Zhou, X, Fan, LX, Sweeney, WE, Jr., Denu, JM, Avner, ED, Li, X: Sirtuin 1 inhibition delays cyst formation in autosomal-dominant polycystic kidney disease. *J Clin Invest,* 123**:** 3084-3098, 2013.

235. Takahashi, H, Calvet, JP, Dittemore-Hoover, D, Yoshida, K, Grantham, JJ, Gattone, VH, 2nd: A hereditary model of slowly progressive polycystic kidney disease in the mouse. *Journal of the American Society of Nephrology : JASN,* 1**:** 980-989, 1991.

236. Olbrich, H, Fliegauf, M, Hoefele, J, Kispert, A, Otto, E, Volz, A, Wolf, MT, Sasmaz, G, Trauer, U, Reinhardt, R, Sudbrak, R, Antignac, C, Gretz, N, Walz, G, Schermer, B, Benzing, T, Hildebrandt, F, Omran, H: Mutations in a novel gene, NPHP3, cause adolescent

nephronophthisis, tapeto-retinal degeneration and hepatic fibrosis. *Nature genetics,* 34**:** 455-459, 2003.

237. Li, Y, Tan, X, Dai, C, Stolz, DB, Wang, D, Liu, Y: Inhibition of integrin-linked kinase attenuates renal interstitial fibrosis. *Journal of the American Society of Nephrology : JASN,* 20**:** 1907-1918, 2009.

238. Grantham, JJ: Clinical practice. Autosomal dominant polycystic kidney disease. *N Engl J Med,* 359**:** 1477-1485, 2008.

239. Malas, TB, Formica, C, Leonhard, WN, Rao, P, Granchi, Z, Roos, M, Peters, DJ, t Hoen, PA: Meta-analysis of polycystic kidney disease expression profiles defines strong involvement of injury repair processes. *Am J Physiol Renal Physiol,* 312**:** F806-F817, 2017.

240. Chang-Panesso, M, Humphreys, BD: Cellular plasticity in kidney injury and repair. *Nat Rev Nephrol,* 13**:** 39-46, 2017.

241. Liu, Y: Cellular and molecular mechanisms of renal fibrosis. *Nat Rev Nephrol,* 7**:** 684-696, 2011.

242. Jackson-Boeters, L, Wen, W, Hamilton, DW: Periostin localizes to cells in normal skin, but is associated with the extracellular matrix during wound repair. *Journal of cell communication and signaling,* 3**:** 125-133, 2009.

243. Guerrot, D, Dussaule, JC, Mael-Ainin, M, Xu-Dubois, YC, Rondeau, E, Chatziantoniou, C, Placier, S: Identification of periostin as a critical marker of progression/reversal of hypertensive nephropathy. *PLoS One,* 7**:** e31974, 2012.

244. Satirapoj, B, Wang, Y, Chamberlin, MP, Dai, T, LaPage, J, Phillips, L, Nast, CC, Adler, SG: Periostin: novel tissue and urinary biomarker of progressive renal injury induces a coordinated mesenchymal phenotype in tubular cells. *Nephrol Dial Transplant,* 27**:** 2702-2711, 2012.

245. Raman, A, Reif, GA, Dai, Y, Khanna, A, Li, X, Astleford, L, Parnell, SC, Calvet, JP, Wallace, DP: Integrin-Linked Kinase Signaling Promotes Cyst Growth and Fibrosis in Polycystic Kidney Disease. *Journal of the American Society of Nephrology***:** ASN. 2016111235, 2017.

246. Satirapoj, B, Witoon, R, Ruangkanchanasetr, P, Wantanasiri, P, Charoenpitakchai, M, Choovichian, P: Urine periostin as a biomarker of renal injury in chronic allograft nephropathy. *Transplant Proc,* 46**:** 135-140, 2014.

247. Ren, Y, Cao, B, Law, S, Xie, Y, Lee, PY, Cheung, L, Chen, Y, Huang, X, Chan, HM, Zhao, P, Luk, J, Vande Woude, G, Wong, J: Hepatocyte growth factor promotes cancer cell migration and angiogenic factors expression: a prognostic marker of human esophageal squamous cell carcinomas. *Clin Cancer Res,* 11**:** 6190-6197, 2005.

248. Tasic, B, Hippenmeyer, S, Wang, C, Gamboa, M, Zong, H, Chen-Tsai, Y, Luo, L: Site-specific integrase-mediated transgenesis in mice via pronuclear injection. *Proc Natl Acad Sci U S A,* 108**:** 7902-7907, 2011.

249. Cluzel, C, Saltel, F, Lussi, J, Paulhe, F, Imhof, BA, Wehrle-Haller, B: The mechanisms and dynamics of (alpha)v(beta)3 integrin clustering in living cells. *J Cell Biol,* 171**:** 383-392, 2005.

250. Mitra, SK, Hanson, DA, Schlaepfer, DD: Focal adhesion kinase: in command and control of cell motility. *Nature reviews Molecular cell biology,* 6**:** 56-68, 2005.

251. Palazzo, AF, Eng, CH, Schlaepfer, DD, Marcantonio, EE, Gundersen, GG: Localized stabilization of microtubules by integrin- and FAK-facilitated Rho signaling. *Science,* 303**:** 836-839, 2004.

252. Butcher, JT, Norris, RA, Hoffman, S, Mjaatvedt, CH, Markwald, RR: Periostin promotes atrioventricular mesenchyme matrix invasion and remodeling mediated by integrin signaling through Rho/PI 3-kinase. *Developmental biology,* 302**:** 256-266, 2007.

253. Kanno, A, Satoh, K, Masamune, A, Hirota, M, Kimura, K, Umino, J, Hamada, S, Satoh, A, Egawa, S, Motoi, F, Unno, M, Shimosegawa, T: Periostin, secreted from stromal cells, has biphasic effect on cell migration and correlates with the epithelial to mesenchymal transition of human pancreatic cancer cells. *International journal of cancer Journal international du cancer,* 122**:** 2707-2718, 2008.

254. Watanabe, T, Yasue, A, Fujihara, S, Tanaka, E: PERIOSTIN regulates MMP-2 expression via the alphavbeta3 integrin/ERK pathway in human periodontal ligament cells. *Archives of oral biology,* 57**:** 52-59, 2012.

255. Chang, MY, Ong, AC: Autosomal dominant polycystic kidney disease: recent advances in pathogenesis and treatment. *Nephron Physiology,* 108**:** p1-7, 2008.

256. Hinz, B: It has to be the alphav: myofibroblast integrins activate latent TGF-beta1. *Nat Med,* 19**:** 1567-1568, 2013.

257. Asano, Y, Ihn, H, Yamane, K, Jinnin, M, Mimura, Y, Tamaki, K: Increased expression of integrin alpha(v)beta3 contributes to the establishment of autocrine TGF-beta signaling in scleroderma fibroblasts. *Journal of immunology,* 175**:** 7708-7718, 2005.

258. Wetmore, JB, Calvet, JP, Yu, AS, Lynch, CF, Wang, CJ, Kasiske, BL, Engels, EA: Polycystic kidney disease and cancer after renal transplantation. *Journal of the American Society of Nephrology : JASN,* 25**:** 2335-2341, 2014.

259. Stupp, R, Hegi, ME, Gorlia, T, Erridge, SC, Perry, J, Hong, YK, Aldape, KD, Lhermitte, B, Pietsch, T, Grujicic, D, Steinbach, JP, Wick, W, Tarnawski, R, Nam, DH, Hau, P, Weyerbrock, A, Taphoorn, MJ, Shen, CC, Rao, N, Thurzo, L, Herrlinger, U, Gupta, T, Kortmann, RD, Adamska, K, McBain, C, Brandes, AA, Tonn, JC, Schnell, O, Wiegel, T, Kim, CY, Nabors, LB, Reardon, DA, van den Bent, MJ, Hicking, C, Markivskyy, A, Picard, M, Weller, M, European Organisation for, R, Treatment of, C, Canadian Brain Tumor, C, team, Cs: Cilengitide combined with standard treatment for patients with newly diagnosed glioblastoma with methylated MGMT promoter (CENTRIC EORTC 26071-22072 study): a multicentre, randomised, open-label, phase 3 trial. *Lancet Oncol,* 15**:** 1100-1108, 2014.

260. Ma, M, Simon, R, Ishikawa, Y, Tian, X, Dong, K, Cai, Y, Zhang, C, Sakai, T, Somlo, S: Fibronectin signaling modulates cyst progression in models of autosomal dominant polycystic kidney disease. *J Am Soc Nephrol supplement,* 27**:** 483A, 2016. CONFERENCE ABSTRACT.

261. Mael-Ainin, M, Abed, A, Conway, SJ, Dussaule, J-C, Chatziantoniou, C: Inhibition of periostin expression protects against the development of renal inflammation and fibrosis. *Journal of the American Society of Nephrology***:** ASN. 2013060664, 2014.